
H. A. AFFELDT. JR.
M.S.

M.S.

M.S.

This is to certify that the

thesis entitled

DIGITAL ANALYSIS OF THE DYNAMIC RESPONSE
WITHIN TRUNK SHAKER HARVESTER SYSTEMS

presented by

Henry Albert Affeldt, Jr.

has been accepted towards fulfillment
of the requirements for

M.S. degree in Agricultural Engineering

John B. Gerrish

Major professor
John B. Gerrish

Date 4 May 1984

DIGITAL ANALYSIS OF THE DYNAMIC RESPONSE WITHIN TRUNK SHAKER HARVESTER SYSTEMS

By

Henry Albert Affeldt Jr.

A THESIS

Submitted to
Michigan State University
in partial fulfillment of the requirements
for the degree of

MASTER OF SCIENCE

Department of Agricultural Engineering

1984

DIGITAL ANALYSIS OF THE DYNAMIC RESPONSE
WITHIN TRUNK SHAKER HARVESTER SYSTEMS

By

Henry Albert Affeldt Jr.

Date: _____

Approved: _____
Major Professor

Approved: _____
Department Chairman

Approved: _____
Committee Member

Approved: _____
Committee Member

ABSTRACT

DIGITAL ANALYSIS OF THE DYNAMIC RESPONSE
WITHIN TRUNK SHAKER HARVESTER SYSTEMS

By

Henry Albert Affeldt Jr.

The decline in productivity of commercial cherry orchards in Michigan has called attention to mechanical fruit harvesting as a potential cause of bark damage to trees; the dynamic characteristics of commercially-available tree shakers had to be measured in order to establish operating procedures which would be safe for the trees.

A C-clamp eccentric mass trunk shaker harvester for cherries was instrumented with transducers to characterize rigid body acceleration, hydraulic circuit pressure and mass and clamp arm position. A 2 MHz 6502 microprocessor-based data-acquisition system was assembled capable of digitizing 14 analog signals at a rate of 21 KHz and processing the resultant data.

Accelerations were integrated to displacement and compared with other physical events. The critical time of putative tree damage appeared to occur during the start-up transient of the shaker. A clamp 'pad relaxation' effect was observed.

To the Spirit of my father and mother,

of which I am so much a part.

ACKNOWLEDGMENTS

The author would like to express his deepest gratitude to the following persons and organizations for their contribution to this study:

To Dr. John B. Gerrish, my major professor, for his professional guidance, cooperation and support provided throughout the duration of the graduate program.

To my guidance committee, Dr. Galen K. Brown (Research Leader, Fruit and Vegetable Harvesting, U.S. Department of Agriculture) and Dr. Clark J. Radcliffe (Assistant Professor Mechanical Engineering) for their time, constructive counsel, and professional interest.

To USDA Mechanical Engineering Technician Richard Wolthius, USDA Electronic Technician Joe Clemens, and undergraduates Phil Richey and Paul Speicher who each contributed many hours of valuable assistance and experience to the project.

To cherry growers David and Philip Friday and the Friday Tractor Company (Hartford, MI) for contributions of equipment and advice which made this project feasible, to technical representative Leonard Wilming (Orchard Machinery Corporation) for the information rendered based on his experience, and to the Vanner Corporation for the

loan of a test model sine wave inverter.

To the Agricultural Research Service, U.S. Department of Agriculture for financial assistance (Research Engineer Recruitment and Development Program) and continued interest in the agricultural foundations of these United States.

To my mother June, my sister Tara, and the branching tree of family and friends whose unfailing love, confidence, and understanding have been a continuing source of strength and encouragement.

TABLE OF CONTENTS

LIST OF TABLES

LIST OF FIGURES

CHAPTER 1

INTRODUCTION

Mechanically induced damage to the world's varied it and nut trees has been a continuing international cern, particularly with the adoption in the early 0's of mechanical shake-and-catch harvesters. The roduction of the mechanical harvester brought about reases in labor efficiency and production capability. k damage associated with the use of these harvesters in commercial cherry orchards of Michigan has caused reasing alarm. Growers' observations of tree and nard decline, particularly among the younger plantings, e also suggested dynamic shaker loading as a possible se of internal tree damage. An estimated 20 to 30 ent of the cherry trees in some orchards annually show ence of some sort of injury (Brown, 1982). A means of uating the dynamic action of a trunk shaker as a ntial cause of bark damage was needed.

This study describes the development of the ware, software, and methodology to characterize the vior of an eccentric mass trunk shaker and a tree in to evaluate the detrimental effects of trunk shakers

tree bark. The information obtained can be employed in ther investigations to determine the stress and strain the bark. Estimates of stress and strain can be ived from peak displacements of the tree and shaker tem. Knowledge of applied bark loading coupled with vious studies of bark and cambium strength could help dict the presence and extent of tissue rupture within living tree. The instrumentation and analytical cedures developed in this investigation are expected to ly to other fruit and nut shake-harvest systems.

1.1 The Bark Damage Problem

The first mechanical cherry harvesters introduced 1958 (Levin et al.) caused tree damage through the ipping of bark resulting from excessive forces exerted the shaker. Insects and disease, especially canker, ld enter through the damaged tissue and spread to thy tissue, often resulting in the death of the tree.

California, the disease causing fungus, tocystis fimbriata, is carried by insects into damaged area where a favorable environment allows d spreading into healthy bark and wood (Devay et al. , 1962, 1965). Fungal vectors can be carried from to tree on shaker pads when continuous harvesting is ucted in a diseased orchard. Temperature and soil ture strongly affect the spread of infectious canker.

Fungal growth and activity are favored by a warm and moist environment typical of the June and July cherry harvest season in Michigan.

The distribution of the clamping and shaking forces on the limb or trunk not only determines external damage but has an appreciable effect on internal damage. Internal stresses in the bark are minimized when the minimum necessary force is transmitted over the largest possible contact area. This is a function of the pad design, clamping pressure, and shaking force.

Excessive clamping forces were found to cause crushing of the bark and internal tissues of the tree (Frahm, 1983). Vital nutrients cannot pass through the ruptured cells to the fruit, leaves, fruit bearing limbs, and roots. Upper limits on clamping pressure have been established which will avoid injury in the static nonvibratory state.

The first limb shakers oscillated in a back-and-forth linear motion. Most modern trunk shakers, however, transmit forces in epicyclic patterns such as cycloids, hypocycloids, cardioids, N-leaved roses, and spirals. The operator can adjust the pattern either by resetting the eccentric masses or stepping through a learned series of hand motions on the hydraulic motor drive controls. Cycloidal patterns require that the shaker pads conform to the tree to provide sufficient

contact area for minimized compressive, longitudinal and tangential stresses.

The physiological condition of the cambium plays an important role in bark strength. In the Spring, the cells in the cambium take in moisture, enlarge radially, and begin to divide causing the cell walls of the two newly formed cells to be thinner than the original parent cell wall (Bukovac, 1984). The cell interiors, as well as the intercellular spaces, become filled with liquid. The cambium readily breaks down at this stage when shear stress is applied and the bark slips over the wood. By Fall, when moisture, cambial activity, and cell growth have begun to decrease, the cell walls have thickened from the growth of the cellulose layers forming the wall. As the cells lose moisture to the environment and shrink, the protoplasm turns to a gel and aligns itself against the cell wall for winter insulation (Priestley, 1930). At this point, the cambial cell walls are less elastic and the intercellular spaces have also lost their liquid contents. This deactivated state (preparing for dormancy) greatly reduces the occurrence of slip (Fridley et al., 1970). This physiological condition also varies during the crop season with changes in environmental and soil conditions. The highly variable physiological activity of the tree can elude the machine operator's efforts to prevent bark damage.

1.2 Extent of Cherry Production

In 1982, Michigan ranked first in the United States in the production value of tart cherries. Sweet cherry production ranked third, with Washington and Oregon ranking first and second, respectively. This corresponded to 117,936 tonnes (260,000,000 lbs) or 83.6% of the nations tart cherries and 30,391 tonnes (67,000,000 lbs) or 21.2% of the nations sweet cherries. The State's production value totalled 26.8 million dollars for tarts and 10.9 million dollars for sweets. The 1982 Michigan tart cherry crop was the second largest since records were started in 1925.

Ninety-seven percent of all tart cherries and 92% of all sweet cherries harvested in Michigan are processed; the small remainder supplies the fresh fruit market. Tart cherries go into juice, wine, jam, and pie, while sweet cherries go into juice, jelly, ice cream, and frozen goods.

In 1982, Michigan reported 4,500,000 red tart cherry trees and 887,000 sweet cherry trees of all ages (Michigan Dept. of Agriculture, 1983b). This was a 17% increase in the number of tart cherry trees and a 9% decrease in the number of sweet cherry trees since the 1978 fruit tree survey (Michigan Dept. of Agricuture, 1979). Although tart tree numbers increased 17%, acreage increased only 14%. This was due to closer tree spacing.

Tree spacing becomes a significant factor in harvester speed, size, operating efficiency and tree damage potential.

Practically all of the tart cherry trees (99%) are of the Montmorency variety, (See Table 1.1). The sweet cherry trees are slightly dominated (31%) by the Napoleon variety. With 82% of the cherry trees in the state as tarts, the uniformity of variety throughout the state aids in design and analysis of mechanical harvest systems.

Over 98% of the Michigan cherry production occurs in the northwest, west central, and southwest districts of the lower peninsula bordering Lake Michigan. Tree ages range from 1 to 22 years or more, (See Figure 1.1). Trunk diameters of commercially harvested trees typically range from 50 mm (2 in) to 406 mm (16 in).

As the older plantings die out and become unproductive, they are replaced with young plantings. Until this occurs, however, the common practice is to replace each damaged and unproductive tree with a new tree. This creates a highly non-uniform orchard and is a significant factor contributing to tree damage when operators fail to reset shakers for different tree sizes.

1.3 Need for Shaker Analysis

Limb and trunk shakers have been used for many

Table 1.1. Michigan Cherry Tree Production by Variety (1982).

VARIETY	NUMBER OF TREES	PERCENT	NUMBER OF GROWERS	STATE HECTARES
TART	4,500,000	100.0	1,383	18,907
Montmorency	4,484,500	99.7		
Other	15,500	0.3		
SWEET	887,000	100.0	775	4,329
Napoleon	275,200	31.0		
Golds	153,500	17.3		
Schmidt	107,600	12.1		
Emperor Francis	94,300	10.6		
Hedelfingen	71,700	8.1		
Windsor	67,800	7.7		
Other	116,900	13.2		
TOTAL	5,387,000		2,158	23,236

Michigan Department of Agriculture, October, 1983a.

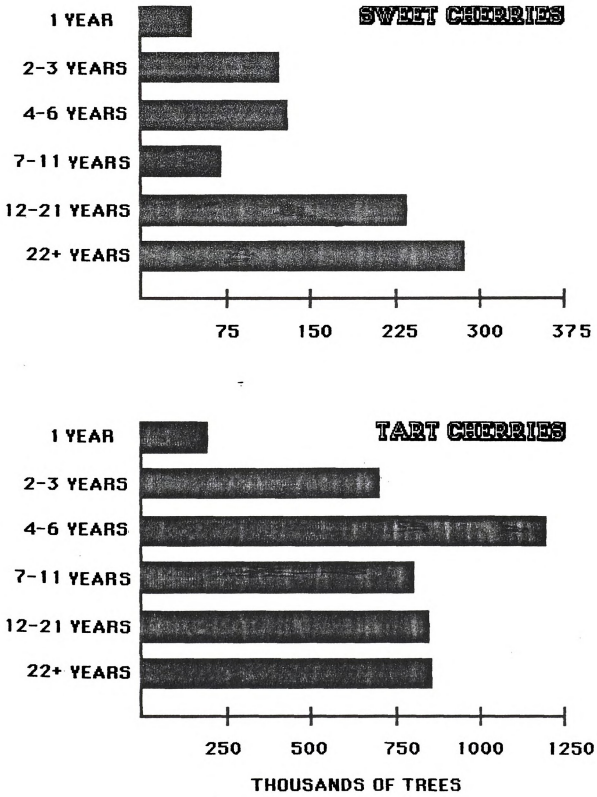

Figure 1.1 Michigan Cherry Trees by Age - 1982 Survey. (Michigan Dept. of Agriculture, 1983b)

years for the mechanized removal of fruits and nuts (Brown, 1983). Over 95% of the cherries annually harvested in Michigan are removed with mechanical shake-and-catch systems (Brown et al., 1982). The majority of these systems use trunk shakers because they provide greater speed, lower harvest cost, and minimized human effort in comparison to limb shakers.

Studies of cherry bark strength indicate that cherry bark is easier to damage than apple or peach fruit tree bark in both longitudinal and tangential directions (Diener et al., 1968). In apple and peach trees, the bark tissue is not rigidly attached to the inner tissues. This provides a tangential bark strength four times that of cherry tree bark, where the bark tissues are rigidly attached.

The force developed by the shaker must overcome the inertia of the tree and provide limb acceleration large enough to detach the fruit from the stem. This force should be transmitted to the tree without exceeding the bark strength properties. Design and operating parameters for mechanical harvesters have been determined which presumably do not damage the tree.

Static forces have been applied to tree trunks through shaker pad-clamp systems with no evidence of bark damage. After shaking, however, tree decline (defined as a reduction in yield, vigor, or total tree numbers per

orchard i.e. tree death), continues to be of great concern to growers. The static forces applied to tree bark do not adequately explain the bark damage problem. Factors that continue to be of concern as potential causes include operator error, clamping force, shaking force, carrier slip, improper shaker and clamp adjustments, improper machine maintenance, inadequate orchard maintenance, and poor choice of harvest date, harvest practice or production practice (Cargill et al., 1982). Several of these factors only occur during the actual process of tree vibration. From these causes and others, repeated machine harvesting has shortened the life of cherry orchards in Michigan (Brown, 1982, Friday, 1983). With 658,042 new tart cherry trees planted since 1978 (15% of the total number of tart cherry trees reported in 1982), the impact of harvesting equipment damage on young trees has become a particular concern. Young trees are more easily damaged than mature trees.

To pursue the causes of the bark damage problem, I decided to conduct an analysis of the real-time dynamic behavior of the tree and shaker system. The stresses which are applied to the tree trunk during mechanical shaking vary in both magnitude and direction. Previous studies of the dynamic behavior of the shaker and tree have not made estimates of these stresses possible. Measurements of the maximum displacements of the tree and

shaker body would provide information which could be used to estimate the maximum imposed stress and strain on the bark. Since the pad is composed of elastic material, relative displacements between shaker and tree act as a strong indicator of stress.

1.4 Objectives of the study

The goal of this study was to determine the relative dynamic displacements between a cherry tree trunk and the attached trunk shaker. Resulting relative displacements would be analyzed for critical maxima. The displacement data could aid in the estimation of force, stress, and strain applied to the bark during shaking, and provide new knowledge useful for the reduction of bark damage. The following specific objectives were selected to meet the need of the investigation:

1. Design a microprocessor-based data-acquisition system capable of characterizing the real-time dynamic behavior of a tree trunk with various vibratory driving forces. The accuracy of digitizing signals with such a system would be evaluated and a process selected so that the relative displacement data were representative.

2. Develop the methodology for analyzing the accelerometer data and obtaining displacement results

therefrom.

3. Determine the peak X, Y, Z and θ relative displacements between the tree and shaker at the clamp area for several driving force situations.

CHAPTER 2

LITERATURE REVIEW

Compared with other fruits, cherries are relatively small and have a short harvest season. Levin (1960) states that yield per worker is quite low when harvesting cherries, meaning long hours of slow picking. Ten times as many man-hours are required to pick a tonne of cherries as are required to pick the same amount of apples, peaches, or pears.

Manual harvesting of the cherry crop requires many migrant workers, so many that the cost of labor during harvest can amount to half the farm value of the crop (Brown, 1980). Public Law (PL) 78, commonly called the "bracero program", allowed supplementary foreign workers to enter the U.S. to meet high seasonal needs. With the termination of PL 78, growers had to choose between mechanical harvesting, switching crops or changing vocation. Recognizing the high long-term investment of orchard crops, growers looked to mechanization and discovered they could economically mechanize and supply the consumer market at lower cost than with hand labor.

Shortage and cost of hand labor, labor unrest,

final product cost to consumers, rough handling, economic risk and other economic barriers had been primary problems in managing a steady flow of produce from the field to the consumer in competitive markets, according to Drake (1983). A non-destructive, non-damaging means of mechanically harvesting fruits, specifically cherries, was sought.

Work was begun in 1956 by Levin et al. to develop a method of mechanically harvesting cherries. The first step was to study the effectiveness of separating red tart cherries from trees with hand and pole shaking methods. Detachment was accomplished by causing the fruit to oscillate until a failure of the stem at the spur or at the fruit occurred. Very little tree damage resulted with the hand and pole method. Finding this procedure unacceptable due to worker fatigue, however, hand-carried mechanical shakers were built in 1957 which hooked to individual tree limbs. These units were heavy, transferred excessive shock to the user, caused slight tree damage, and worked successfully only on the smaller limbs.

In 1958, a tractor-mounted, hydraulically-activated boom shaker, used previously on the West Coast for harvesting nut crops, was tried on sour cherries by Levin et al.. It operated at 12-17 Hz (700-1000 cpm) and used a 3.8 cm (1.5 in) stroke. It provided 95% fruit

removal in seconds with little operator fatigue. The clamp was a bear-hug style covered with rubber padding to cushion tree contact. Bark damage to limbs due to clamp slip, excessive pressure, or deviation from a 90 degree attachment angle ranged from no damage to very serious damage. Removal of sweet cherries with this same shaker caused considerable tree damage due to the violent action required to remove immature fruits for the brining market.

Adrian et al. (1963, 1965) described their attempts to transfer forces from shakers to fruit and nut trees with minimal tree damage. Metallic fasteners were placed permanently or semi-permanently into main scaffold limbs or trunks for shaker attachment. This permitted direct transfer of force to the structural wood rather than through the vulnerable bark and growing tissues. After repeated occurrences of fastener bending, breakage, withdrawal and limb splitting, Adrian et al. concluded that direct clamping of a shaker to a tree through a cushioning pad was the most efficient method of trunk or limb attachment.

When mechanical harvesting was adopted in Michigan in the 1960's, drastic modification of tree structure was necessary for efficient harvesting. Large scaffold limbs trained low to the ground for hand harvesting were eliminated leaving only three or four main scaffolds. Willowy branches were pruned to improve fruit

removal by eliminating the damping effect of a long branch. Newer, younger orchards were trained for mechanical harvesters, too.

Harvester design also changed through the 1960's. Small limb shakers with little power yielded to large trunk shakers with greater forces and redesigned clamps and pads. Larger stresses, varying in magnitude and direction (i.e. radial-compressive, tangential, longitudinal) were imposed on the tree, Figure 2.1.

Mechanical harvesting of cherries is presently accomplished by securely attaching the shaking mechanism to a single limb or trunk through a thick rubber pad to transmit the energy into the tree system for fruit detachment, Figure 2.2. Mechanically harvested fruits are most often used for processing. Tennes and Brown (1981) have noted that conventional low density orchards of 75 to 200 trees/ha are presently being harvested at acceptable rates with these stop-and-go shaker harvester systems. Higher density plantings (200-400 trees/ha) may have lower yield per tree, and therefore require higher speeds for equivalent volume per unit time. Continuously-moving harvesting systems are being developed for these high density orchards (Peterson and Monroe, 1977, Peterson, 1984). Trunk shakers with self-propelled catching frames can harvest 60-120 cherry trees per hour. Thanks to mechanization over the last 20 years, 65 man-hours per

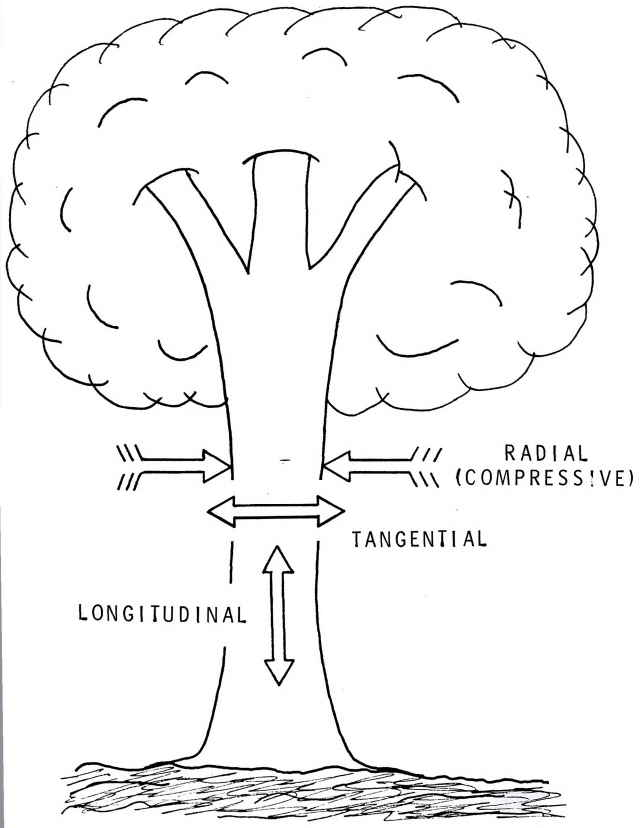

Figure 2.1 Possible stress directions when using trunk shaker harvesters.

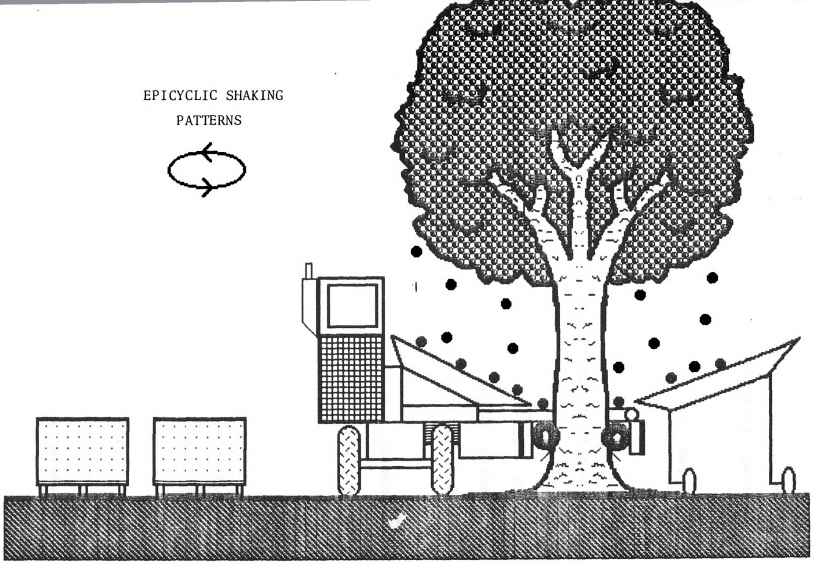

Figure 2.2 Two piece trunk shaker harvester for cherries.

hectare of hand picking have been reduced to 4 and 8 man-hours per hectare to mechanically harvest tart and sweet cherries, respectively.

Labor shortage and costs in New South Wales prompted Hutton and Brown (1981) to attempt to mechanically harvest cherries, peaches, plums, pears, apples and apricots in the orchards of the Murrumbidgee Irrigation areas with the new trunk shakers. Harvesting proved satisfactory in most crops. Cherries were harvested for the fresh and canning markets but fresh market harvesting proved feasible only on dark colored, firm fleshed varieties.

Mechanical harvesters are common in most commercial orchards for reasons of speed and economy. Brown et al. (1982) reports that 95% of the sweet and sour cherry trees in Michigan in 1982 were harvested mechanically. According to the Michigan Department of Agriculture (1982), this amounts to 5,118,000 trees of bearing age. Reports by growers have indicated that orchards of all ages are showing signs of tree deterioration (Brown, 1982, Friday, 1983).

The negative impact of tree decline in the fruit industry, particularly cherries, has prompted current efforts to determine and eliminate the causal factors. Cherry trees have a long productive life exceeding 50 years; bark damage can shorten the life of a tree by 10

years or more.

Tree damage, as analyzed by Cargill et al. (1982), occurs in three forms: 1) damage to the bark at the point of shaker attachment, 2) breakage of large stiff limbs and, 3) breakage of small branches or detachment of leaves and other new, young growth. The authors list 19 possible factors that can result in bark damage on trees. These causes, exacerbated by repeated machine use, may shorten the productive lives of cherry trees and orchards.

Brown et al. (1982) noted that untrained operators are often unaware of the damage caused by their machines. The separation of the bark from the wood at the cambial zone is often externally invisible to these operators, yet later can provide an ideal environment for disease organisms and insects. Unattended tree damage, combined with adverse winter weather, insect and disease attack, poor nutrient supply from the soil, improper use of growth regulators or poor irrigation practices, can cause an orchard to decline quite rapidly.

2.1 General Causes of Bark Damage

Bark damage is easily recognized when conditions exist that cause stripping, cracking or wetting of the bark at the trunk or limb of the tree. Often, however, conditions only cause a slight cracking or internal

separating of the bark from the wood at the cambium, Figure 2.3. This lesser injury is not apparent to the untrained machine operator and thus, goes unnoticed and uncorrected. The influence of disease, weather, insects and obstructions of nutrient flow with time in the damaged area add up to a major problem of total tree decline (Figure 2.4).

Diener et al. (1968) studied damage problems and found that the amount of bark damage inflicted on a limb or trunk is determined by the bark properties, the radius of the limb or trunk, and the resistive forces of the shaken object.

Fridley and Adrian (1960) attempted to determine the power and optimum frequency of vibration in fruit removal with minimal tree damage. One possibility was to vibrate the tree at the natural frequency of the fruit. Combinations of frequency and displacement that cause instability at the point of fruit suspension, however, were difficult to transmit through the branched tree system due to colliding limbs and damping by leaves. Collision of fruit and limbs when the shaker frequency reached the natural frequency of a limb could cause damage to tree and fruit.

The other possibility was to vibrate the tree at one of the natural frequencies of the tree. The selection of the proper natural frequency was dependent on the

Figure 2.3 Tart cherry tree trunk six months after trunk shaker harvesting. - No apparent evidence of bark damage.

Figure 2.4 Tart cherry tree trunk 18 months after trunk shaker harvesting. Obvious tree decline from uncorrected bark damage.

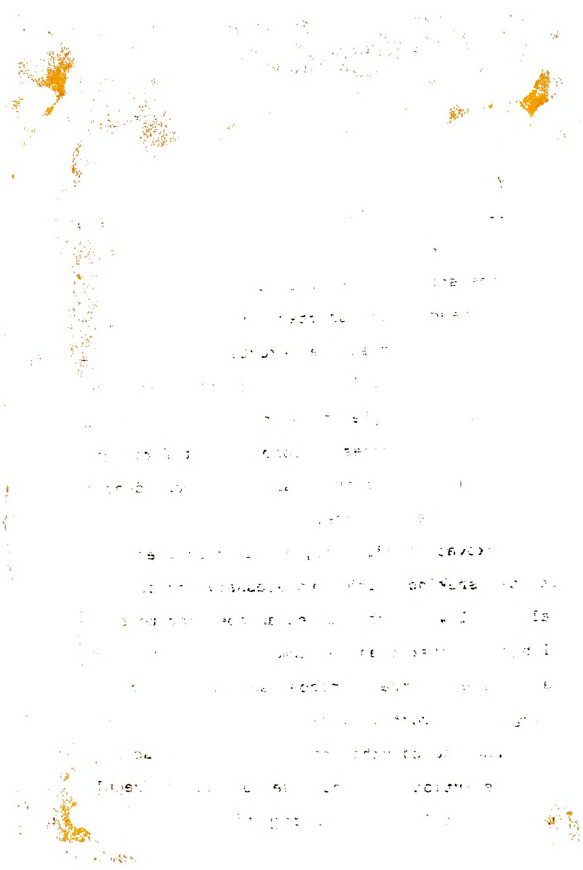

stroke needed to remove the fruit at that frequency, the power required and the resulting tree and fruit damage. Power was needed to remove a volume of fruit with long strokes and low frequency; increase of either stroke or frequency, however, caused an increase in tree damage, though stroke was the major determinant. Placing the clamp at an anti-node for a given natural frequency allowed the stroke to reach a maximum for that frequency. Higher frequency with shorter strokes resulted in minimum damage. A force must be exerted perpendicular to the trunk or limb to minimize damage and power required, for as the included angle between the shaker and the object deviated from 90 degrees, a component of force parallel to the trunk or limb induced shear and was identified as a direct cause of bark damage.

Bukovac (1983) suggested that tree decline is a result of shaking with "unnecessary force" when fruit removal is low which causes an operator to shake harder and longer. Other than the common damage at clamp points, Bukovac believes that improper shaker usage may result in "breaking of roots, interfering with the conduction systems, and doing other harm which is not so apparent". Bukovac's solution is the use of plant regulators to loosen fruit and get high crop yields without stressing the trees and causing premature death to orchards.

Beljakov et al. (1979) studied the effects of

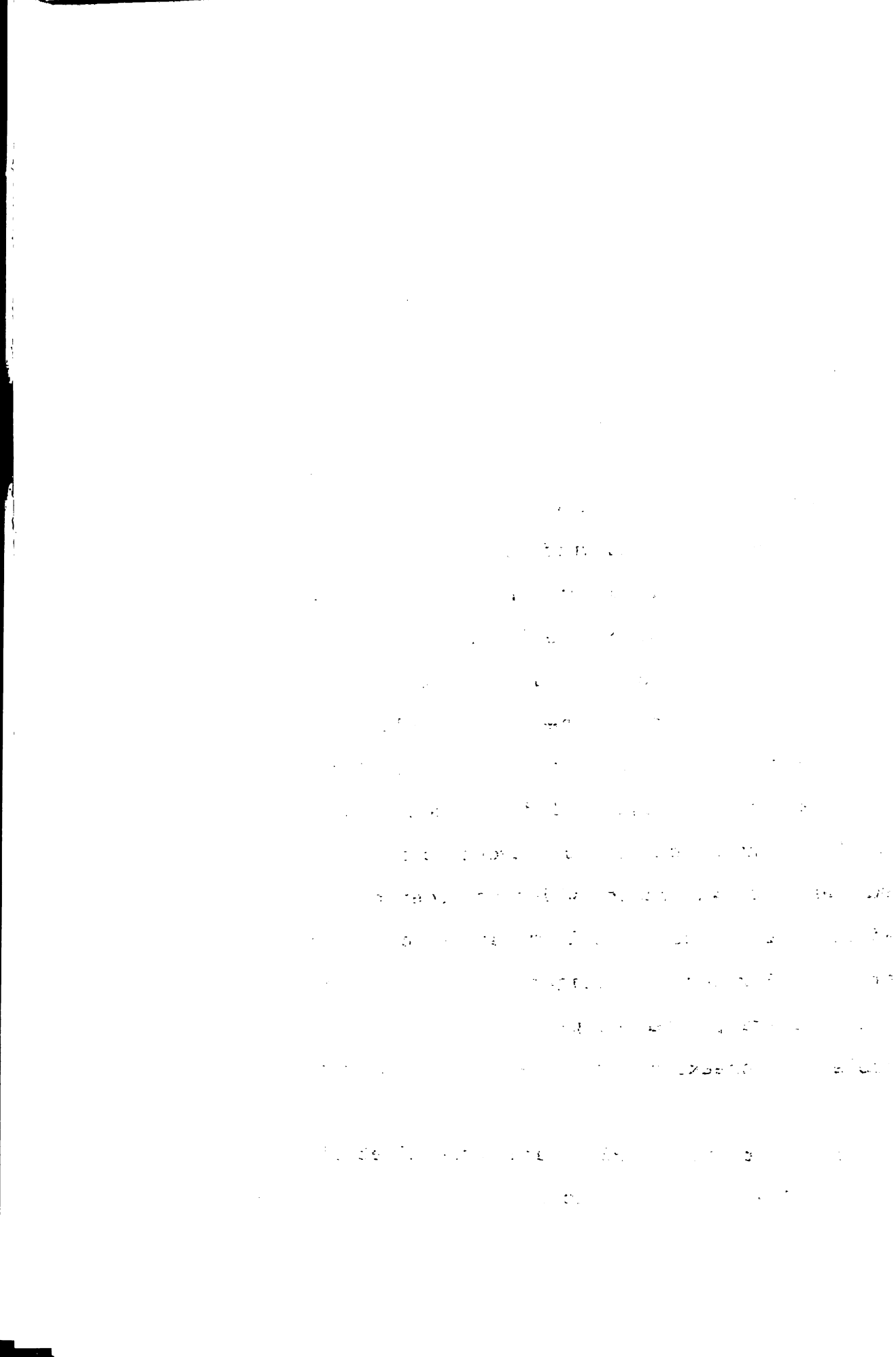

shaker harvest on the root systems of sweet and sour cherries, peaches and plums. The exciting force was developed by an eccentric mass trunk shaker, clamped 20 cm (7.9 in) above the earth and operated at 15-18 hz with 2.4-3.0 cm (1.0-1.2 in) strokes. A radioactive tracer, P-32, was injected into the soil and along with C-14, was applied to leaves to study photosynthetic activity. Results indicated that there was no adverse effect on tree growth, and only an insignificant number of roots were severed (less than 0.05% of the roots by weight of diameter 0.1 cm (0.04 in) or smaller).

Heavy wind and rainfall in August and September of 1979 blew over or loosened many 7.6-12.7 cm (3-5 in) diameter peach trees in Northern Virginia. The following Spring, trees grew poorly, failed to produce normal leaves and died. Investigation by Lyons and Yoder (1981) revealed dead crown roots which had been broken by wind and killed by excess soil moisture or pathenogenic infestation. Further investigation found poorly anchored trees, in general, had deeper crown roots and were more susceptable to breakage by external attack from wind or shaking.

Brown et al. (1982) and Cargill et al. (1982) made direct field observations and classified ten general causes behind the bark damage problem as follows:

1. Operator error and inadequate operator

training (Operators, due to a lack of time or training constraints, may not follow recommended procedures to minimize bark damage).

2. Improper shaker adjustment.
3. Improper clamp adjustment and maintenance.
4. Improper shaker clamp attachment.
5. Poor judgement in selection of a machine for young trees and/or failure to adjust existing machines for tree size.
6. High cambial activity at harvest due to excessive irrigation, rainfall, or physiological activity.
7. Immature fruit requiring an excessive force for removal (this tempts the operator to overshake for satisfactory fruit removal).
8. Improper machine design.
9. Settling or moving of the shaker due to soft soil conditions or excessive side hill slope.
10. Improperly pruned trees requiring excessively long shaking cycles.

The critical concept is the transmission of the proper force to a tree to remove fruit, but to do so without harming the living tissues of the tree. This is a

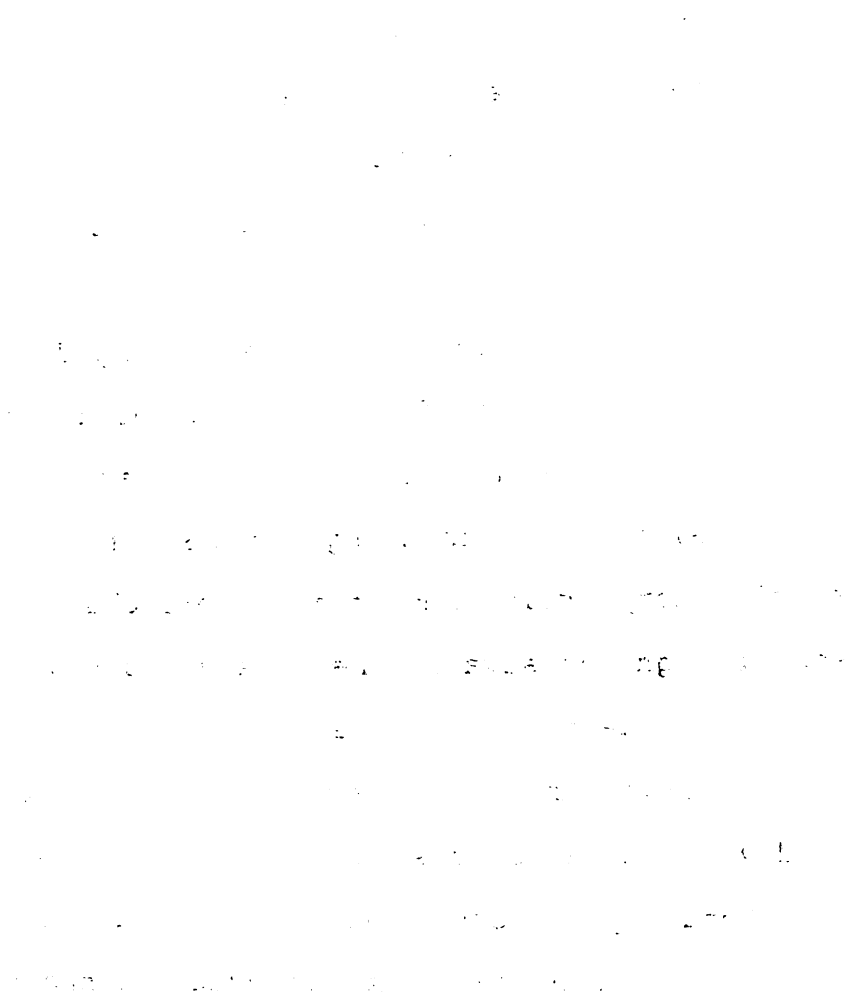

difficult task for, as Brown et al. (1982) noted, bark and cambium damage on cherry trees will occur at lower stress levels than on other fruit trees.

2.2 Harvester Factors in Bark Damage

Halderson (1966) suggests that damage to trees occurs in three forms: a) physical injury by the shaker, b) trunk injury by positioning catching frames or shaker and, c) root damage from tree vibration. In field experiments, all movement of the roots ceased approximately 15.2 cm (6 in) below the soil surface and did not appear to be a major problem. Bark damage by attachments was minimized with good clamp design. Level ground, providing perpendicular attachment to the tree, was considered such an important factor as to necessitate leveling devices on catching frames and harvesters. Tangential clamp slip and twist were observed to cause problems, though not always immediately apparent.

Many details of tree and fruit response to mechanical harvesting have yet to be resolved. Gentry (1980) developed a citrus harvester in 1978 to harvest lemons. Rotating masses totalling 114 kg (250 lbs) were rotated up to 5 Hz (300 cpm) in order to shake trees up to 40 cm (16 in) in diameter. The shaker mechanism weighed 565 kg (1245 lbs) and was attached at a height of 36 cm to 1 m (14-40 in) above the tree base. After

repeatedly running into the skinned trunk problem on lemon trees, Gentry switched to grapefruit, finding less damage after shaking due to a tougher bark. Without explanation, however, in three consecutive years, Gentry's grapefruit harvest steadily increased and tree appearance improved when using the mechanical shaker.

Tennes and Brown (1981) developed a sway bar shaker for the continuous harvest of horticultural tree crops. A pair of horizontal bars was pivoted at the front end of the harvester and was powered at the back end by two synchronized rotating eccentric masses. A roller assembly was mounted along each bar to eliminate sliding motion between the bark and the contact surface of the bars. The entire harvester was found to move 3-6 cm (1-2 in) during each cycle of the sway bar. Bark damage to the central leader of apple trees was still observed to be a problem; the putative cause of bark failure was the shearing impact discussed by Fridley et al. (1970). A solution to prevent bark damage was needed before a shaker of this design would become practical.

In 1982, Helden removed fruit from Valencia and Hamlin orange trees with two shakers, one providing a linear motion and the other being a multidirectional shaker. Average shaken tree diameter was 16.2 cm (6.4 in). Static clamping pressures were 6.5 kg/cm^2 (93 psi) for the linear shaker and 12.4 kg/cm^2 (176 psi)

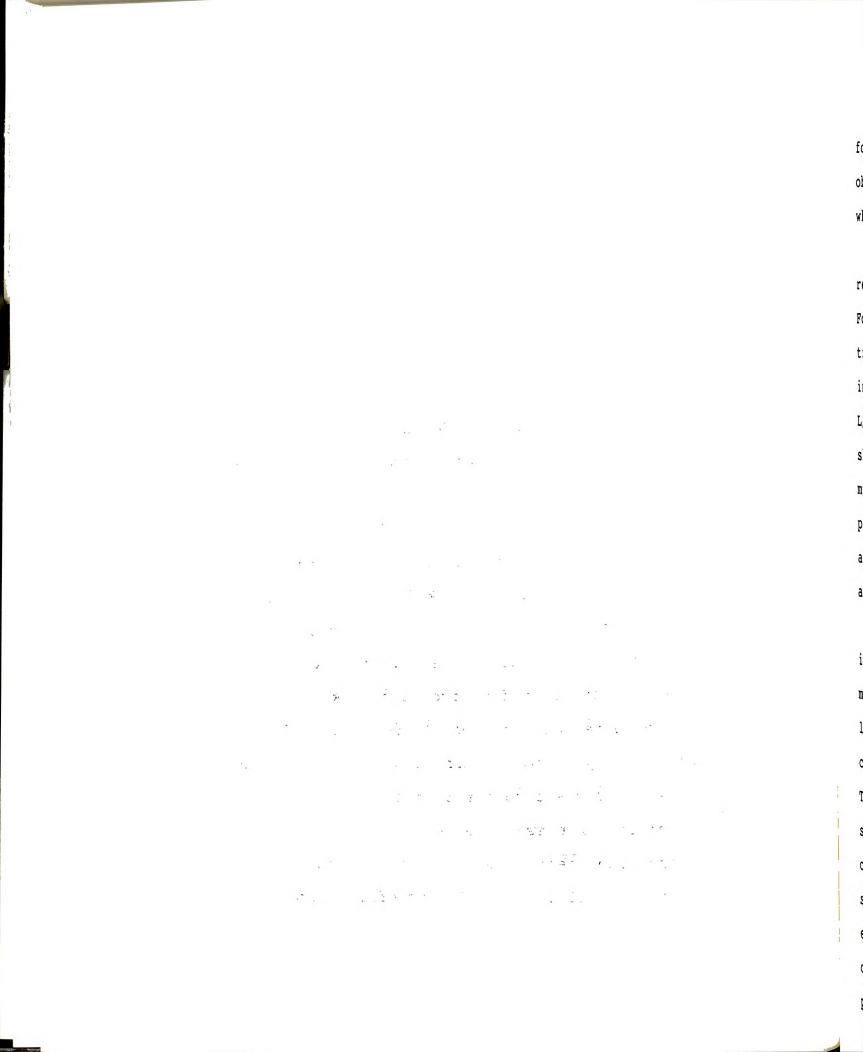

for the multidirectional shaker. Minimal bark damage was observed in all tests, even for the Valencia orange trees which are in a growth state at the time of harvest.

Millier et al. (1983) developed and tested a recoil impact shaker for fruit removal from apple trees. Force was applied in a single linear direction at the trunk of the tree. Four displacement cycles were applied in 30 s with a 141 kg/cm^2 (2000 psi) pressure at a 30 L/m (8 gpm) flow rate. Tests showed that the linear shaker performed better on Y-shaped trees than did a multidirectional shaker, easily removing fruit on limbs parallel to the applied force, but requiring violent action to remove fruit on limbs perpendicular to the applied force. No obvious trunk damage occurred.

The general design of some shakers naturally induces damage to the shaken tree. Counter-rotating masses are usually offset from the shaker clamp so as to locate the center of rotation of the shaking force several centimeters away from the center of gravity of the tree. This offset induces a torque as the shaker moves through a select pattern because the center of force is at a point other than the center of gravity of the tree. As the shaking occurs, different twisting effects are induced and energy is applied to the shaker mounts and carrier. Part of the input energy goes into friction as the tree and pads attempt to resist the torque. A lubricated flap

between the pad and tree reduces the shear and torque transmitted to the bark. Shear may also be reduced by increasing the pad contact area. The pressure on the bark is reduced as a fixed applied force is transmitted through a larger and larger bark contact area.

Many other studies conducted on mechanical fruit harvesters have reported that bark damage can be serious in some cases. Conditions under which shaking is performed such as weather, environment, soil, terrain, labor, cultivation practice, tree type or variety, or machine are seldom the same; hence, pinpointing the most likely common causes of tree damage and decline has been difficult. In 1982, Brown et al. expanded their general observations of bark damage in order to isolate specific operator and machine inaccurracies that may account for the observed tree damage. The list of critical points included:

1. Failure to center the clamp on the trunk.
2. Clamping too firmly to the tree causing excessive radial stress, hence, crushing and splitting of the bark.
3. Clamping too loosely during shaking where the pads tend to scuff and tear the bark (tangential shear).
4. Clamp pads not slipping internally due to the wrong pad design or improper lubrication

of slip surfaces causing high shear forces (e.g. pads becoming heated, sticking together, inducing shear force and deteriorating).

5. Excessive eccentric mass setting causing excessive tree displacement and bark strain.
6. Excessive power applied to small trees.
7. Shaker "gallop" during startup and stop (causing torque (shear) in the bark).
8. Settling of the shaker carrier into the earth during shaking (causing excessive longitudinal shear).
9. Shaking forces not perpendicular to the trunk (causing longitudinal shear).
10. Clamping too low to the ground where trunk is most rigid (causing excessive forces to be applied to the trunk).
11. Clamp pads too small or firm causing high stress in the bark due to a small contact area.
12. Longitudinal shear caused by clamping to a leaning trunk.
13. Longitudinal shear caused if shaker is tilted when clamping to trunk.

The above list of causal factors fell into three main categories:

1) Operator error during shake and clamp,

2) Improper pad design, and

3) Improper machine design or setting.

Little damage can be blamed on a well-trained, well-informed and experienced operator. Shaker pads have been studied in a static state and will be discussed in the succeeding sections. Machine design and selection of operating settings require knowledge of static and dynamic biological tree tolerances, as well as the dynamic reaction of shaker pads to force transmission. Little work has been done to define the dynamic reaction of the pads and bark because of the lack of practical measurement and analysis technologies.

2.3 Bark Structure

Diener et al. (1968) describe the structure of cherry bark as having a thin, nonliving outer periderm, a large, spongy, nonfunctioning phloem in the center and a thin, functioning phloem next to the cambium. The directional strength properties of cherry bark can be accounted for from the alignment of the constituent cells. Phloem cells have their long axis in a longitudinal (vertical on the trunk) direction, whereas periderm cells have their long axis in the tangential (horizontal on the trunk) direction. The periderm consists of thin-walled dead cells encrusted with waxes which lubricate the dead

tissue and allow slippage between cells (Esau, 1965).

When the bark is damaged so that it separates from the wood (xylem) of the tree, the flow of fluids containing the essential life sustaining elements is interrupted in that area. Usually, hairline cracks are formed in the bark tissue, through which air enters and oxidizes the cambial tissues so that they appear brown (Adrian et al. 1965). Devay et al. (1962) notes that these damaged areas are open invitations for insects and disease, especially tree canker, a gummosis disease caused by the fungus Ceratocystis fimbriata, evidenced in the fruit orchards of California. The fungus, C. fimbriata infects bruised bark tissue, gradually spreading to healthy surrounding tissue, slowly causing tree death. A depression in the infected tissues, accompanied by the production of an orange frothy gum, characterizes the canker attack (Devay, 1960).

In 1960, Devay et al. reported increasing incidence of canker in California almond orchards as a result of fungus attack in damaged bark areas caused by mallets and mechanical shakers. The cause of the spread of the fungus is not primarily a search for nutrients but rather to escape its own lethal environment of dead bark cells and tissues. Hence, the live fungi are only found at the canker margin. The fungus expansion occurs all year, but is most rapid in the warm and moist months. In

19
mo
de
in
th
su
Fu
fr
wo
tr
bas
obv
ind
of
myc
thu
occ
par
(19
alm
whi
fac

1965, Devay et al. discovered that extremes in bark moisture do not greatly affect fungus growth (canker development) but that soil moisture plays a primary role in the spread of the fungus by insects from tree to tree; the spread is most pronounced when soil moisture is high such as within the first few weeks after irrigation. Fungus development is particularly pronounced on stone fruit trees that are irrigated 1-2 weeks before injury. A wound dressing (Cerano) was successfully developed to treat canker wounds in almond and plum trees.

Damage by a powerful trunk shaker affects the base structure of the entire tree. Damage to the trunk is obviously much more critical than damage caused to individual scaffold limbs by limb shakers. Continued use of shakers in diseased orchards can spread spores and mycelial fragments to bruised tissues of healthy trees, thus propagating tree cankers. Death of injured trees can occur within a few years.

2.4 Bark Strength

Bark strength was studied to develop design parameters for mechanical harvest systems. Fridley et al. (1970) studied the bark strength of prune, peach, apricot, almond, and olive trees. They reported that the stress which bark can withstand is directly related to seasonal factors such as moisture content and cambial activity.

When moisture content or cambial activity is high, the bark slips easily and bark strength is low. "Slip", as defined by Cargill et al. (1982), is the separation of bark from the wood at the cambium zone. Slip occurs mainly in the Spring when cells are enlarging radially and dividing. Cell contents change from a solid to a liquid consistency. The walls of cells at this time of year are not as thick due to continuous cell division (Bukovac, 1984). Therefore, cells tend to break easily and the bark slips.

In the Fall, cambial activity ceases, cell walls thicken as moisture content drops in the bark and cambium, and slip does not occur because of the toughened fibers. Shear strength of cherry bark decreases as cells are ruptured by excessive radial forces.

Directional strength properties of the periderm layer were opposite to that of the bark of cherry according to Diener et al. (1968). Periderm strength was highest in the tangential direction, parallel to the long axis of the constituent cells. The periderm exhibited five or six times the tangential elongation before rupture as did the phloem. The important fact here is that tangential shear stress or strain from shaker torsion or clamp pressure can cause the phloem underneath the periderm to rupture without rupturing the periderm itself, therefore the phloem damage can be concealed.

Phloem strength was greatest in the direction parallel to the long axis of its cells, the longitudinal direction, and weakest in the tangential direction. Results indicated that cherry bark would typically have a tangential strength of approximately 420 N (95 lb) per inch of width rather than 110 N (25 lb) if the cherry periderm was not attached to the bark. Rupture due to elongation of cherry phloem and periderm was found to be quite dependent on direction; this is opposite the response of peach and apple bark.

Failure of bark cells in the longitudinal direction was found to occur from incremental fiber and tissue rupture, accompanied by sliding and continued failure. Bark behaved as a viscoelastic material until yield occurred. Failure at the cell borders with tangential loading took place at very low forces; in tangential loading, a force was applied perpendicular to the long axis of the cells. On a curved surface, bark tended to realign its tissues in the direction of the applied force. The amount of stress absorbed increased slightly with time until rupture.

Sweet cherry bark is about twice as easy to damage as tart cherry bark on equal diameter trees. Young cherry bark (up to 8 cm trunk diameter) damages more easily than bark of older trees. Brown et al. (1982) demonstrated that compressive failure in the cambium of

sweet cherries occurred at surface pressures on the bark above 10.5 kg/cm^2 (150 psi). Sour cherry compressive failure was evident above 24.6 kg/cm^2 (350 psi). Compressive tests showed that cherry bark ruptures completely at 84.4 kg/cm^2 (1200 psi). Pressures of 10.5 kg/cm^2 (150 psi) and 24.6 kg/cm^2 (350 psi) for sweet and sour cherry, respectively, were accepted as clamping pressure limits. The pressure limits can vary from these values subject to moisture content and cambial activity.

Shear strength for sweet cherry bark was also lower than for sour cherry. Average cherry cambial shear strength was suggested by Brown et al. (1982) to be only 4-7 kg/cm^2 (60-100 psi). Sweet cherry bark shear strength decreased as moisture content increased but this trend was not convincing for tart cherry bark. The shear strength increased as clamping pressure increased, apparently due to friction. According to Adrian et al. (1965b), tangential shear failure in fruit and nut trees occurred only with complete bark failure and at significantly lower stress levels than those which caused cambium browning following compression. Dynamic stress in tests by Adrian et al. (1965b) was only 75% of static stress and still caused cambium browning. This would indicate that acceptable static clamping pressures may be much too high to prevent tree damage in a dynamic

(shaking) state. Radial design stress was limited to 17.6 kg/cm^2 (250 psi). Tangential stress was limited to 7.0 kg/cm^2 (100 psi) to prevent tissue injury in prunes, peaches, almonds, olives, and apricots.

Fridley et al. (1970) used cambium browning as an indicator of radial stress failure. Browning increased with increasing pressure. The inner bark appeared porous and degenerated when browning occurred. Radial stress of 70.3 kg/cm^2 (1000 psi) visibly cracked bark to the cambium in 20-year-old prune trees, with subsequent occurrences of C. fimbriata canker. Cracking and canker in six-year-old trees occurred at 75% of these stress values.

As radial stress increased, strength decreased at high moisture content but increased at low moisture content. Bark was found to withstand three or four times the radial stress (compression) as longitudinal or tangential stress (shear). Fridley et al. (1970) found that the inner bark (phloem) of prune trees resisted the longitudinal loading while the outer bark (periderm) resisted tangential loading. Outer bark failed at 10% of the ultimate longitudinal tension making a clean break. Inner bark failed similarly under small tangential loads.

Fridley et al. (1970) demonstrated that a primary factor in bark injury is the application of forces having either a tangential or longitudinal component with the

limb. Field tests of total tangential shear stress showed that injury and infection occurred only when bark failed completely. Shear failure at the cambium and tensile failure at the bark combined to cause injury with the tensile failure occurring both perpendicular and longitudinal to the bark fibers. Results showed that tangential shear strength was 50-70% of total tangential strength. Low shear strength occurred at high moisture while high shear strength occurred at low moisture. As moisture increased, the presence of radial stress became less effective in preventing longitudinal shear failure. This demonstrates the importance of avoiding irrigation near harvest if bark damage prevention is desired. Since slip depends on moisture content, irrigation and rainfall during periods of rapid growth will reduce bark strength. The harvesting of Michigan cherries in June and July makes this crop more susceptible than most other fruit trees.

Bark strength varies from location to location, depending on climate, soil type and practices of production. The susceptibility of young trees makes these factors a particular concern when looking at methods of reducing damage. Excessive clamping pressure and shear forces can combine to increase the likelihood of bark damage when moisture content is high.

2.5 Shaker Pads

Forces are transmitted from the shaker body to the tree through a pad which acts as cushion, damper, and spring. Minimum stress occurs in the bark when the required vibrational energy is transmitted over the largest possible area. Longitudinal and tangential forces from the epicyclic shaking patterns must be efficiently communicated to the tree by means of a pad that conforms well to the tree structure. The pad must be firm enough to transmit shaking energy without pad slip, but not such that compression and splitting result. Scouring of the bark or excessive shear stress may result if pad contact area or clamping pressure are insufficient. During shaking, these inefficiencies may be observed as slipping action (tangential or longitudinal) or beating action (radial). If contact area is sufficent, but clamping pressure is too great, the bark may be crushed or split. As clamping pressure is increased, shaker pads become stiffer (smaller pad deflection per force increment) and a harder shake is imposed on the tree. Excessive torque may arise during shaking if clamping pressure is very high, because the pad is unable to internally flex or slip. Until recently, pad design has been a trial-and-error process. The use of a poorly designed pad would likely cause bark damage regardless of attempts to control other damage factors during shake harvesting.

Methods of pad construction have included a round hollow tube, bags filled with sand or ground nutshells, solid rubber pads with small holes drilled parallel to the tree trunk axis, preformed clamp jaws and rubber pads, and other conforming materials.

In 1982, Brown et al. made preliminary tests of C-clamp shaker pads for contact area and peak contact pressure at the manufacturer's recommended hydraulic circuit clamping pressures. This hydraulic pressure range was assumed to cover the unknown peak pressures between the pad and the tree during shaking. They found peak pressures between the pad and bark of 23.9 kg/cm^2 (340 psi), 35.2 kg/cm^2 (500 psi), and 42.2 kg/cm^2 (600 psi) on an 11 cm (4.5 in) diameter trunk (actually an instrumented steel pipe). This suggests that certain recommended clamping pressures may be excessive and cause compressive failure of high moisture cambium for both sweet and sour cherries, as well as, splitting of the inner bark in sweet cherries. Failure of the cambium from compressive stress (radial) was initiated at lower clamping pressure on sweet cherry 10.2 kg/cm^2 (145 psi) than on tart cherry 23.5 kg/cm^2 (335 psi). Brown also states that "Peak contact pressures higher than observed in these stationary tests certainly occur during shaking, but we have not progressed to the point of estimating dynamic pressures".

Frahm et al. (1983) evaluated four commercial trunk shaker pads for peak bark pressure, bark contact area and pad stiffness. Pad pressure patterns are not uniform and differ for each manufacturer. If a peak bark pressure of 21.1 kg/cm^2 (300 psi) was not exceeded, when bark contact area and pad stiffness were adequate, the pads were judged to be safe. This pressure presumably would not cause compressive failure in sour cherry tree bark, which exhibited an average ultimate compressive strength of 24.6 kg/cm^2 (350 psi) and it would cause only minimal damage in sweet cherries, with a corresponding strength of 10.5 kg/cm^2 (150 psi). Results showed that recommended manufacturer's clamping pressures on all pads developed peak pressures exceeding the estimated 21.1 kg/cm^2 (300 psi) limit, indicating that all tested pads could potentially cause bark damage.

Reduced clamping pressures which would limit the peak pressure under the pads to 21.1 kg/cm^2 (300 psi) were identified. This procedure was possible on some pads but resulted in insufficient contact area on others.

The Friday Tractor Co. (1982) has developed a "tri-clamp" composed of three pads contacting areas of a tree trunk 120 degrees apart to completely surround the tree. An eccentric rotating mass was centered in line on each side of the tree to provide a center of gravity of the masses at the center of gravity of the tree. This

design provided a complete wrap of the pads around the tree for no-slip and presumably directed all forces through the center of gravity of the tree to prevent torque damage. A firmer grip on the tree was the result.

2.6 Tree Response

Kronenberg (1964) studied the effects of fruit detachment forces in attempting to mechanically harvest cherries. He found the detachment force decreased as the fruit ripened. The difference between the force ten days before harvest and that on the traditional picking day varied with the equation:

$$Y = -48X + 428$$

Where X = 9 - Number of Days before Harvest

Y = Grams Force

Unripe cherries came off with stems, whereas ripe cherries did not. With careful shaking, healthy leaves would not come off with mature fruit. This suggests that cherries might be harvested selectively and should first be harvested 4-7 days prior to the traditional picking day.

Halderson (1966) studied the relationship between percentage of cherry fruit removal and elapsed shaking time. He found that long shaking time was required for over 85% removal when fruit was immature, but little

shaking time was required when fruit was mature. The rate of fruit removal was determined mainly by the shaking frequency. Eighty-five percent removal was obtained in 2 s of shake with 95% removal after 8 s at a frequency of 16 Hz (950 cpm). A frequency of 13 Hz (800 cpm) was determined to be a minimum for adequate removal. A maximum stroke of 1.9 cm (.75 in) was adequate at frequencies of 17 Hz (1000 cpm). Using this setting, the fruit fell straight to the ground (no whipping action).

Tests by Adrian and Fridley (1958) indicated that fruit removal was affected by applied acceleration and the number of hangers (limber fruit-bearing branches) in a given tree, as well as, the frequency and stroke of shake. More fruit were removed on rigid trees than on trees with an abundance of hangers; breakage of limbs increased with increasing stroke. Minimum damage occurred between 12-15 Hz (700-900 cpm).

Studies by Fridley and Adrian (1960) showed minimum force and power were needed to vibrate a tree when clamping was at an anti-node and shaking speed was at a natural frequency. The first resonant frequency of a vibrating cherry tree is very low (e.g. 50 cpm) (Halderson, 1966). Less power was needed with larger strokes and lower frequencies although tree and fruit damage increased. Clamping closer to a tree trunk and increasing the trunk or limb size each increased the power

and force requirements.

According to Cargill et al. (1982) the force and power when shaking fruit trees vary with frequency, stroke, shaker design, clamp position on the tree, diameter of the tree trunk, tree species, tree yield and fruit stem detachment strength. Power for increasing trunk displacement is proportional to the square of the ratio of the increased displacement to the original displacement. Power required to increase frequency varies as the cube of the frequency. The proper frequency and stroke required for adequate fruit removal depend on the type of fruit and maturity level.

In 1976, Alder et al. investigated the effect of the applied frequency and the point-of-force application on resultant amplitudes at the points of fruit suspension and at the zone of force application on orange trees. Vibrations that developed at these points were described by harmonic displacements. The tree system, when excited by a shaker, went from a transient-state to a steady-state and back to a transient-state during a shaking test. The vibration amplitudes in a shaken branch at points of fruit suspension were found to increase as the force application point was moved further from the main branching point. If a constant force was applied, then the momentum transferred to nearby branches through the joint link remained constant as the application point was moved.

Vibration amplitudes at points of fruit suspension remained the same with and without attached fruit.

Except at very low frequencies or very low amplitudes, changing applied frequency and amplitude had little effect on cherry fruit removal unless the combination resulted in a change in acceleration (Bruhn, 1969). Frequencies of 16-20 Hz (1000-1200 cpm) with a stroke of 3.8 cm (1.5 in) provided adequate removal of tart cherries. Accelerations at outer portions of a tree exceeded those applied to the trunk or base limb in all cases. Bruhn's conclusion was confirmed by Tennes et al. (1981) in later tests of a sway bar shaker for over-the-row harvesting of apples. The magnitudes of acceleration on apple trees increased proportionally with the frequency and the distance from the point-of-force application.

Yung and Fridley (1975) developed three special elements that mathematically described the components of a general hanging fruit tree system. Elements were standard geometric shapes assumed to be elastic, homogeneous, and isotropic. The tree system was assumed to be made up of: a) a tree structure consisting of trunk, secondary branches and hanger branches; b) fruits and stems, and; c) leaves and twigs. The three elements were incorporated into a finite element analysis of several tree models to accurately predict tree response to free and forced

vibration.

Yamamoto (1979) investigated the response of total limb-branch systems of cherry and oak trees. He studied the natural frequency of each branch of the system from limb excitation and analyzed the resultant oscillatory wave through a range of frequencies. He found that the fruit became injured when the main branch system in a limb was excited at the first resonant mode. The fruit and twigs at the fruit zone responded in an unstable fashion as the amplitudes of branch tops magnified considerably. Resonance of two branches adjacent to one another occurred in cases where a phase angle of 3.14 radians was present between the motions. If the natural frequency of one branch differed from the other, the two branches could collide and break, damaging the tree. Finally, when the first resonant mode of a main limb occurred, almost all branches on it were moving in linear paths with large amplitudes, parallel to the exciting direction. When the frequency was such that the small branches on the limb were resonant from exciting frequencies of 4-8 Hz, the trajectory of each branch became an ellipse or circle which had components perpendicular to the exciting force. He concluded that the elliptical pattern effectively detached fruit but it may have induced undesirable reaction forces at the force application point.

Vibrations can be transferred to a tree via a number of shaker patterns. On some machines, patterns can be preset, while on other machines there is an undefined pattern which continuously changes with each movement of the controls by the operator. The common patterns listed by one manufacturer are shown in Figure 2.5. With inadequate clamping force, force transmission in many of these patterns may induce reactive forces in undesirable directions causing radial stress, shear stress, or vertical slip of the machine or carrier. Often, shaker force and pattern are not independently adjustable. Shaker patterns that present only a few strokes per complete cycle of a pattern (i.e. a 3-leaved rose presents three strokes per pattern cycle) deliver a lower frequency shake to the tree at a given power setting than a pattern that produces many effective strokes per pattern cycle. Increasing the frequency of the few stroke pattern requires a higher rpm of shaker masses and more power. Higher shaker mass rpm requires a higher hydraulic system pressure, and on some machines may result in excessive clamping pressure where the clamp and shaker motor circuits are interconnected.

2.7 Suggestions for Reducing Bark Damage

Adrian et al. (1962) found that a linear shaker which would apply force to the tree in line with the

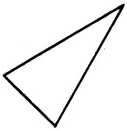

TRIANGLE
(Cycloidal)

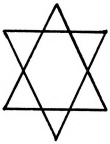

DUAL TRIANGLE
(Cycloidal)

THINNING
(Hypocycloidal)

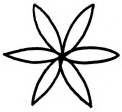

STAR
(6-Leaved Rose)

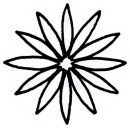

MODIFIED STAR
(12-Leaved Rose)

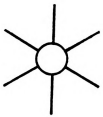

SPIKES
(Cardioidal)

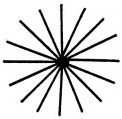

STANDARD
(Cycloidal)

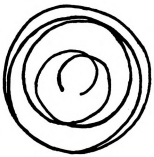

SPIRAL
(Spiral)

Figure 2.5 Some possible epicyclic trunk shaker patterns.
(Orchard Machinery Corp., Yuba City, CA)

generated force resulted in minimum bark damage. Adjusting the shaker properly, pruning trees to accommodate the shaker mechanism and employing attentive operators were significant factors in damage prevention. Advising operators to avoid canker infected areas on trees and employing preventive sanitation measures to retard the spread of disease mitigated orchard losses.

Adrian and Fridley (1963) developed four possible pad designs which would minimize damage. A pad containing magnetic particles and oil caused no injury but was unacceptable due to its weight and deformation characteristics. Two parallel flat belts were tried as a conforming clamp surface for limbs and showed no evidence of limb injury. Bolts mounted permanently into tree trunks proved to be strong and remained secure in younger trees, but failed in older trees. A flexible inelastic pad filled with an incompressible viscous fluid was designed but not evaluated.

Devay et al. (1965) prevented and controlled C. fimbriata canker by: avoiding bark injuries that provide insect attractive environments; shaving away bruised bark tissue and painting the wood with an appropriate dressing (Cerano); cutting away diseased internal tissues and applying a subsequent dressing, or lastly; removing entire infected limbs or scaffolds. All the diseased tissue removed was immediately collected and

burned.

Adrian et al. (1962) used a C-type clamp on shakers because it resulted in minimal damage at the point of attachment.

In summary, adequate removal of cherries by mechanical shakers requires a stroke of approximately 3.8 cm (1.5 in) and a frequency of vibration of 15-20 Hz (900-1200 cpm) (Gaston et al. 1966, Bruhn 1969, AERD 1964). Shaking periods of 3-5 s gave the best results in fruit removal without excessive tree damage, trash accumulation, or bruising of fruit (AERD, 1964).

2.8 Triboelectric Phenomena

I investigated the feasibility of making direct force measurements between the shaker pad and the tree bark using a phenomenon called triboelectricity. A dielectric material (such as the rubber composing the shaker pads) exhibits certain electrical characteristics which may be calibrated and interpreted as meaningful physical events.

The compression of a dielectric material on a hard substance causes strain in the intermolecular structure. When a piece of rubber, a dielectric, is stretched or compressed, the surfaces under stress become charged, similar to the piezoelectric effect. This charge is sufficiently large as to be useful (Memmler, 1934).

Richards (Memmler, 1934) conducted tests on rubber pads as dielectrics and found that pressure applied by a hard surface to these rubber pads resulted in very small negative charges. The charge on rubber in contact with steel was found to be -17.2 esu/cm^2 and in contact with lead was -17.0 esu/cm^2. This effect has been attributed to a combination of the piezoelectric effect, the Volta effect and the rubber's surface expanding under pressure causing friction.

Since the charge has been found to be proportional to strain for a given contact area and material, it would also be proportional to stress.

$$q \sim e = \frac{\sigma}{E} = \frac{\Delta l}{L}$$

The stress for a given area then determines a force.

$$\sigma = \frac{F}{A}$$

It would then be possible to obtain force measurements from the charge output of rubber pads.

$$F = A\sigma = AEe \cong Aq \cong q$$

Where A has been found invariant (Brain and Richards (Davis et al., 1937)).

Shaw (Davis et al., 1937) showed that triboelectrification was influenced by surface conditions, the composition of material and other factors. He found

at least ten factors that determine the sign and magnitude of charge when two materials are brought into contact.

Coehn (Memmler, 1934) noted that a material of higher dielectric constant assumed a positive charge when brought into contact with a material of lower dielectric constant. Since rubber is toward the negative end of the triboelectric series, it normally takes a negative charge. Soft rubber has a dielectric constant of 2.1 to 4.2 while hard rubber is around 3.02 (the ratio of the capacitance with a dielectric to the capacitance in a vacuum is called the dielectric constant of a material where the vacuum capacitance is given the base value 1.0). Deodhar, however, noted various anomalous responses of both hard and soft rubber, which may be explained in part by Shaw's factors determining charge.

Later investigations by Brain and Richards (Davis et al., 1937) found that electrification was in the rubber itself and was not a friction or voltaic effect. Compressing the rubber against seven different hard surfaces produced no variation in results which could be attributed to the nature of the contact surface.

Brain found that for small loads, the charge was proportional to the load, but for large loads, the charge increased more slowly. Hysteresis and fatigue were also observed. This behavior was attributed to a piezoelectric effect similar to the effect in some crystals.

Brain and Richards showed that small loads produced a charge independent of the cross section of the specimen. Hard rubber developed charges of 0.02 esu/kg-load up to 0.151 esu/kg-load. When the load was removed, the charge was opposite in sign and equal in magnitude to that obtained when the load was applied. Soft rubber developed greater charges when compressed, in the range of 15.5 to 21.7 esu/cm^2. Loads ranged up to 2 kg/cm^2 (28 psi). At low pressures, the electrification increased with increasing pressure but raising the pressure from 2-5 kg/cm^2 (28-71 psi) produced no increment in the electrification.

2.9 The Need For Tree Preservation

Fruit and nut growers have a high, long term investment in their crops (Brown, 1980). The cost of switching to another crop requires major changes financially. Problems of obtaining and economically managing labor have led growers to mechanize production and harvesting. Mechanization of labor-intensive fresh market crops is presently occurring in the U.S., Japan, Australia, New Zealand, Israel, South Africa, the Socialist Block Countries, Canada, and many countries in South America. Efficiency and reliability in production have been necessitated by the world population growth, as well as the competition in food production and marketing.

The need to preserve existing crops while increasing productive land and methodology has an immediate impact in prevention of near-future crop failures and shortages.

CHAPTER 3

THEORETICAL CONSIDERATIONS

3.1 Sampling Rate and Resolution

Bruhn (1969) states that vibratory harvesters remove cherries from their stems by applying modified sinusoidal acceleration to the tree or major limbs. Acceleration is transmitted through the tree structure to the stems. If the arriving acceleration levels for an inertial force exceed the stem-to-cherry attachment strength of 1.5 to 2.9 N when ripe, then the cherry detaches. If the cherry is not immediately removed, assuming the induced force is less than the attachment strength, then the attachment strength will gradually be reduced by succeeding cycles of vibration which result in bending fatigue failure.

Characterizing shake-harvesting of fruit involves an analysis of dynamic events which are continuous (analog) during the shaking period. An analog signal can be characterized by an integral number of points in a specified time, provided that each interval of time is sufficiently small to detect the changes occurring during the course of the event. Since most sensors, such as

accelerometers, have analog output while most data acquisition and processing is now done with digital computers, an analysis of the required conversion speed between the two forms is necessary.

A triangular wave can be thought of as an extremely rough approximation of a sine wave. Digitally characterizing a triangular wave (originally of unknown form) would require a minimum of five points per cycle taken at equal time intervals. The inclusion of additional points between any two given endpoints increases the accuracy of modelling the time-dependent analog signal.

Sampling a signal for digital data analysis is usually performed at equally spaced time intervals. The problem of determining the appropriate sampling interval Δt involves a knowledge of the highest desired frequency of interest. The sampling of points at an extremely short time interval can yield correlated and highly redundant data. Sampling at a time interval too large will lead to confusion between low and high frequency components of the original data. This latter problem, called aliasing, can be avoided by sampling data at twice the highest frequency of interest (Bundat and Piersol, 1971). This sampling frequency is termed the 'Nyquist frequency' and has a cutoff of:

$$f_c = \frac{1}{2\Delta t}$$

The Nyquist frequency was developed on the theoretical consideration that at least two samples per cycle were required to define a frequency component in original data where the original sampling interval was Δt. Thus, the Nyquist frequency sampling interval becomes $2\Delta t$. With the Nyquist frequency as a minimum, aliasing can be avoided by choosing Δt sufficiently small so that it is physically unreasonable to find data above an associated cutoff frequency. Vibration of cherry trees at 20 Hz (1200 cpm) then dictates a Nyquist sampling frequency of 40 Hz (2400 cpm). However, it may be desirable to sample at a frequency higher than this when looking for peak amplitudes from bumps at the shaker-tree interface.

Work by Fridley and Adrian (1960), Yamamoto (1979) and others revealed sinusoidal or nearly sinusoidal response when trees and limbs are forced to vibrate by eccentric mass inertial shakers. Halderson (1966) notes that when a tree is vibrated, it displays nodes and anti-nodes similar to those appearing on a vibrating cantilever beam.

In order to digitize an analog accelerometer signal for computer storage, an accurate sampling rate had to be determined. Taking the midpoint of each segment forming one cycle of the triangular wave, and then the

midpoints of the segments formed by those points, a total of 16 points results when added to the endpoints (the final endpoint is ignored in this cycle and counted as the initial point for the next cycle). A safety factor of two was assumed giving a total of 32 points to characterize a cycle of a sinusoidal input wave, Figure 3.1.

Operating at the lower frequency for removal of cherry fruits, a sampling rate of

$$\frac{900 \text{ cycles}}{\text{min}} * \frac{1 \text{ min}}{60 \text{ s}} * \frac{32 \text{ points}}{\text{cycle}} = \frac{480 \text{ points}}{\text{s}}$$

was required.

At the upper end of the frequency range, the sampling rate is:

$$\frac{1200 \text{ cycles}}{\text{min}} * \frac{1 \text{ min}}{60 \text{ s}} * \frac{32 \text{ points}}{\text{cycle}} = \frac{640 \text{ points}}{\text{s}}$$

These sampling rates fulfill the Nyquist frequency requirement for a 15 Hz (900 cpm) or a 20 Hz (1200 cpm) input wave, respectively. Using a standard 16 channel analog-to-digital converter (ADC) with the same sampling rate for each channel, the sum of all channels would require a sampling rate of:

$$\frac{640 \text{ points}}{\text{s per channel}} * 16 \text{ channels} = \frac{10{,}240 \text{ points}}{\text{s}}$$

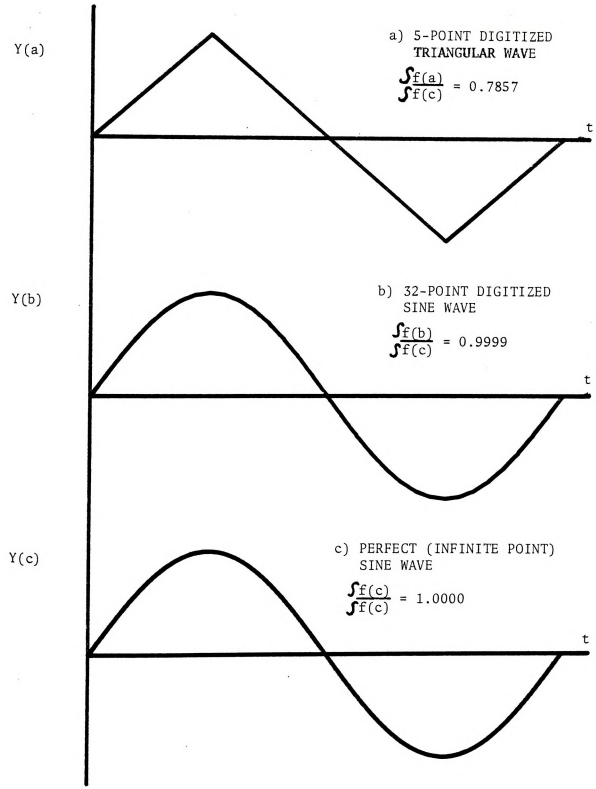

Figure 3.1 Comparison of integration accuracy of several waveforms: (a) 5-point digitized triangular wave (b) 32-point digitized sine wave and (c) a perfect (infinite point) sine wave.

This is the minimum required sampling rate to operate the ADC for response curves of cherry harvest vibrations at frequencies up to 20 Hz (1200 cpm). This speed must accomodate the sample and hold, conversion, and settling time of the ADC's internal amplifiers. The digital processor must process the program instructions, access the ADC ports and access memory for storage in less than 1/10,240 seconds.

The input increment required to give a small definite numerical change in output is the 'resolution' of a device (Doeblin, 1983). Resolution is extremely important in analog-to-digital conversions where an analog signal must be characterized over a limited digital interval. The interval is bounded by the number of bits for which it was designed. A typical 12 bit ADC has 2^{12} = 4096 increments for a processing interval of 0-4095; thus one increment of input is 1/4096 of the selected processing range. Converters usually have processing ranges of 0 to +5 volts, 0 to +1 volt, 0 to +0.5 volts and 0 to +0.1 volts, as well as bipolar ranges of -5 to +5 volts, -1 to +1 volts, -0.5 to +0.5 volts, and -0.1 to +0.1 volts. Ranges above and below these are available, but are not standard.

The resolution of a 0 to +1 volt processing interval is 1/4096 of +1-0=+1 or 244 μV. When digital bits represent analog signals, there is an inherent

quantization error of plus or minus half of the least significant bit ($\pm$ 1/2 LSB) or $\pm 1/2^{n+1}$ * voltage range (V_{max}-V_{min}). The above example has a quantization error of $\pm$ 122 μV.

In analog-to-digital data conversion, it is wise to select the processing range closest to but greater than the expected input signal limits. Suppose a 0 to +4 volt sine wave is collected on a 0 to +5 volt range in a 12 bit ADC: then the resolution is 1.22 mv. The resolution on a 0 to +10 volt range would be 2.44 mv. Twice as many points would characterize the signal on the smaller range as on the larger.

3.2 Frequency Response

The use of physical sensing elements in measuring real world events requires knowing the sensor's capabilities to detect those events. The expected output is a function of the input signal and the transformation performed by the instrument itself. The transfer function for second order instruments such as accelerometers is of the form (Doeblin, 1983):

$$\frac{e_o\ (D)}{x_i} = \frac{[\ k_g/(C w_n^2\ )]\ * \tau D}{(D^2/w_n^2\ +\ 2\zeta D/w_n + 1)(\tau D + 1)}$$

where K_g is the static sensitivity, w_n is the undamped natural frequency, τ is the time constant, and ζ is the

damping ratio. For a sinusoidal input, the transfer function takes the form:

$$\frac{e_o(iw)}{x_i} = \frac{K}{(iw/w_n)^2 + 2\zeta iw/w_n + 1}$$

Where $K = \frac{K_q/Cw_n^2 * \tau_D}{\tau_D + 1}$

i is the complex operator

Then:

$$\frac{e_o/K \quad (iw)}{x_i} = \frac{1}{[1 - (w/w_n)^2]^2 + 4\zeta^2 w^2/w_n^2} \quad e^{i\phi}$$

$$\phi = \tan^{-1}\left[\frac{2\zeta}{w/w_n - w_n/w}\right]$$

It is evident that increasing w_n increases the frequency range for which the amplitude ratio curve is constant (flat). Most piezoelectric accelerometers have a very high natural frequency (w_n) caused by mechanical resonance at 30-40 kHz. Such a high value of w_n allows shock and high frequency vibration measurements at lower frequencies. The low frequency response is limited by the piezoelectric characteristic $\tau_D/(\tau_D + 1)$. A large τ will give accurate low frequency response; a large τ requires the use of high impedance voltage amplifiers or "charge amplifiers". The time constant is $\tau = RC$ where C normally depends upon the amplifier output capacitance and R depends on the data-logging instrument input impedance. A time constant also exists between the transducer and its

amplifier. However, the theoretical infinite input impedance of an amplifier makes τ quite large and therefore, it can be neglected in most instrumentation operations. Time constants are offered in a variety of ranges by manufacturers.

Built-in impedance converters of piezoelectric accelerometers act like emitter-followers, producing a linear output at a low impedance of nominally 100 ohms. Accelerometers are capable of delivering linear output signals to full scale when used to measure vibration.

The damping in piezoelectric accelerometers occurs normally as a result of material hysteresis absorbing some energy. The damping ratio is therefore very low (about 0.01) and can be taken as 0 for practical purposes. With a zero damping ratio, $\phi = \tan^{-1}(0) = 0$. No phase lag is evident between the input and the output of such a sensor.

Adrian et al. (1960, 1963b), Adrian (1964), AERD (1964), and Bruhn (1969) suggest applying sinusoidal energy to a trunk or limb at 10-20 Hz (600-1200 cpm). The response of limbs to excitation was studied by Adrian et al. (1963b) and Hussain et al. (1975). The natural frequencies of experimental apple limbs were in the range of 2-4 Hz for the first mode, 10-13 Hz for the second mode and 20-30 Hz for the third mode of vibration. The response of the tree as a total system was around 1.0 Hz.

Therefore, the frequencies of interest are far below the natural frequency of the instrument and should indicate the exact magnitude of the actual acceleration with negligible phase lag.

The fact that the frequency of forced vibration is in the same range as the natural frequency of the tree and limb may suggest that upon startup, during shake, and/or during shutdown, the shaker may induce resonance in the tree system. Tree resonance could result in large vibration amplitudes at the point of shaker attachment, and in turn cause magnified reactive forces against the shaker. Ultimately, these forces along with tilting or twisting of the shaker, may develop excessive radial, tangential, and/or longitudinal stresses in the bark system. As these magnified stresses may exceed the ultimate strength levels of the bark, visible and invisible bark damage may occur.

3.3 Numerical Integration

Numerical integration or numerical quadrature involves the estimation of the quantity:

$$I(f) = \int_a^b f(x)dx$$

A problem occurs when the integration cannot be performed exactly due to a messy function or when the function f(x) is known only at a finite number of points. If x_o, $x_1 \ldots x_n$ are n+1 distinct points on the real axis and f(x) is a

real-valued function defined on an interval (a,b) containing these points, then there is at least one polynomial $p_K(x)$ of degree $\leq n$ which interpolates f(x) at the points $x_o \ldots x_n$ and satisfies:

$$p(x_i) = f(x_i) \qquad \text{for } i = 0 \ldots n$$

The polynomial form employed to develop this interpolating equation is called the LaGrange formula (Conte et al., 1980) and is written as:

$$p(x) = a_o r_o(x) + a_1 r_1(x) + \ldots + a_n r_n(x)$$

with the weights $r_K(x) = \prod_{\substack{i=o \\ i \neq K}}^{n} \frac{x - x_i}{x_K - x_i}$ $\qquad k=0,1 \ldots n$

and $r_K(x_i) = \begin{cases} 1 & i=k \\ 0 & i \neq k \end{cases}$ $\qquad i=0,1 \ldots n$

The function $r_K(x)$ is the product of n linear factors which makes it a polynomial of degree n.

The value of the integral I(f) can then be approximated by $I(p_K)$ where $p_K(x)$ is the LaGrange polynomial of degree $\leq$ n that agrees with f(x) at the points $x_o \ldots x_n$. The approximation of I(f) can be written as

$$I(p_K) = A_o f(x_o) + A_1 f(x_1) + \ldots + A_n f(x_n)$$

where $f(x_o)\ldots f(x_n)$ are the known function values. The weights are calculated as $A_K = I(r_K)$ with $r_K(x)$ being the ith LaGrange polynomial where:

$$r_K(x_i) = \prod_{\substack{i=o \\ i\neq K}}^{n} \frac{x-x_i}{x_K-x_i} \qquad k = 0,1\ldots n$$

Thus, for any point x_i:

$$p(x_i) = \sum_{K=o}^{n} a_K r_K(x_i) = a_i \qquad i = 0,1\ldots n$$

Therefore, the coefficients $a_o \ldots a_n$ in the LaGrange polynomial are the values of the polynomial $p_K(x)$ at the points $x_o \ldots x_n$. It follows that:

$$p(x) = \sum_{K=o}^{n} f(x_K) r_K(x)$$

for any arbitrary function f(x). If f(x) is smooth on an interval (c,d) and

$$f(x) = p_K(x) + f(x_o \ldots x_K, x)\ \psi_K(x)$$
$$\text{where } \psi_K(x) = \prod_{j=o}^{K}(x-x_j)$$

then the error in the estimate of I(f) is:

$$E(f) = I(f) - I(p_K) = \int_a^b f[x_o \ldots x_K, x]\ \psi_K(x)dx$$

The general nature of the curve to be integrated suggests the type of polynomial fit for least error (best

fit). A triangular wave is characterized by a finite series of trapezoids divided at points of inflection. The trapezoid rule of numerical integration (k=1 case of LaGrange) sums the areas over the total interval (a,b) of the individual trapezoids each with area:

$$\left[\frac{f(x_{K-1}) + f(x_K)}{2}\right](x_K - x_{K-1}) = \frac{b-a}{2n}\left[f(x_{K-1}) + f(x_K)\right]$$

Since $f(x) = f(x_0) + f[x_0,x_1](x-x_0) + f[x_0,x_1,x]\,\psi_1(x)$, the trapezoidal rule becomes:

$$\int_a^b f(x)dx = \frac{b-a}{2n}\left[f(x_0) + 2f(x_1) + 2f(x_2) + \ldots + f(x_h)\right]$$

With a characteristic sine curve and many substantial divisions with a cycle, a piecewise quadratic function

$$f(x) = p_2(x) + f[x_0,x_1,x_2,x]\,\psi_2(x)$$

provides a closer fit (k=2 case of LaGrange). Each fit requires a minimum of three points for quadratic regression:

$$p(x) = f(x_0) + \frac{f(x_1)-f(x_0)}{h}(x-x_0) + \frac{f(x_0)-2f(x_1)+f(x_2)}{2h^2}(x-x_0)(x-x_1)$$

The individual areas under the quadratic piece fitting are summed for the integral of p(x) where:

$$\int_{x_1}^{x_2} p(x)dx = \frac{h}{3}[f(x_0)+4f(x_1)+f(x_2)]$$

$$= \frac{b-a}{3n}[f(x_0)+4f(x_1)+2f(x_2)+4f(x_3)+\ldots+f(x_n)]$$

This rule, known as Simpson's Rule, holds for any continuous function on (a,b). The maximum error terms for the trapezoid $(b-a)^3M/12n^2$ and Simpson's $(b-a)^5M/180n^4$ (M is the maximum of the numbers $|f''(x)|$ for trapezoid and $|f''''(x)|$ for Simpson's) suggest that the latter is preferred for a sufficiently smooth f(x) and the former otherwise, without the complexity of high degree polynomial integration. Therefore, the selection of an integration procedure depends on the nature of the recorded signal.

CHAPTER 4

EXPERIMENTAL TECHNIQUES

A high-speed microprocessor-controlled data-acquisition system was assembled to characterize the real time dynamic behavior of a mechanical tree shaker and a cherry tree. The shaker was obtained from the Friday Tractor Co., Hartford, MI, a company with similar research interests. The C-clamp shaker was typical of those employed in commercial cherry orchards, Figure 4.1. At any point in time, sensors and signal conditioning devices provided the microprocessor system with digital inputs that represented the X, Y, and Z accelerations of the tree and shaker, the position of the rotating masses, the relative linear position of the clamping arm and the pressure in the clamping cylinder. The high rate of data sampling across 16 channels provided accurate digital characterization of analog transducer inputs. Waveforms were reconstructed from digitized data; accelerations were integrated twice to give absolute displacements and relative displacements between the trunk shaker and the tree.

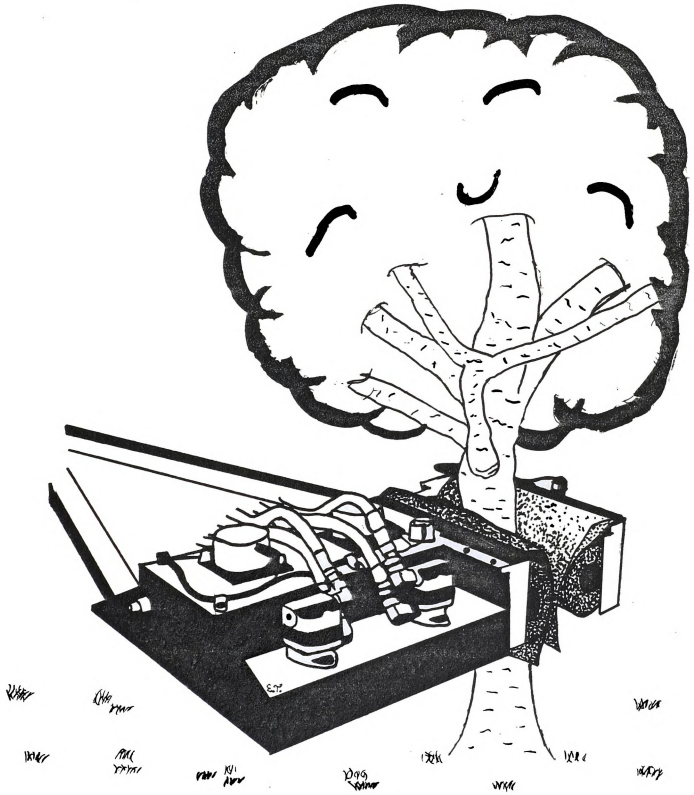

Figure 4.1 C-clamp style eccentric mass trunk shaker used in commercial fruit harvesting.

4.1 Triboelectric Phenomena

In order to determine the feasibility of measuring a force between the shaker and the tree directly from the output charge of a rubber pad, tests were conducted to verify the phenomenon and, if present, to calibrate the charge with shaker pad compression.

A rubber cylindrically shaped shaker pad was mounted on a 422 kg/cm^2 (6000 psi) hydraulic press with its cylindrical axis horizontal. On each circular end of the pad, four wire electrodes were inserted at a radius of 70 mm (2.8 in) 90 degrees apart. The pad face was forced against a 20 cm X 25 cm (8 in X 10 in) steel plate at various pressures. (See Figure 4.2). Probes from a Kistler Model 503 charge amplifier were connected to the electrodes. Output from the charge amplifier was observed on a Tektronix oscilloscope. The variation in charge was recorded for increments of pressure, both increasing and decreasing. Remaining charge after pressure release and the effects of charged objects passing nearby were observed.

Results of this test (Table 5.1) showed that direct force measurements from pad compression would not be possible because of hysteresis phenomena and the sensitivity of the output charge of the pad to environmental electrical effects. A possible alternate solution to detect force transmission between the shaker

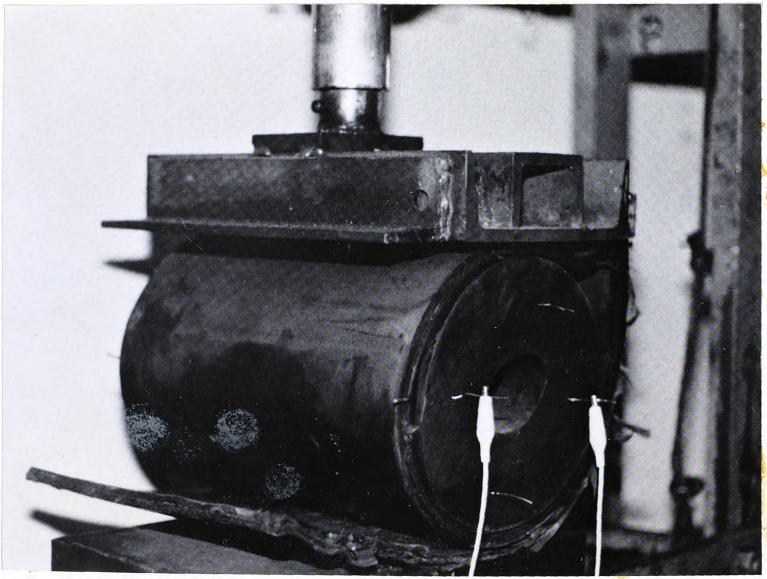

Figure 4.2 Rubber shaker clamp pad mounted on a 422 kg/cm^2 hydraulic press for the triboelectric test. Clip leads extend from the electrodes inserted in the pad to a charge amplifier and oscilloscope for charge quantization.

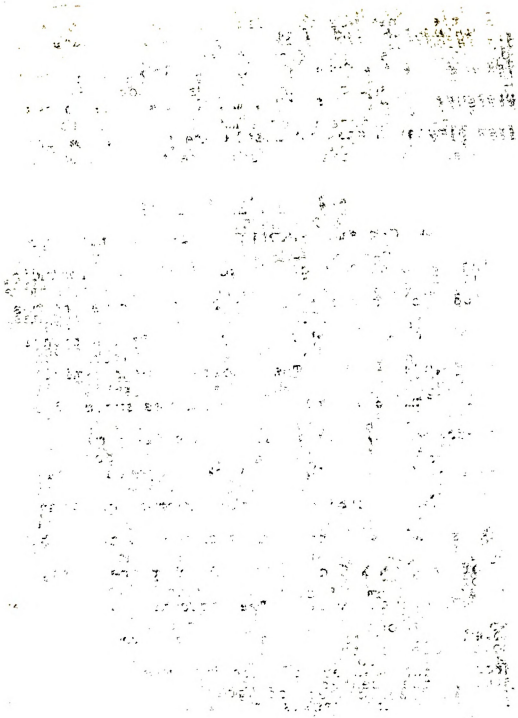

and the tree was to measure the tree and shaker real-time displacements and from these data, simulate the critical maximum displacements in a laboratory test. Using pressure tranducers on a model tree, the forces generated from simulated maximum displacements could be estimated.

4.2 The Trunk Shaker

A C-clamp eccentric-mass inertial trunk shaker having a total mass of 544 kg (1200 lbs), including two 40 kg (88 lb) semicircular unbalanced rotating masses, was mounted on a 56 PTO Hp Hydro 84 International Tractor (See Figure 4.3). The radius of each semicircular mass was 17.1 cm (6.75 in). Each mass was attached to a shaft, chain-driven by individual 2.8 L/s (44 gpm) 105 kg/cm^2 (1500 psi) counter-rotating Vickers hydraulic vane motors.

The location of the center of gravity of the trunk shaker was obtained by balancing the machine on the tip of a 5 cm X 5 cm (2 in X 2 in) piece of angle iron on two orthogonal axes. The eccentric masses were not removed due to the difficulties involved in disassembly. Instead, the center of gravity was corrected for the presence of the masses by taking measurements on the appropriate axis with both masses inward, then outward and then calculating an average. This provided an accurate measurement of the location of the center of gravity of the shaker without the masses.

Figure 4.3 C-clamp eccentric-mass inertial trunk shaker mounted on the lift of a 56 PTO Hp Hydro 84 International tractor.

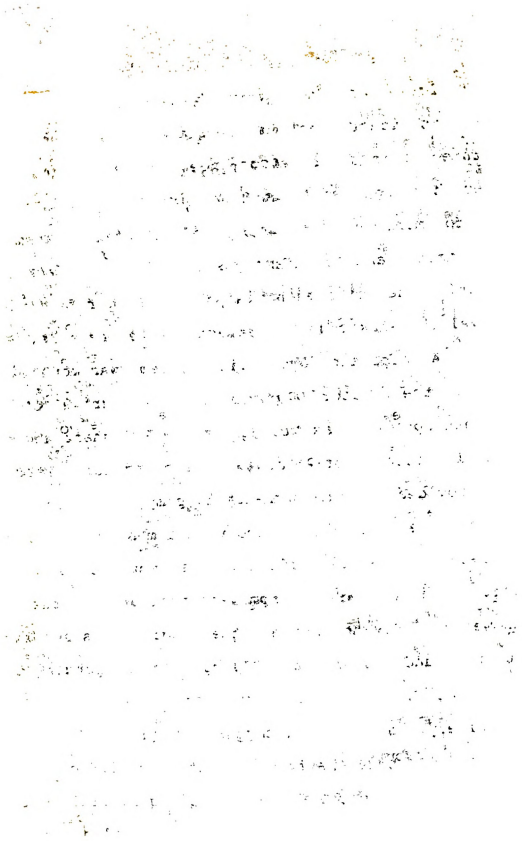

The shaker was mounted on the 2250 Mount-O-Matic loader frame of the Hydro 84 International Tractor. A frame was constructed on the loader to suspend the shaker at three points as recommended by the manufacturer. Rubber bushings were used on both ends of the suspension bars to minimize the amount of vibration transmitted to the tractor and to damp oscillations fed back from the tractor. The tilt mechanism of the loader frame was used to level the shaker during attachment to the tree.

A separate hydraulic system was mounted on the rear of the tractor to power the shaker drive motors. A 35 tooth sprocket was mounted on the PTO shaft and chained to a 13 tooth sprocket on a Hydreco hydraulic gear pump. This provided a 2.7:1 increase in pump drive rpm. A 150 L (40 gal) reservoir, equipped with a master shut off valve and return line oil filter, was mounted above the PTO shaft. Engine and PTO rpm were monitored on the tractor tachometer. During shake, the engine was set first at 1500 rpm and later at 2200 rpm, corresponding to pump outputs of 1.9 L/s (30 gpm) and 2.5 L/s (40 gpm), respectively, at 105 kg/cm^2 (1500 psi). The hoses used to distribute the flow were at least 1.9 cm (0.75 in) ID. A 50-50 flow divider allocated equal fluid volume to an individual continuously variable flow valve controlling each shaker drive motor. The separate variable flow control valves regulated oil flow to each shaker drive

m
i
t
s
a
e
e

W

F
c
r

i
a
c
i
r
p
k
c
d

motor such that speed for each motor could be independently selected. Each shaker drive motor then transmitted power from a 45 tooth sprocket to an 18 tooth sprocket mounted on the shaft of the eccentric mass. At any given engine speed, the full rotational frequency of each mass (assuming both were being driven) followed the equation:

$$\text{Frequency} = \frac{[\text{Engine RPM} - 100] * 0.4}{60}$$

Where Frequency is in Hertz

Frequencies of 9.3 Hz (560 cpm) and 14.0 Hz (840 cpm) corresponded to engine test settings of 1500 and 2200 rpm, respectively.

A double acting 8 cm ID X 61 cm stroke (3 in X 24 in) hydraulic cylinder, mounted on the back of the shaker, activated the opening and closing of the C-clamp. The clamping pressure for shaking 11.4 cm (4 in) to 15.2 cm (6 in) diameter trunks was set at 49 kg/cm^2 (700 psi), as recommended by Frahm et al. (1983). The cylinder clamping pressure was monitored on the hydraulic system with a 105 kg/cm^2 (1500 psi) pressure gauge. Check valves in the clamping circuit presumably prevented clamp movement during shake.

The clamping cylinder was connected directly to

the tractor's hydraulic system which operated at 0.7 L/s (11.0 gpm) 127 kg/cm^2 (1800 psi) at 2200 engine rpm and operated at 0.4 L/s (6.2 gpm) 127 kg/cm^2 (1800 psi) at 1500 engine rpm. Clamp pressure was set at 49 kg/cm^2 (700 psi). Clamping to the tree was then accomplished independently of the operation of the shaker motor hydraulic system. This configuration prevented any interaction between the clamping pressure on the tree trunk and the pressure required to drive the shaker motor at the desired shaking frequency.

Two cylindrical rubber pads (19 cm OD, 8 cm ID and 55 cm long) were fastened in support slings within the clamping jaw. The facing of each sling was coated with a lubricant (grease) and covered with an attached rubber flap. This followed the manufacturer's recommended practice for reducing shear force on the tree bark by allowing the slip to occur between the pad sling and the flap.

4.3 Sensing Elements and Calibration

Sensors were placed at strategic points on the trunk shaker to characterize the planar motion of the inertial shaker in real time. Planar motion can be described by a minimum of three accelerometers, two at one location and a third at a known fixed distance from the two. Three accelerometers were placed in such

configuration, both on the shaker and on the tree. Accelerometers were located at the shaker's center of gravity to detect X and Y motion, and a set of three accelerometers were located at the base of the pad on the shaker frame to detect X, Y, and Z motion (See Figure 4.4). A second Z axis accelerometer was centered on the clamp arm at the pad base to complement the first Z axis accelerometer and define the vertical shaker position as vectors at opposite sides of the tree (See Figure 4.5). Vertical motion (Z) of the tree was assumed zero.

Two 0.8 cm (5/16 in) diameter holes were drilled radially in each tree trunk at 90 degrees separation and 46 cm (18 in) above the ground plane. In one hole, a single X axis accelerometer was placed. In the second, a 16 cm^3 (1 in^3) aluminum block was mounted and X and Y axis accelerometers were then mounted on the block, Figure 4.6. This combination of three accelerometers permitted calculations of X and Y linear displacement of the trunk, as well as angular displacement of the trunk.

Sunstrand (Sunstrand Data Control Inc., Redmond, WA) and General Radio (General Radio Co., Concorde, MA) accelerometers were used in all tests. Resonant frequencies of the accelerometers were 40 Khz, well above the operating range of the shaker system. The time constant of each accelerometer was 20 s allowing frequency response of 0.02 to 5000 Hz with 5% low error at the low

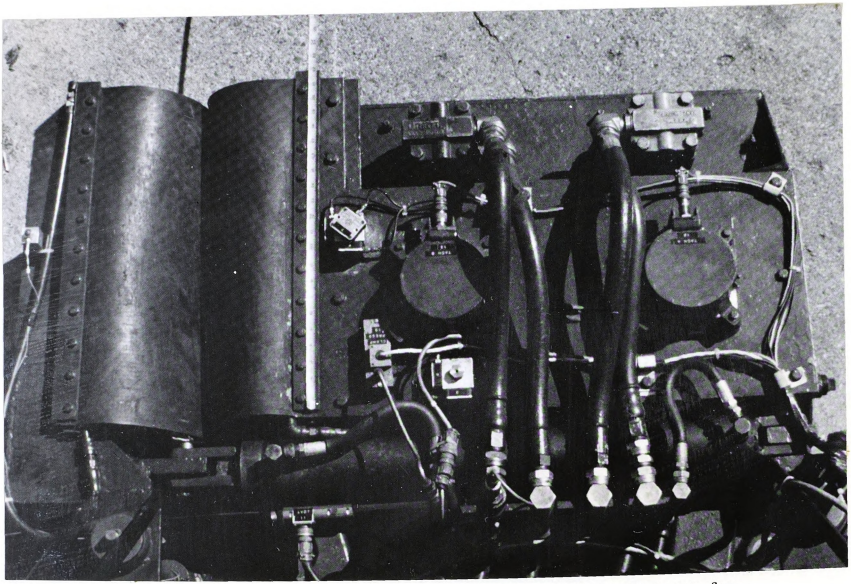

Figure 4.4 Top view of trunk shaker revealing strategic locations of sensors for detection of acceleration, displacement, and position.

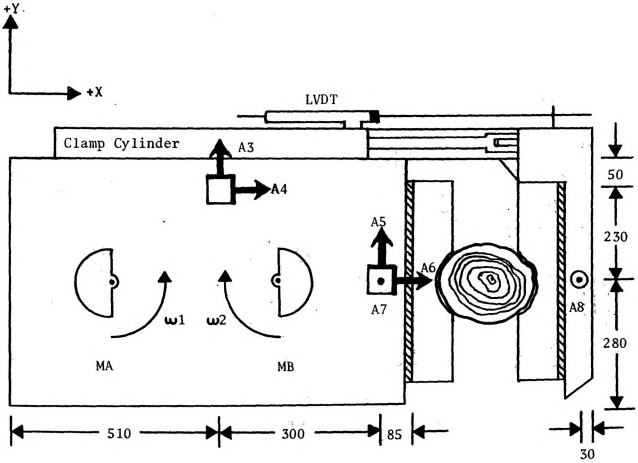

Figure 4.5 Dimensioned trunk shaker showing accelerometer and LVDT locations. (All measurements in millimeters)

Figure 4.6 Orthogonal location of X and XY accelerometer blocks mounted on a cherry tree trunk.

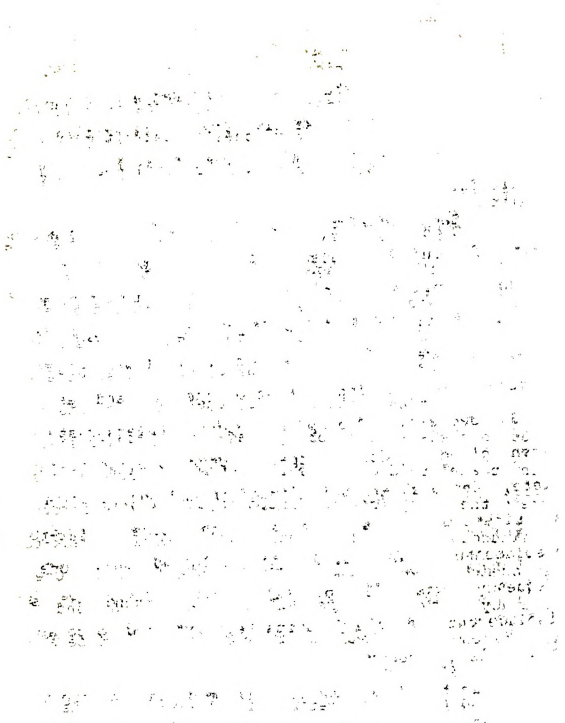

frequencies and 5% high error at the high frequencies. This covered the shaker operating range with an amplitude response of almost exactly one. Acceleration range was ± 250 g (1 g = 9.8 m/s^2) with $\pm$ 1% linearity in amplitude.

Each accelerometer was calibrated in a separate test for output voltage per unit displacement. A fixed linear displacement plunger unit was mounted on a lathe. The lathe provided rotation to the input shaft of the unit, Figure 4.7. A teflon disk (swash plate) was attached to the input shaft of the unit and was inclined at 30 degrees. Two spring-loaded plungers rested on the swash plate 180 degrees apart. Upon rotation of the swash plate, the plungers were forced in and out, each providing a sinusoidal displacement with time. Peak-to-peak displacement was 1.09 cm (430/1000 in). Operating frequency was 676 cpm (11.3 Hz). Trunk and shaker displacement in field tests were expected to be about 10 mm at this frequency.

Each accelerometer was mounted on the plunger shaft, and its output was amplified with a Piezetron Coupler or a Kistler Model 503 charge amplifier, then integrated twice by hardware integrators (See Figure 4.8). The integrator input and output signals were monitored on an oscilloscope and recorded on a strip chart recorder. Several signals were also recorded on a four

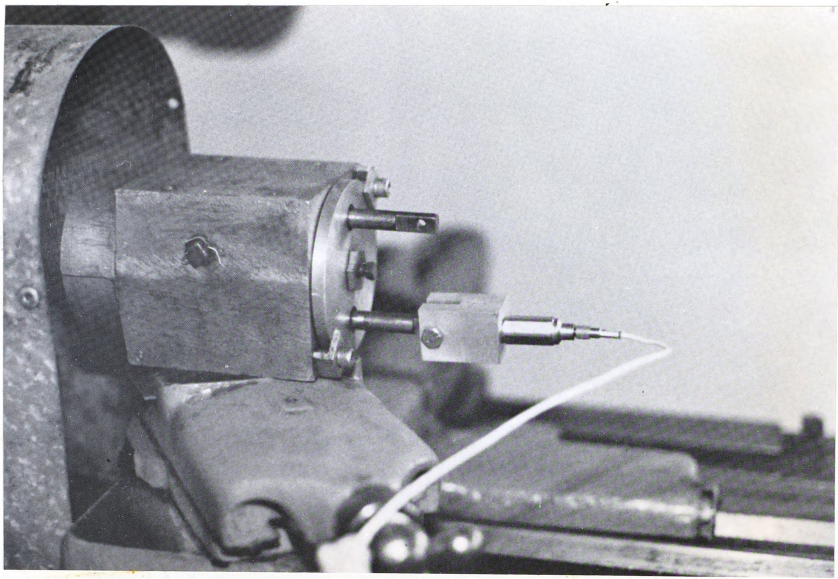

Figure 4.7 Accelerometer mounted on a fixed-displacement variable-frequency reciprocating plunger unit for calibration.

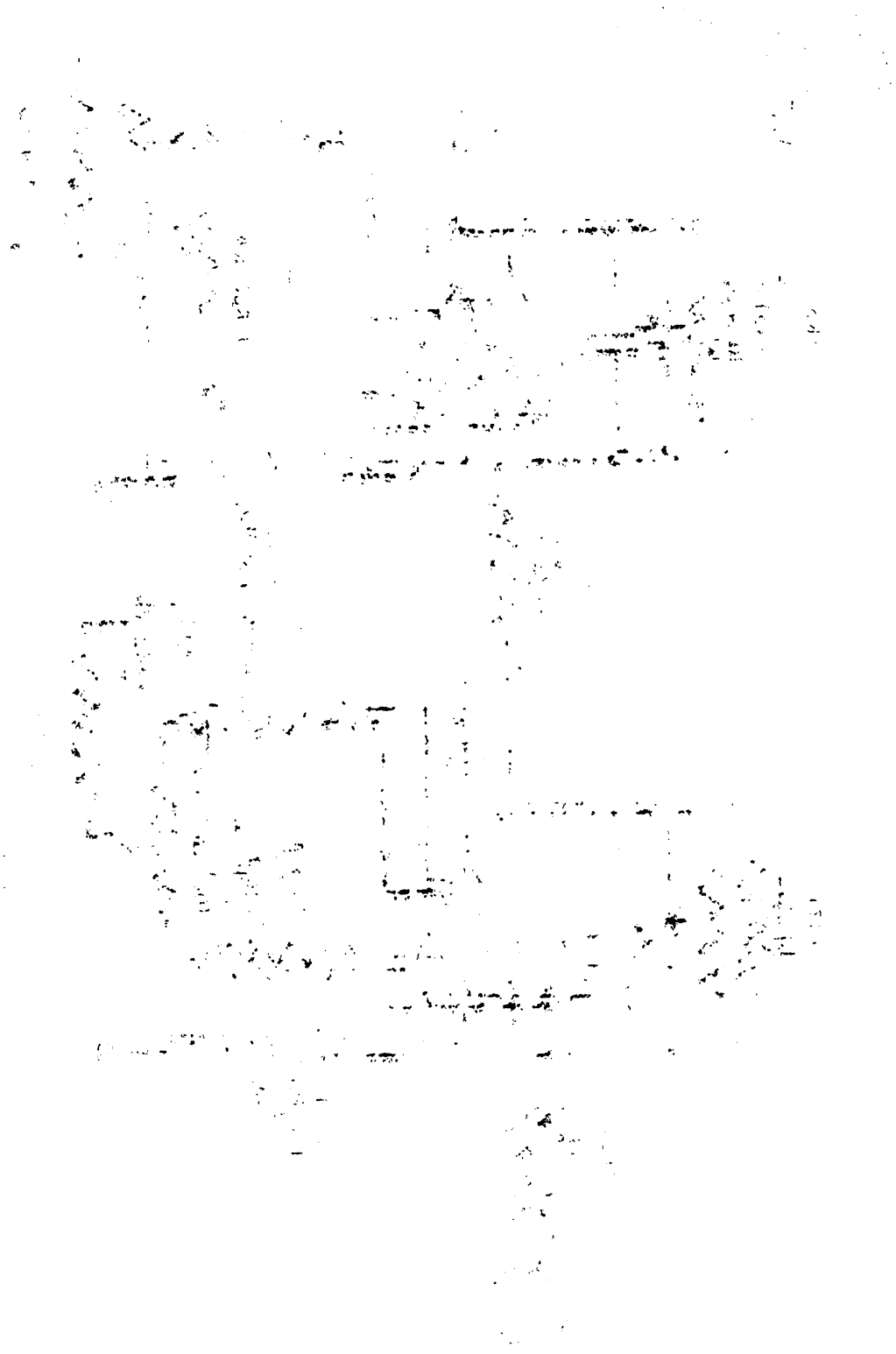

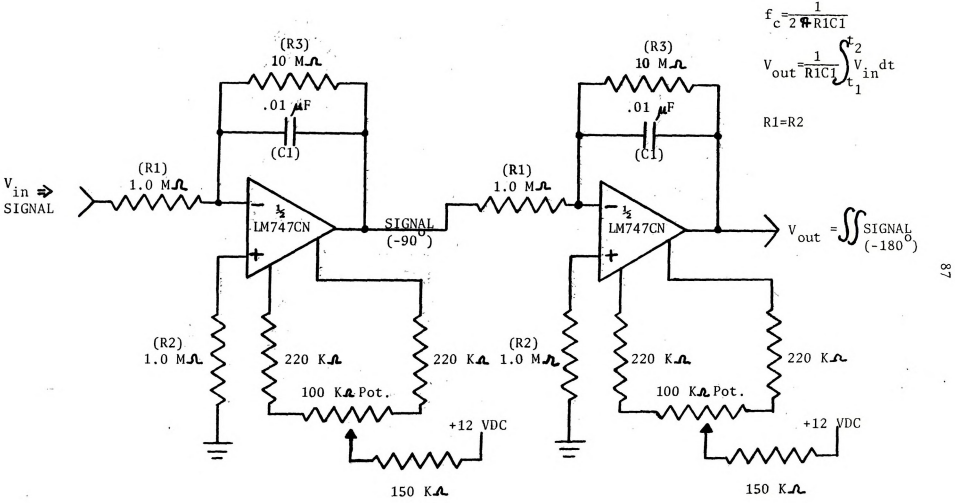

Figure 4.8 Hardware (double) integrator circuit using operational amplifiers. (Amplifier power ± 12 VDC)

channel analog tape recorder for future reference. Voltage ranges were tentatively selected from these tests for setting scales in the ADC data acquisition routine.

A proximity sensor on the shaft of each eccentric mass provided both frequency and angular position information for each mass. The proximity sensors operated on electromagnetic induction principles whereby the change in reluctance in a magnetic field induced a current in an internal coil. A small rectangular steel bar protruding from the side of each shaft provided the change in reluctance needed to cause a flux change in the magnetic field of the proximity sensor each time the shaft was in a particular position. Pulse voltage was proportional to angular shaft velocity.

These proximity pickups were adjusted (by adjusting the gap between sensor and shaft) to provide a maximum -5 to +5 volt pulse at shaker operating frequencies. The shaker drive motors were unidirectional in operation. For purposes of uniformity, the proximity sensor leads were connected to respond with a positive lead pulse from each shaft.

To detect relaxation or tightening of the clamp, a linear voltage differential transformer (LVDT) was connected across the back side of the clamp opening. A Daytronic Model 300C amplifier with a Type 61 Module provided a 3 volt excitation for the LVDT. The output

voltage from the LVDT was linearly proportional to rod displacement on the ± 0.025 cm (± 0.010 in) scale. The output voltage range was ± 40 millivolts DC. The LVDT provided information on clamp opening or closing movement during the shake which may not have been accompanied by a noticeable change in the hydraulic pressure of the clamp cylinder.

The Daytronic amplifier and LVDT were calibrated by zeroing the amplifier output, incrementally displacing the transformer rod, and recording the output voltage as it varied from zero.

A 0-211 kg/cm^2 (0-3000 psia) Servonic potentiometric pressure transducer (Servonic Instruments Inc., Costa Mesa, CA) was mounted in the pressure line to the clamping cylinder to monitor clamp pressure. Resonant frequency of this device is very high; it is well suited for vibration measurements. Input excitation of ± 10 volts DC provided a linear output of 0 to 3 volts. A 422 kg/cm^2 (6000 psi) hydraulic press was used to apply pressure to the pressure transducer for calibration. Electrical output was recorded for a unit change in pressure.

4.4 The Acquisition Processor Hardware

A data acquisition system was assembled that was capable of operating at very high speeds, collecting up to

16 channels of data sequentially, and storing this information on a "floppy disk" (See Figure 4.9). An analog-to-digital converter (ADC) (Interactive Structures, Inc.) and a 6502 microprocessor system (Apple Computer, Inc.) were selected and interfaced.

All direct and amplified transducer signal carrier lines were connected to a common terminal box where they merged into three main cables. These cables, each of four pair twisted shielded wire, linked the sensing element outputs to the ADC and the microprocessor housed inside an air conditioned van that provided protection from dust and temperature effects (See Figure 4.10). Writing to the disk was a sensitive process and could have failed if tiny particles of foreign matter got between the disk and the writing head of the disk drive.

The box also contained three Piezetron couplers which provided a current source and amplified the accelerometer signals on the tree. A variable DC power supply energized the clamp-cylinder pressure transducer with $\pm$ 10 VDC. Six Kistler Model 503 Charge Amplifiers, fastened to a portable cart, amplified six of the accelerometer signals from the shaker.

The 16-channel, 12-bit ADC unit provided software-scaling of signals on 8 ranges with 0.024% resolution. Each channel was read in 20 μs with a sample-and-hold amplifier circuit. ADC ranges were

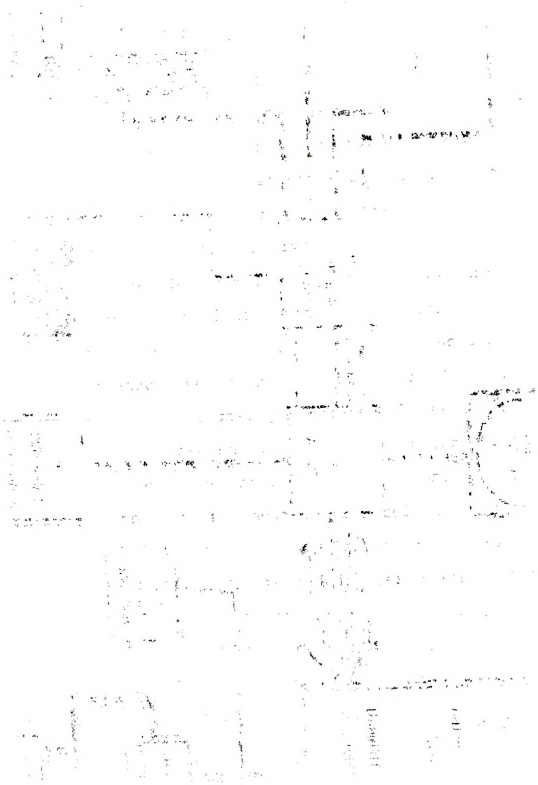

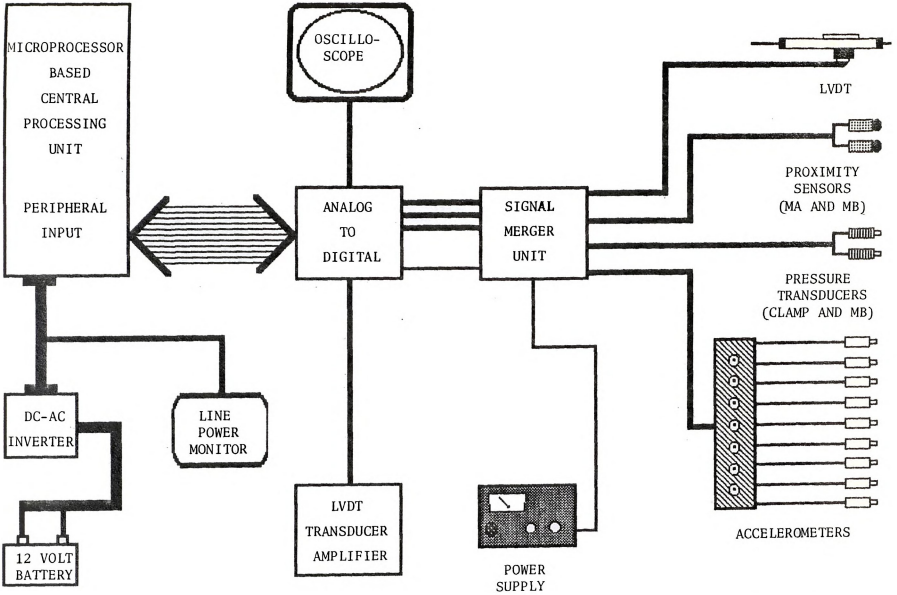

Figure 4.9 Hardware block diagram of the microprocessor-based data acquisition system for trunk shaker vibration analyses.

Figure 4.10 The data acquisition equipment was assembled in an air conditioned van to protect it from dust and temperature.

[illegible]

selected by programming the microprocessor to access the proper I/O port. Range, channel, order and sampling speed were software-controlled.

The 6502 microprocessor system was the hardware operating system of the Apple III Computer. A 2 Mhz crystal controlled the system speed. Expanded memory provided 256 Kilobytes (1 byte = 8 bits) of Random-Access-Memory (RAM) with 2 Kilobytes of masked Read-Only-Memory (ROM). An interface between the keyboard and the video screen provided easy programming of the microprocessor. A system disk drive allowed storage of 140 K of data on a 13 cm (5.25 in) soft disk. Buffered I/O ports permitted the addition of a second 140 K disk drive, as well as connection to the ADC.

The microprocessor controlled the operation of the ADC, retrieved and stored values in RAM, and dumped all information to the two soft disks at the end of a test. User-friendly messages were directed to the video screen to provide information on the status of a test. With the video screen on, the microprocessor speed was reduced to 1.4 Mhz. Therefore, during actual data collection the screen was shut off (by the software) thereby increasing clock frequency to 1.8 MHz.

4.5 The Acquisition Processor Software

The main function of the software was to control

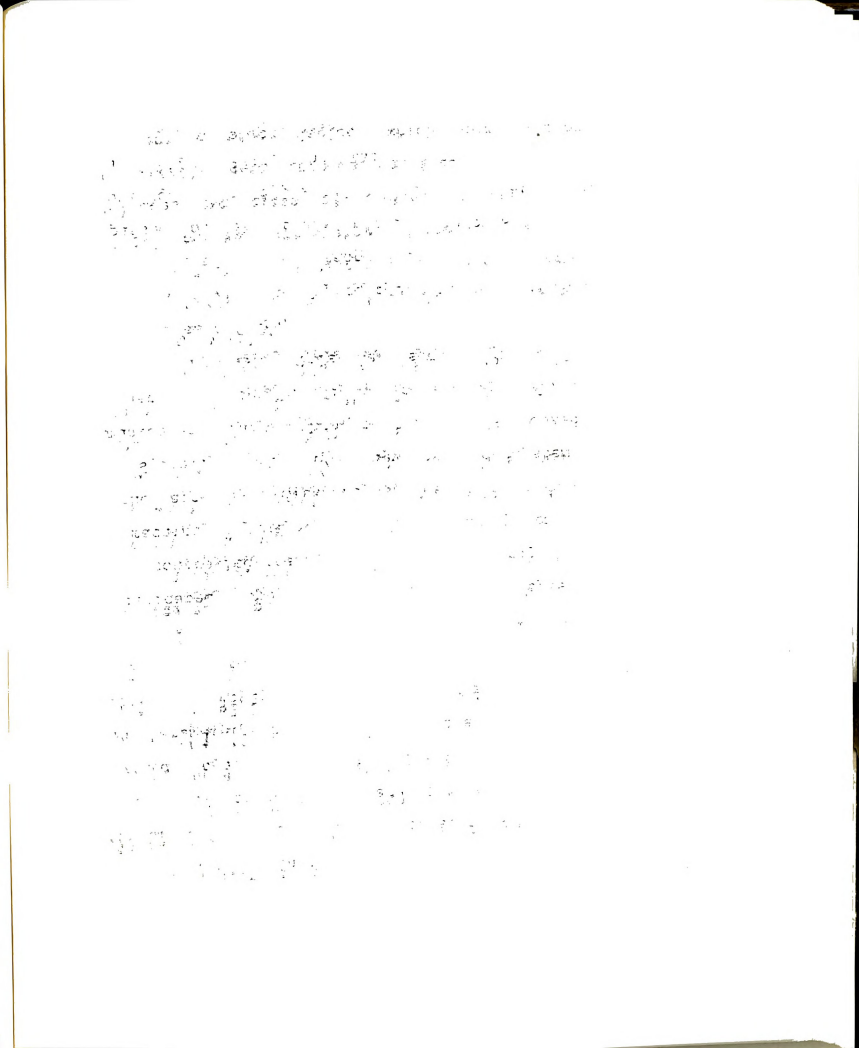

the conversion of analog data signals in the ADC and place the information into memory for later disk storage. The program was written as a series of subroutines to keep sections of operation independent of each other. This provided ease in troubleshooting when failure occurred or when parameters needed to be altered. Programs were written in 6502 assembly code. A Pascal operating system was available to assemble the program code.

A central software program called the Sophisticated Operating System (SOS) (Apple Computer, Inc.) controlled the means by which all programs could use the machine hardware. This operating system was located on the main system disk and was needed to start up and run the system. All I/O devices and system hardware communicated only through SOS. SOS looked at all peripherals (console, disk drives, speaker, printers, etc.) as devices. This was similar to looking at each peripheral as a file.

A device is a part of the system hardware or a piece of external equipment that can allow information to be passed between the system and the outside world. SOS acknowledges two types of devices: a character device, which normally gets information into and out of the system; and a block device, which normally stores and retrieves information.

SOS contains special programs called device

drivers. These take information from SOS and translate it into a machine action, or take a machine action and convert it into information for SOS. Any message sent to a device must first be sent to SOS by a program. SOS will then send it to the driver and the driver will send it to the device. Therefore, any device added to the system, not inherent in the operating system, must be accompanied by a special device driver program. Device drivers for the disk drives, the console, the speaker and several printers are part of the system start-up diskette.

The ADC is a general purpose piece of hardware intended for use with many microcomputers. No device driver program existed for the ADC; a device driver had to be written for the ADC so that SOS could recognize the ADC as a device and communicate with it. The ADC was a character device, receiving streams of characters, and processing them one at a time. An explanation of the complete operation of SOS would be voluminous and is beside the point of this subsection. A brief explanation of the function of the device driver program will be presented followed by a discussion of the actual acquisition program. The annotated ADC device driver program is given in Appendix B.

When SOS starts the system, it checks all device drivers to verify the existence of their accompanying devices. At this time, absent devices or device driver

programs are noted to let SOS know what resources are available. The needed devices are initialized and any required internal resources are allocated. Any time a user program wishes access to a device, it must "open" the device through the device driver program by a 'Call' to SOS. The device driver required for the ADC was written to allow a 'Read Data' request to be implemented from an operating program. FFFE (65,534) bytes of information were requested in one call. The driver accepted the request, probed the ADC device with a preprogrammed channel-gain sequence and returned the data to a buffer memory. The channel-gain sequences were preprogrammed in the driver; this permitted greater operating speed and a reduction in programming time. To change the sequence, however, required a significant amount of reprogramming. It is suggested that the next version of this driver should accept keyboard entered requests of the channel and gain that can be passed from the user keyboard through SOS to the driver. Figures 4.11 and 4.12 show the block diagrams for the ADC device driver program preparation and execution fields.

The ADC appears to SOS as a block of memory locations. The address of the block is determined by the expansion slot number in the machine, indicating in which slot the ADC is located. The starting address of this memory block was (hexadecimal) ADC = C080 + SLOT * 10. A

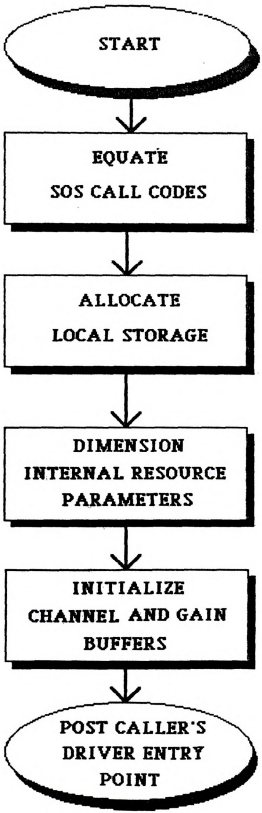

Figure 4.11 Simplified Block Diagram of the Allocation Field of the Analog-to-Digital Converter Device Driver.

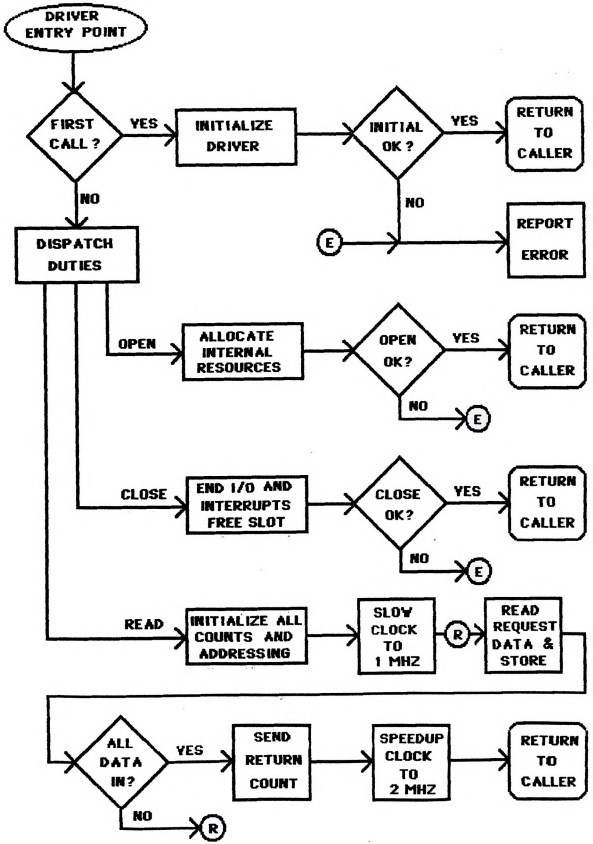

Figure 4.12 Flow Diagram of the Execution Field of the Analog-to-Digital Device Driver.

single "Write" command directed to one of the locations in a memory block caused the ADC to read a selected channel on a chosen voltage range (selectable gain). The result of the conversion was then returned in two bytes from the same memory location. Since the result was a 12 bit value of 0-4095, two bytes were used but the upper half (4 bits) of the most significant byte was not used and was stripped off before data storage. All ranges were electronically calibrated such that zero corresponded to the low end and 4095 to the high end. When an amplified conversion required the 0.5 or 1.0 volt range, a timing delay of 45 microseconds had to be inserted into the software to allow hardware settling of the sensitive amplifier gain settings. This delay was subsequently inserted in the device driver program to cover this situation, as well as to keep the time interval between all data points constant.

When the requested datum was entered in the buffer memory by the read request in the user program, control was returned to the user program. At the end of the user program's need for the device, a SOS call to 'Close' the device had to be implemented. This call finished any I/O, disabled all interrupt capability, confiscated any device-dedicated resources and returned control again to the user program. At this point, the device no longer existed in the "eyes" of the user

program.

The ADC device driver was written in the prescribed format for SOS. At first, operation of the driver program produced fatal misbehavior of the system. Careful examination of the microcomputer programming manual revealed an addressing routine which incorrectly allowed the user to dedicate a buffer memory in an area which was actually reserved for SOS. The addressing routine would fail when more than 32 kilobytes of data were sent to the buffer memory. The routine was then rewritten to utilize the maximum amount of memory available, Figure 4.13.

In summary, the ADC device driver makes possible communication between the ADC device and the user program through a master program called SOS. Thusfar, the main program in the machine has been referred to as the user program. Here follows a discussion of this user program.

The start-up routine of the 6502 system consisted of loading and operating three programs from a disk. SOS always resides in memory even while the machine is in use and is referred to as the 'Kernel'. The Kernel should only be altered by the manufacturer. All special device communication programs were stored in a special SOS format in a file called the 'Driver' file. Finally, a machine code user program was written in a file called the 'Interpreter'. The Interpreter was loaded thirdly and

6502 ASSEMBLY LANGUAGE MACRO FOR ADC DEVICE DRIVER

INCREMENTS 3 BYTE ADDRESS AND CHECKS FOR PROHIBITED RESULTS

```
*************************************************************

      .MACRO INCADR          ;Begin Address Increment Macro

       INC     %1            ;Increment Low Byte of Address
       BNE     $310          ;If not zero, then skip Hi byte
       INC     %1+1          ;If low byte is 0, Inc. Hi byte
       LDA     %1+1          ;Load the Hi byte for checking
       CMP     #0A0          ;Are we in SOS Hi address?
       BEQ     $120          ;If so, fix it so we are not

$110   CMP     #00           ;Are we in SOS Low address?
       BNE     $310          ;If not, skip this correction
       SEC                   ;We are, so fix it
       ROR     %1+1          ;Reset Hi byte of Address
       INC     %1+1401       ;Increment to next memory bank
       JMP     $310          ;Leave

$120   LDY     %1+1401       ;Where in SOS are we?
       CPY     #8F           ;Are we in the zero bank?
       BNE     $130          ;If not, repair differently
       LDA     #80           ;If so, do a general fixup
       STA     %1+1          ;Set Hi byte to 80
       STA     %1+1401       ;Set extension bank to 80
       JMP     $310          ;Done, now leave

$130   CMP     #00           ;Are we in SOS zero page?
       BNE     $310          ;If not, we are OK
       SEC                   ;If so, fix it
       ROR     %1+1          ;Reset Hi byte of address
       INC     %1+1401       ;Increment next memory bank

$310   .ENDM                 ;End of Macro

*************************************************************
```

Figure 4.13 Device driver address incrementation routine that allows maximum utilization of internal memory without the production of system-fatal memory pointers.

contained programmed code (which I wrote in a special SOS format) that directed the machine to carry out specific actions. I wrote the Interpreter program in such a way that the machine could execute the program from a "cold start" in the field, i.e. all initial user rituals were bypassed.

The Interpreter, communicating through SOS and the device drivers, first allocated 196 kilobytes of RAM for data storage, opened the screen and keyboard (console) for reading and writing, and set up the ADC driver to acquire transducer signals. Block diagrams of the Interpreter program header and execution fields are shown in Figures 4.14 and 4.15. All communication to devices through drivers by user programs such as the Interpreter required information in a SOS executable format. This formatted information is noted in the Interpreter program documentation in Appendix A.

4.6 Data Capture

The Interpreter made a 'Call' to read the ADC driver three times, each time requesting FFFE (65,534) bytes. This totalled 196,602 bytes of data. The starting and ending time of each read call was obtained from the system clock as the linear time base for the real-time analysis. The video screen was turned off by the Interpreter program before data collection to increase the

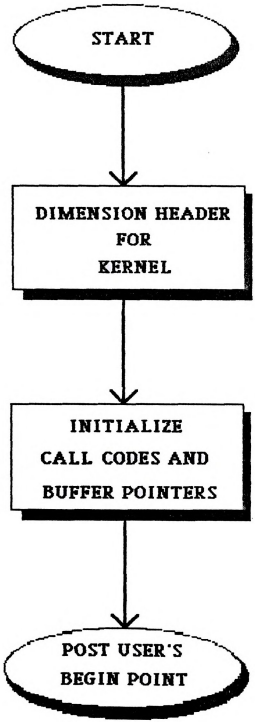

Figure 4.14 Simplified Block Diagram of the Header Field of the Analog-to-Digital Converter Interpreter.

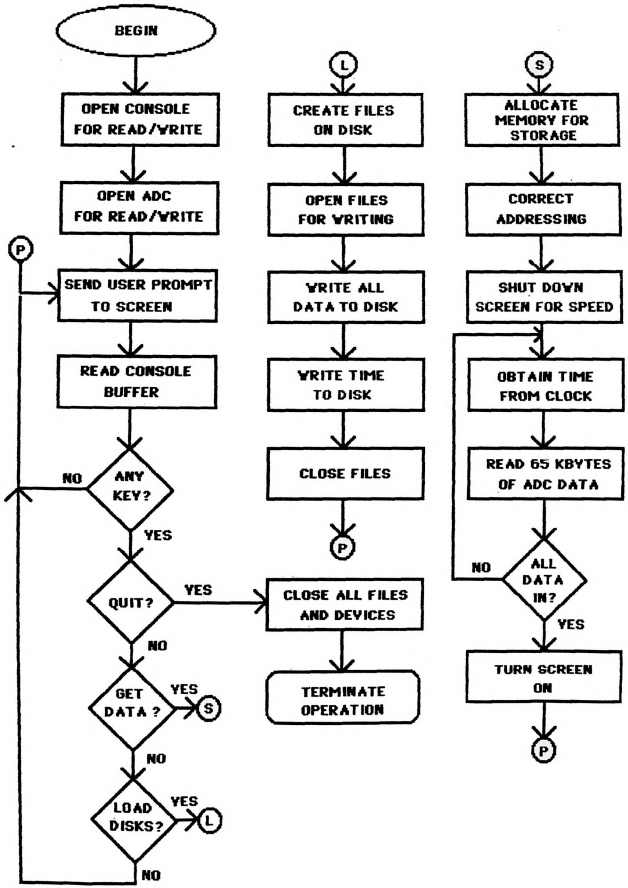

Figure 4.15 Flow Diagram of the Execution Field of the Analog-to-Digital Converter Interpreter.

system speed to 1.8 Mhz. The video was turned on at the end of the data collection in order to send messages to the user. System clock speed then reduced to 1.4 Mhz.

Data in memory could then be stored on two 13 cm (5.25 in) "floppy disks". Specific data sent to SOS allowed a disk driver program to create, open, write to, and finally, close 'data' files and one 'time' file. The system was then prepared to make another test. As a safety feature, data in memory were not destroyed unless another test was begun or the machine was turned off. Therefore, if a disk problem arose or if the user forgot to insert disks into the drives, new disks could be inserted and the data restored.

4.7 Transcription to Disk

Six 'write-to-disk' operations transferred the data of the three 'read ADC' operations to disk. Although a write operation could accept up to FFFF (65,535) bytes, SOS memory management did not allow continuous data in memory to be written to a file without inserting undesired information from a reserved buffer. The memory of the SOS system consisted of fifteen 32 kilobyte areas called banks. Two special memory areas, at low address (0000 to 00FF) and at high address (A000 to FFFF), were reserved for SOS. Between this area (2000 to 9FFF), one of the fifteen banks could be called for data access. Extended

indirect addressing, which specified a bank and a two byte memory address via a pointer, was utilized to store and retrieve information.

The Interpreter program stored the data as high byte first, low byte second, starting at a low memory address. Fourteen codes were continuously cycled in the driver program indicating to the ADC which channel and gain to select. Data storage locations are specified in Figure 4.16.

Overall collection rate was 196,602 data bytes in 9.148 s. Out of the 9.148 s, an average tree shake lasted 3-6 s; thus there was enough time to cover the shaker startup and shutdown activity. The 'write-to-disk' process required 1.9 minutes. Two bytes of data were required to produce one value in a code range of 0-4095. The first 7 of the 14 channels of data were each characterized by 7,023 data points in 9.148 s. The second set of seven channels received 7,020 data points. The missing three points of the channels in the second set occurred because the three 'read requests' were not multiples of 28, which was the required number of bytes for 14 channels.

4.8 Displacement Tests

A Vanner Model 80-500 (12 VDC to 120 VAC, 60 Hz, 500 Watt) sinusoidal voltage inverter, lent by the Vanner

User Identified Data Storage Locations

BANK NO.	BANK ID.	ADDRESSABLE MEMORY	SYSTEM MEMORY	CONTENTS
0	8F	2000-9FFF	2000-A000	DATA
1	80	8000-FFFF	2000-A000	DATA
2	81	8000-FFFF	2000-A000	DATA
3	82	8000-FFFF	2000-A000	DATA
4	83	8000-FFFF	2000-A000	DATA
5	84	8000-FFFF	2000-A000	DATA
6	85	8000-FFFF	2000-A000	DATA

Reserved Operating System Memory Locations

(Apple Computer, Inc.)

LOW S BANK	0F	0000-1FFF	0000-1FFF	KERNEL OPERATIONS
HI S BANK	10	A000-FFFF	A000-FFFF	KERNEL OPERATIONS
LOW S BANK	0F	1A00-1AFF	1A00-1AFF	INTERP ZERO PAGE
LOW S BANK	0F	1600-16FF	1600-16FF	INTERP EXTEND PAGE
LOW S BANK	0F	1B00-1BFF	1B00-1BFF	INTERP STACK
LOW S BANK	0F	1800-18FF	1800-18FF	DRIVER/SOS ZERO PAGE
LOW S BANK	0F	1400-14FF	1400-14FF	DRIVER/SOS EXTEND PAGE
LOW S BANK	0F	0100-01FF	0100-01FF	DRIVER/SOS STACK
HI S BANK	10	FFEF	FFEF	BANK SELECT REGISTER
HI S BANK	10	A000-B7FF	A000-B7FF	INTERP/DRIVERS
HI S BANK	10	B800-FFFF	B800-FFFF	SOS KERNEL

Figure 4.16 Data storage locations for the 6502-based data acquistion system in the Sophisticated Operating System Environment.

Corporation (Columbus, Ohio), provided electric power at 120 VAC. Our acquisition system full load voltage was 120.2 VAC with smooth sinusoidal output. No-load voltage was 123.8 VAC with a voltage spike at points of maxima and minima in the output waveform. Frequency was constant at 60 Hz with and without load.

The inverter was connected to the battery posts of the van for input power. During use, the engine idle on the van was increased to maintain the necessary charging capacity.

The van body was taken as ground potential when connecting electrical devices. Problems later arose with charge build-up in the van body from the frictional charge-separating action of the engine fan belts on the pulleys. A galvanized-steel ground-rod was driven 76 cm (30 in) into the soil near the vehicle and connected to the vehicle body with #12 stranded copper wire. This eliminated the charge build-up problem.

Displacement tests were conducted on tart cherry trees in the Michigan State University Horticultural Orchards. All trees were in the same general location and were presumed to have the same soil base. Six trees were chosen to be shaken. A period of three days was required for data collection. Trees were tested twice each, once at 1500 shaker rpm and once at 2200 shaker rpm. These speeds provided frequencies of 9.3 and 14.0 Hz,

respectively, for each of the two eccentric masses. The actual frequency of vibration imparted to the tree was a combination of individual frequencies. Three trees of 11 cm (4.5 in) and three of 16 cm (6.5 in) trunk diameter at clamp height were selected for testing. The clamp was positioned according to common practice, which, on older trees, was normally 25-30 cm (10-12 in) above ground level. The shaker body was positioned orthogonal to the tree axis. The trunk was centered in the pad, Figure 4.17. For greater accuracy in shaker clamp positioning, the tractor driver was guided to the trunk by a flagman; in production operations, this precaution is not taken due to the time and expense of a second worker.

The following were recorded: clamp height above the soil surface, clamp opening, and accelerometer location with respect to the tree center and the soil surface, date, engine rpm, and tree identification data.

All amplifiers were zeroed before each test. The LVDT slide rod was centered for zero readout and was then fastened to the clamp. The tree was clamped at a recommended pressure of 49 kg/cm^2 (700 psi). The desired engine speed was obtained and the control system was initialized for data collection. After 1-2 s, the shaker operator was signaled to begin the shake. A shake lasted 3-5 s. The shaker operator was then signaled to end the shake; there were 2-3 s of shut-down data at the

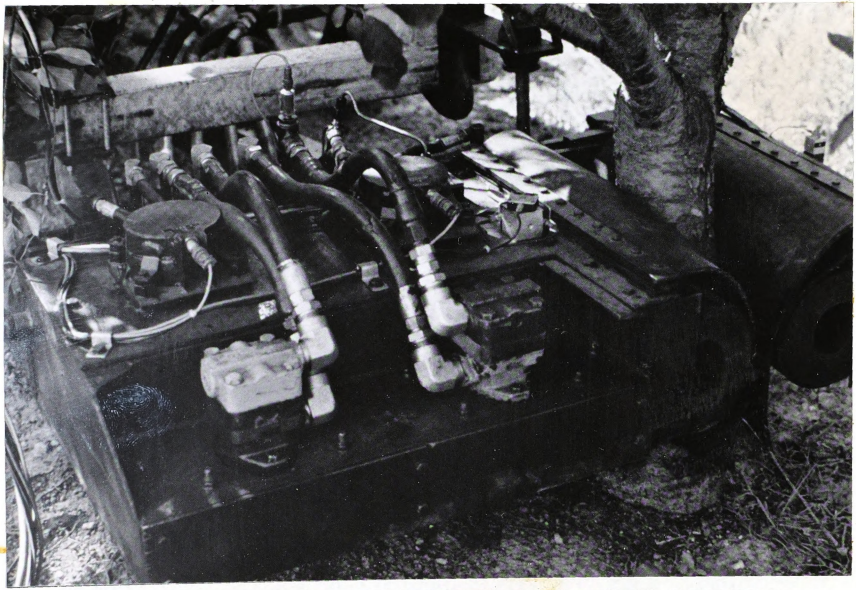

Figure 4.17 Cherry tree trunk centered in shaker clamping jaw. Flaps between the tree and the cylindrical pads are coated with grease to reduce shear stress on the bark.

end of the data acquisition period.

The data were stored on two 140 kilobyte "floppy disks". While the 196 kilobytes of transducer data and time information were being transferred to the magnetic media (1.9 minutes), the LVDT was unfastened and the clamp was released from the tree. The process was repeated for each test such that all instrument settings and clamping pressures were the same at the start of every run.

For each tree diameter, the last tree to be shaken was analyzed for pivot motion about the tree base. The XY block of accelerometers was removed from the tree and a hole was drilled in the tree in the X direction below the pad, vertically in line with the previous single X sensor. Average height from soil surface was 8 cm (3 in), Figure 4.18. Shaking tests were repeated with the sensor at this point. Therefore, X movement was detected at 8 cm (3 in) and 46 cm (18 in) above soil surface. The relative difference would be an indicator of pivot motion about the tree base.

A test at each engine speed was conducted for free shake (no tree in the clamp) and free idle (tree in clamp with no shaking, engine running at shaking speed). This information may be useful for detecting otherwise unnoticed vibrations inherent in the mechanism.

The pressure of the clamping cylinder was checked for constancy and maximum deviation during a test. The

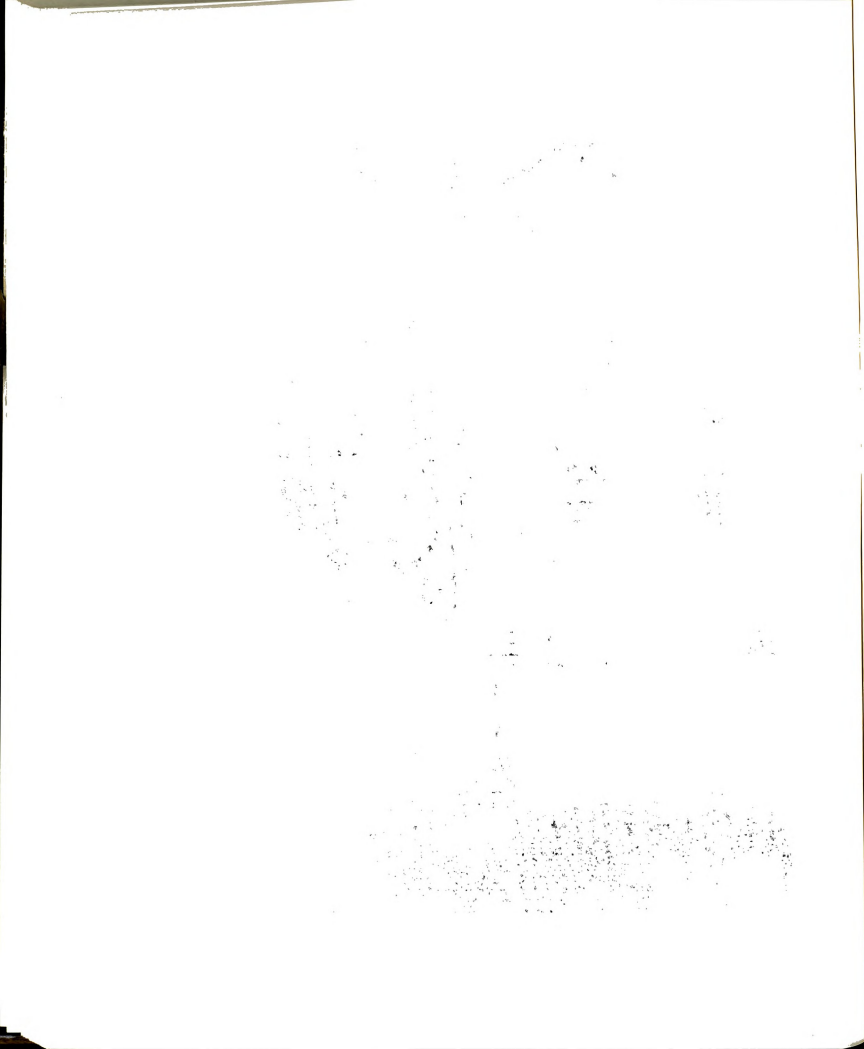

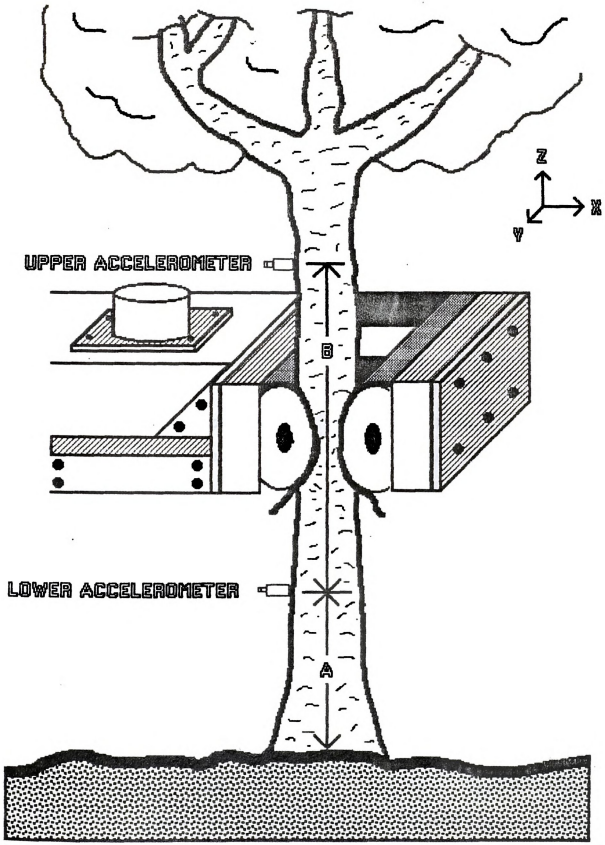

Figure 4.18 Physical Location of Tilt Detecting Sensors Relative to the Tree and the Shaker.

LVDT correlated clamp displacement with time. The electromagnetic sensors detected the times at which masses were in a known position. The microprocessor's real-time clock provided the time to which all physical events occurring during the shaker tests were referred.

4.9 Method of Data Analysis

Data on each floppy disk were analyzed with a Pascal-programmed integration and calibration algorithm. The original order of data in a file was high byte, low byte starting at low memory address. Every two bytes represented the code of one voltage reading. Since 14 consecutive channels were scanned, every 28th and 29th bytes starting with bytes 0 and 1 were Channel 0 data. A program was written to read the original encoded information by byte and display the codes on the video screen in order to verify the data. The Pascal language required an integer to be in the form low byte, high byte. Therefore, in order to read coded information with UCSD (University of California, San Diego) Pascal into the integration and calibration program, it was necessary to flip the byte order for each integer. During this process, the data were separated into files according to channel number, then re-stored in six files with file seven containing time.

Calibration was accomplished with constants

obtained in laboratory tests with the instruments employed. The integration-calibration program read in the coded information, converted codes to voltages (knowing the scale from which the ADC read a channel), filtered amplifier offsets from the voltages, integrated acceleration data twice to get displacement, and finally, plotted the results as they varied with time. The maxima and minima of the values were secured and displayed. The plots could be stored on disk for later retrieval and printing.

The double integration was a digital linear quadratic fitting process. Piecewise quadratic integration allowed a smooth fit to a sinusoidal curvature without the oscillations of higher-powered fittings. More complex methods would not have necessarily provided a better fit for a simple waveform. Observations of collected data verified sinusoidal or nearly sinusoidal acceleration waveforms for the shaker and tree tests conducted.

Difficulties arising from variable frequencies and irregular amplitudes prevented calculation of displacements in all directions on the shaker. Displacement vectors were obtained in the X direction only for the sensors at the bark-pad interface. Digital integration of the acceleration traces produced superimposed displacement waveforms in several

frequencies. Some low frequency components prevented accurate interpretation of the higher frequency displacements of major interest. Therefore, attempts were made to remove any low frequency components and/or amplifier drift or external unidentified interference.

Using piecewise linear regression to translate the data base did not provide an easy, intelligible means of interpreting results. Steady state shaker traces were less obscured by this method than the transient start-up and shut-down regions of an accelerometer waveform. System memory and processing time constraints prevented programming of high order polynomials to remove undesired underlying signals. Several traces with amplifier drift displayed exponential waveforms underneath the true data. The time constant of this exponential was usually much longer than the period of data acquisition and was not estimable. The resulting displacement traces were meaningful but not completely accurate. Therefore, not all accelerometer traces were integrated. For purposes of presenting the difficulties encountered, several of the displacement traces are presented in Chapter 5.

CHAPTER 5

RESULTS AND DISCUSSION

Rubber clamp pads were investigated for the triboelectric phenomenon as a tool for force measurement. Machine and tree response to shaker vibration were characterized in digital waveform with the instruments and data acquisition system described in Chapter 4. Shaker frequencies of 9.3 and 14.0 Hz were applied to both 11.0 cm (4.5 in) and 16.5 cm (6.5 in) diameter trees. Acceleration data were twice integrated to displacement for determination of critical maxima in the X direction. Clamping cylinder pressure was evaluated for constancy; clamping motion of the clamping arm was also monitored. A discussion of the error associated with the digital data acquisition process, including suggested improvements, concludes this chapter.

5.1 The Triboelectric Test on Shaker Clamp Pads

The compression of a rubber clamp pad (a dielectric) on a 20 cm x 25 cm (8 in x 10 in) steel plate in a hydraulic press produced small negative charges similar to those described by Richards (Memmler, 1934).

These results are shown in Table 5.1 with probe position shown in Figure 5.1. Measurements are in volts as detected by the measurement system. Conversion to a unit standard employs the following relation:

$$\frac{\text{Given Volts}}{\text{Given Pressure (psi)}} * 3.2828 = \frac{\text{esu}}{\text{kg/cm}^2}$$

Where esu = 1 electrostatic unit
= 1 Stat-couloumb
= 3 x 10E-9 Coulombs

As pressure was applied to the pad, small negative voltages were monitored from the charge produced in the dielectric. A typical plot is shown in Figure 5.2. The small negative charges which developed in the pad were linearly proportional to the applied load for loads up to 2.8 kg/cm^2 (40 psi), but for larger loads, the increase in charge diminished. At large loads, there is probably discharging from the rubber to the surroundings overriding the charge increase for any further increase in load. The charge increase per load increment is shown in Figure 5.3.

For small loads up to 2.8 kg/cm^2 (40 psi), when the load was removed, the charge was opposite in sign and equal in magnitude to that resulting from the applied load. Removal of the larger loads resulted in a hysteresis effect with no apparent proportionality to

Table 5.1. Output voltage (volts) from the charge generated by compression of a rubber shaker clamp pad (triboelectric phenomena). Position reference Figure 5.1. Multiply volts/psi by 3.2828 to get esu/kg/cm^2.

Probe Position	Pressure psi (kg/cm^2)																		
	0 (0)	10 (0.7)	20 (1.4)	30 (2.1)	40 (2.8)	50 (3.5)	60 (4.2)	70 (4.9)	80 (5.6)	90 (6.3)	80 (5.6)	70 (4.9)	60 (4.2)	50 (3.5)	40 (2.8)	30 (2.1)	20 (1.4)	10 (0.7)	0 (0)
A - B	0	-1.28	-2.32	-3.20	-3.92	-4.24	-4.32	-4.24	-4.00	-3.60	-3.28	-2.88	-2.32	-1.66	+2.40	+5.60	+6.80	+7.04	+10.00
A - C	0	-0.56	-1.12	-1.52	-1.84	-1.92	-2.00	-1.84	-1.68	-1.52	-1.36	-1.20	-1.04	-0.80	-0.64	-0.56	+0.48	+0.76	+ 4.24
A - D	0	-1.20	-2.24	-2.88	-3.28	-3.52	-3.52	-3.36	-3.20	-2.80	-2.56	-2.32	-2.00	-1.44	+1.04	+1.48	+1.68	+2.40	+ 7.20
B - C	0	-0.96	-1.52	-1.68	-1.68	-1.60	-1.44	-1.12	-0.96	-0.64	-0.40	-0.32	-0.16	-0.04	+0.08	+0.88	+0.98	+1.20	+ 2.96
B - D	0	-0.80	-1.68	-1.92	-2.00	-1.92	-1.76	-1.52	-1.28	-1.04	-0.96	-0.72	-0.48	-0.32	-0.08	+0.44	+1.20	+2.00	+ 3.06
C - D	0	-3.20	-5.60	-6.16	-6.32	-5.84	-5.20	-4.72	-4.24	-3.28	-2.80	-2.72	-2.32	-1.84	-1.44	-0.80	+1.28	+2.20	+ 6.08
E - F	0	-2.48	-4.64	-5.52	-5.92	-6.08	-6.00	-5.84	-5.62	-5.20	-4.96	-4.68	-4.32	-3.68	-3.12	-2.56	+0.88	+3.20	+ 5.16
G - H	0	-0.56	-0.88	-1.12	-1.20	-1.12	-1.04	-1.04	-1.04	-1.04	-1.04	-1.04	-0.72	-0.08	+0.88	+4.16	+6.40	+8.00	+10.16
G - I	0	-2.56	-4.40	-4.80	-4.72	-4.32	-3.68	-3.20	-2.88	-2.32	-2.00	-1.76	-1.20	-0.24	+0.40	+3.28	+4.00	+6.00	+10.20
G - J	0	-1.52	-2.80	-3.12	-3.20	-3.12	-2.96	-2.88	-2.80	-2.64	-2.32	-2.16	-1.68	-0.64	-0.24	-0.48	+4.16	+4.88	+ 9.84
H - I	0	-1.60	-2.88	-3.28	-3.12	-2.80	-2.48	-2.08	-1.76	-1.44	-1.20	-0.96	-0.56	-0.08	+0.32	+1.76	+4.32	+5.28	+ 9.86
H - J	0	-1.68	-2.56	-2.80	-2.72	-2.48	-2.24	-2.08	-1.84	-1.60	-1.36	-1.12	-0.64	-0.08	+0.64	+3.18	+3.36	+4.40	+ 9.84
I - J	0	-3.68	-3.92	-4.08	-4.08	-3.84	-3.52	-3.28	-2.96	-2.40	-1.92	-0.96	-0.16	+3.68	+3.82	+6.48	+8.56	+8.92	+ 9.84

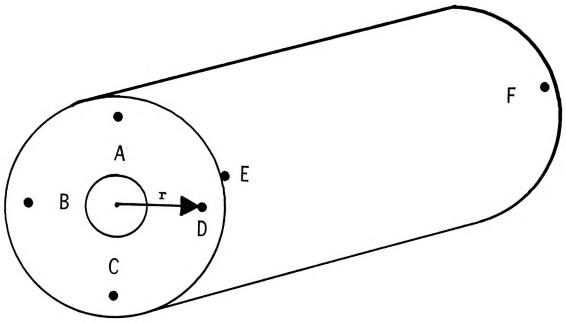

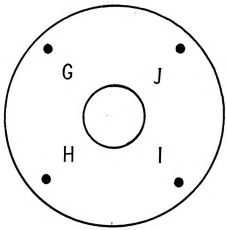

Figure 5.1 Geometry of probe connections on rubber pads. (r=70 mm).

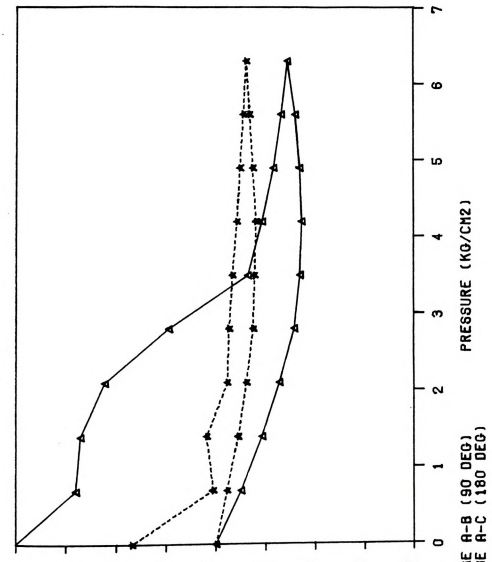

Figure 5.2 Amplified response of rubber clamp pads to applied load.

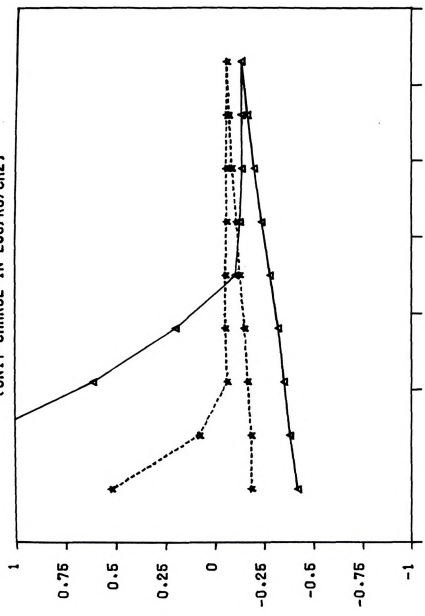

Figure 5.3 Output charge increment for a load applied to rubber clamp pads.

pressure where the final charge was greater than the charge during application of the load. This charge was also dependent on the geometry (direction of strain) in the pad as can be observed from the different charges arising at different measurement locations on the pad for the same load. The charges observed for small loads (0-3 kg/cm^2) agree with those presented by Brain and Richards (Davis et al., 1937) for a material that might be classified as a pliable, semi-hard rubber. These charges ranged from -0.2 to -0.4 $esu/kg/cm^2$ load.

An impulse created with a steel hammer produced charge impulses proportional to the applied force. After repeated impulse application, however, charge was produced on both the hammer and the rubber pad which appeared to be opposite in signs. Movement of the statically charged hammer near the charged pad produced a momentary change in the charge exhibited by the pad. This effect caused me to notice that the charge responded to the passing of any charged object near the pad. Interference of the two electric fields apparently altered the electron-hole density distribution regulated by the pad's static field.

The above observations covered static and impulse loadings. Observation of dynamic loading starting at very low frequencies (30 cpm) revealed a charge saturation effect occurring after only a few cycles. The depletion of charge upon removal of the load appeared to have a

definite time constant which I could not reproduce at a frequency above this. Observation of this application of this low cyclic loading suggested material fatigue. Material fatigue would prevent the reproducible recording of a time varying force from a charge measurement.

The exhibition of hysteresis and saturation, the susceptibility to weak stray electric fields, and the low maximum loading which produced an output change in the pad charge made the triboelectric phenomena impractical for force measurement on the cherry shaker. Perhaps for small, near-static loading in an electrically isolated environment, the triboelectric effect could be useful.

5.2 Pad Deformation by Displacement Measurements

A new idea for a two step (indirect) force measurement was conceived. The measurement of shaker and tree displacement would allow reproduction of maximum displacement conditions of the shaker and tree in a laboratory environment where pressure transducers, mounted inside a model tree (steel pipe), could characterize the concentration of force beneath the pad's surface. In this manner, the simulation of the tree and shaker could provide critical information leading to the classification of maximum potentially-damaging stress conditions imparted by the shaker.

Accurate real-time displacement measurements

could be obtained by the double integration of acceleration measurements. This process was carried out as in Chapter 4. The results of the shaker and tree sensors follow.

5.3 Firmness of Clamp

This investigation of the forces a shaker imparts to a cherry tree was initiated partly on the hypothesis that tree decline results from internal (unseen) trunk damage caused by shaker harvesters. A sub-hypothesis is that trunk damage may result from the unintended beating of the tree by a loosened clamping-arm. Inadequate or variable clamping pressure would cause the clamp arm to periodically grip and release as the forces change direction.

Clamp arm movement was detected using a linear voltage differential transformer (LVDT) which had a conversion factor of 4.0 mV/mm. Several tests were conducted on trees of different diameters. Data for these tests are given in Table 5.2 (c.f. Figure 5.4). The results of clamping force tests are shown in Table 5.3. All data are presented in Figures 5.5-5.8. The initial values are the values of the LVDT before shaking began. This is given in the table to be consistent with the graphs and to allow meaningful difference calculations. A positive-bound peak in the plot indicates a motion of the

Table 5.2. Physical measurements at tree - shaker interface (c.f. Figure 5.4). All measurements in cm.

Test Date	Tree ID	Tree Dia at Clamp	Tree Dia at Accel.	a[1]	b[1]	c[1]	Accelerometer Height from Ground	Clamp Height from ground
9/8/83	1	16	20	13	10	26	46	23
9/9/83	2	17	16	11	10	26	58	36
9/9/83	3a	16	19	11	13	25	47	25
9/12/83	3b*	16	19/22	-	-	25	47/9	25
9/12/83	4	12	12	9	7	25	46	28
9/12/83	5	12	12	9	7	23	47	30
9/12/83	6a	12	12	9	7	22	46	28
9/12/83	6b*	12	12/12	-	-	23	46/8	28

* Data designated by "b" are from a separate tilt test discussed in Chapter 4.

1. See Fig. 5.4.

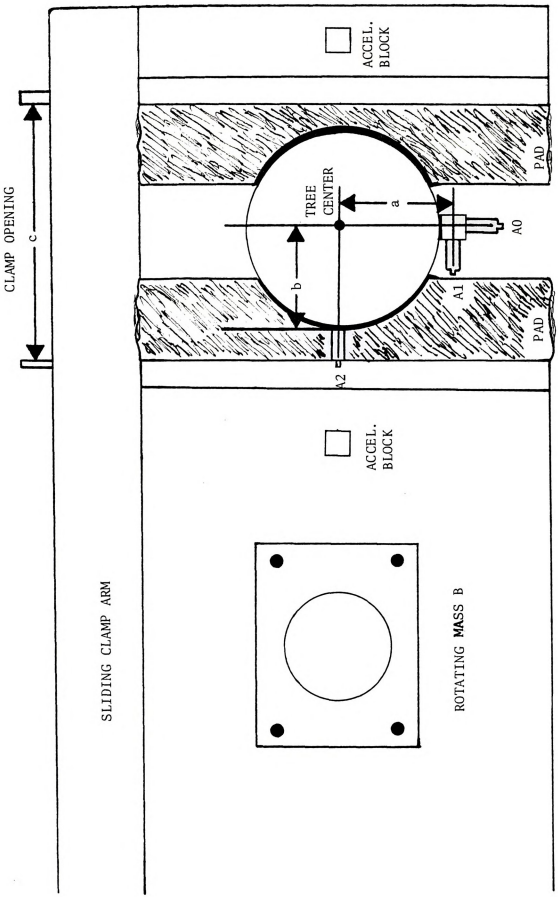

Figure 5.4 Tree and shaker geometry depicting variables measured for trunk shaker vibration tests.

Table 5.3. Linear movement of the shaker clamping arm during harvest. (All values in mm.) Positive values indicate a loosening action, negative values indicate a tightening action.

Tree ID	Tree Diameter	9.3 Hz				14.0 Hz			
		Positive Deflect.	Negative Deflect.	Average Deflect.	Final Deflect.	Positive Deflect.	Negative Deflect.	Average Deflect.	Final Deflect.
1	16.0 cm (6.3 in.)	1.61	-1.76	-0.53	-0.50	1.21	-2.64	-1.05	-1.25
2	17.0 cm (6.7 in.)	1.06	-1.80	-0.67	-1.10	2.60	-1.61	-0.39	-0.45
3a	16.3 cm (6.4 in.)	3.42	-3.01	-1.34	-1.75	0.55	-2.65	-0.90	-1.20
3b	16.3 cm (6.4 in.)	2.52	-1.90	-0.80	-0.90	3.08	-2.52	-0.82	-1.12
4	11.7 cm (4.6 in.)	0.00	-2.20	-2.14	-2.20	0.18	-2.65	-0.90	-1.13
5	11.9 cm (4.7 in.)	2.39	-2.45	-0.54	-0.57	2.26	-2.57	-0.36	-0.36
6a	11.7 cm (4.6 in.)	2.57	-3.34	-1.07	-1.07	2.15	-2.43	-0.48	-0.53
6b	11.7 cm (4.6 in.)	1.85	-3.10	-0.83	-0.90	2.26	-2.19	-0.65	-0.65
Free		0.65	-1.25	-0.12	0	0.60	-1.25	-0.04	-0.06

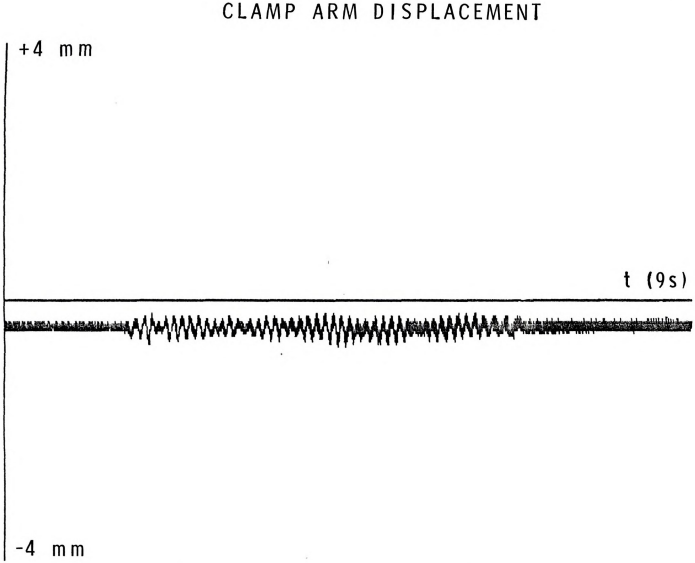

Figure 5.5 Linear Voltage Differential Transformer Trace displaying clamp arm Movement. Test: Eta, 9.3 Hz, No Tree.

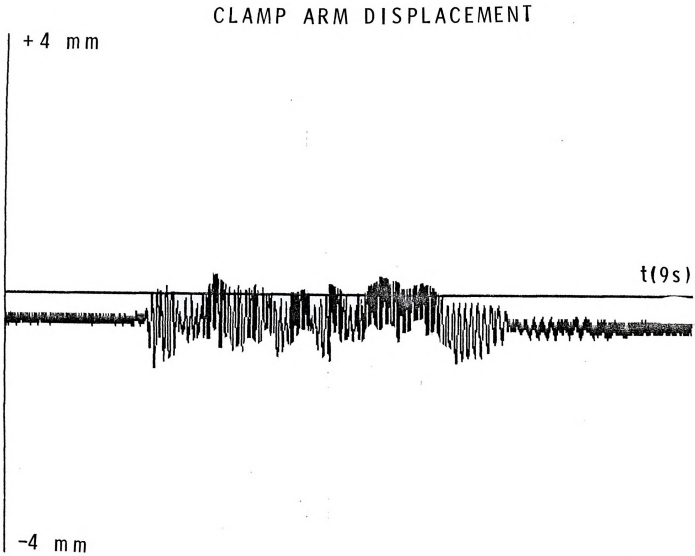

Figure 5.6 Linear Voltage Differential Transformer Trace displaying clamp arm Movement. Test: Zeta, 14.0 Hz, No Tree.

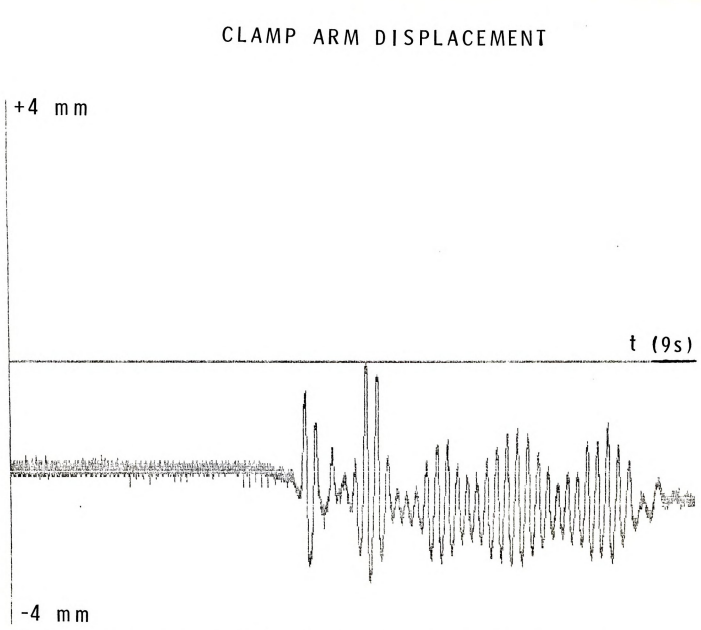

Figure 5.7 Linear Voltage Differential Transformer Trace displaying clamp arm Movement. Test: Alpha, 9.3 Hz, 16 cm (6.5 in) Tree.

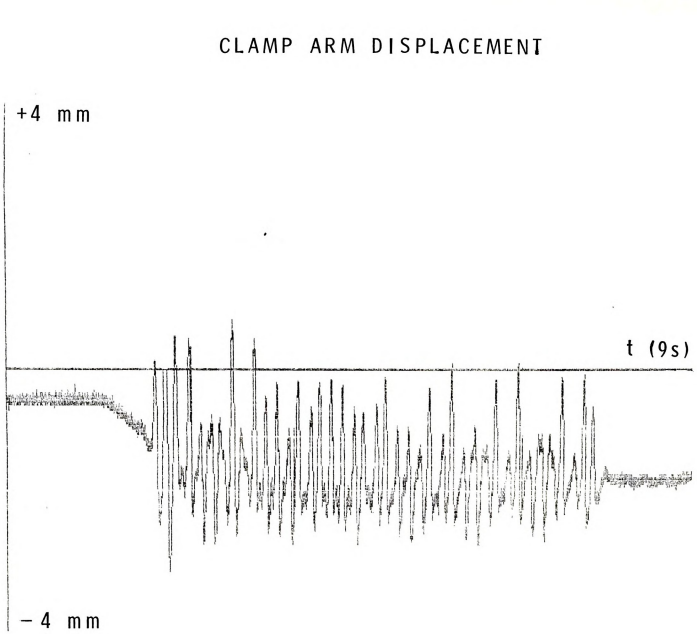

Figure 5.8 Linear Voltage Differential Transformer Trace displaying clamp arm Movement. Test: Beta, 14.0 Hz, 16 cm (6.5 in) Tree.

clamp arm in the positive X direction (c.f. Figure 4.5) which would be a loosening of the arm from around the tree. A negative-bound peak then indicates a tightening of the clamp arm from a given starting position.

The data indicate that in all cases, motion of the clamping arm was less than 0.5 cm. This motion always occurred during the first second of shake and was evidenced as a tightening effect of the clamp arm (Figure 5.9). The most probable explanation for this event is a physical 'relaxation' positioning of the shaker pads around the tree. As the initial tightening of the clamp occurs, a momentary release follows soon after as a one time maximum event. The clamp arm appears to be tightened during a period of transient action of the harvester and then momentarily releases during a transient response to the harvester or tree as a system.

This initial motion could be caused by stickiness in the clamp where the initial vibration allows the clamp to seek its final position. Clamp arm movement inward could also be related to air in the cylinder and hoses, as well as hose expansion. The diameter of the tree may even change slightly as the rough protruding bark is compressed by clamping forces.

While these very small clamp arm displacements may be insignificant in terms of tree damage, they do give a very important indication that tree damage potential may

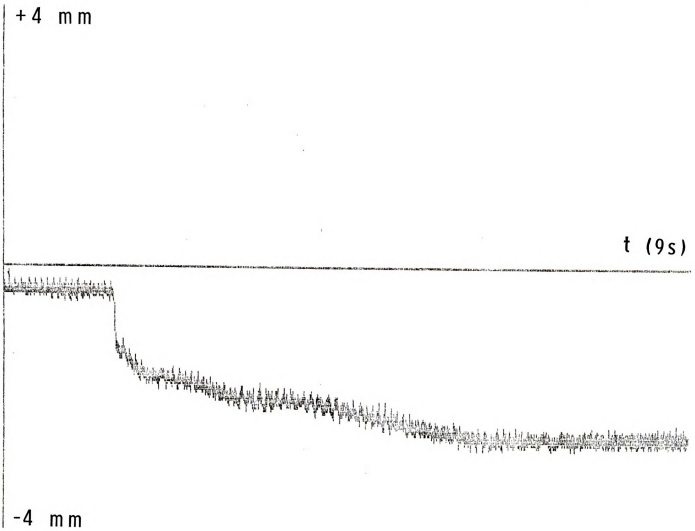

Figure 5.9 Linear Voltage Differential Transformer Trace displaying clamp arm Movement. A tightening occurs in the clamp arm immediately after shaking begins. Test: Omicron, 9.3 Hz, 11 cm (4.5 in) Tree.

be more crucial during the transient operations of start-up and shut-down than during the quasi-steady state operation. This, in turn, may be due to a response by the shaker or the tree passing through frequencies of resonance.

5.4 Pressure Factors in Slip

A major concern in damage to stone fruit trees, particularly cherries, has been the slippage of the shaker pads across the surface of the tree. This slippage can occur longitudinally, tangentially, or in combination.

Changes from the recommended clamping pressure (49.3 kg/cm^2, 700 psi) were considered critical since a significant increase in pressure could cause the bark to split or crush while a significant decrease in pressure could allow the pad to slip over the bark.

A pressure sensor placed in the clamp's high pressure line monitored the clamp pressure throughout each test (Figures 5.10-5.13). The results are presented in Table 5.4.

The clamping pressure exhibited a worst case of 14% overclamp and 11% underclamp from the recommended pressure. The average pressures are observed to be within 15% or less for all tests. The ending pressure in every test is less than the beginning pressure which would indicate at first glance that a loosening of the clamp arm

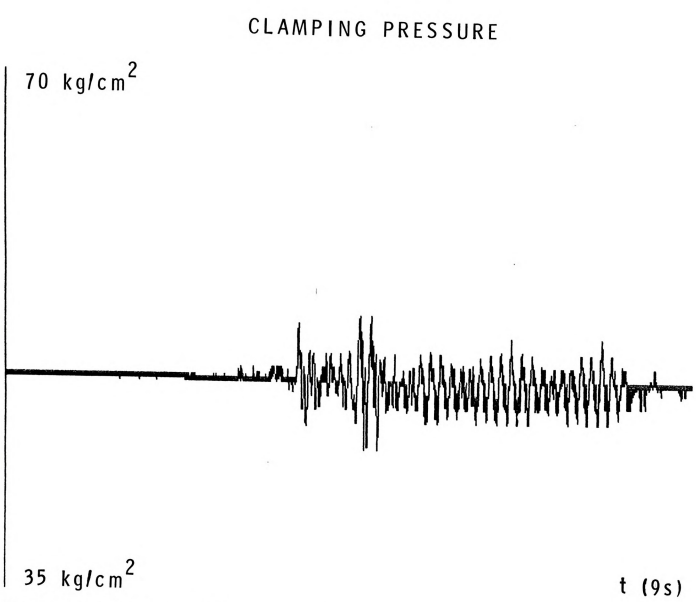

Figure 5.10 Clamping cylinder pressure trace revealing peak pressures during shake harvesting of cherry trees. Test: Alpha, 9.3 Hz, 16 cm (6.5 in) Tree.

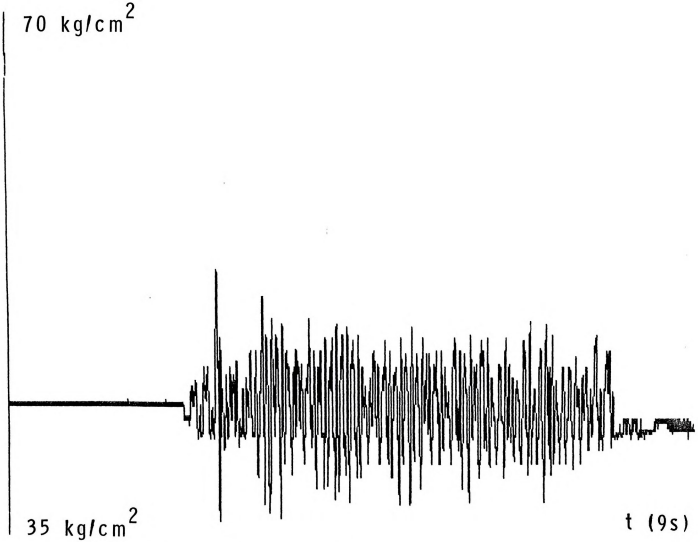

Figure 5.11 Clamping cylinder pressure trace revealing peak pressures during shake harvesting of cherry trees. Test: Delta, 14.0 Hz, 16 cm (6.5 in) Tree.

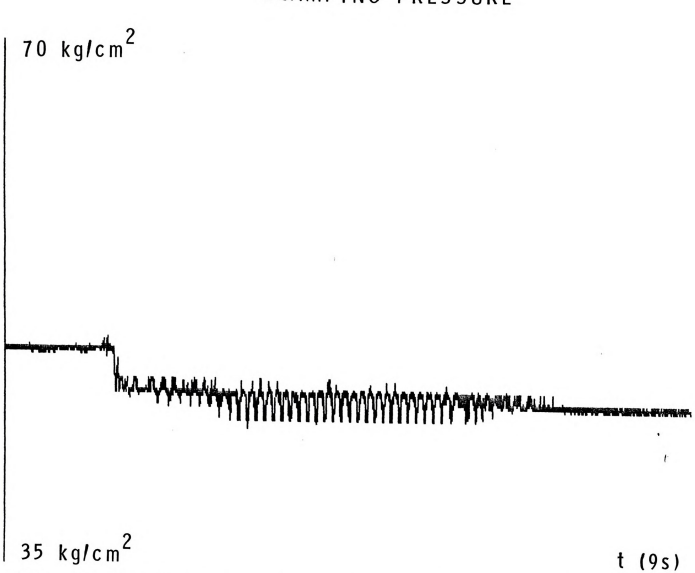

Figure 5.12 Clamping cylinder pressure trace revealing peak pressures during shake harvesting of cherry trees. Test: Omicron, 9.3 Hz, 11 cm (4.5 in) Tree.

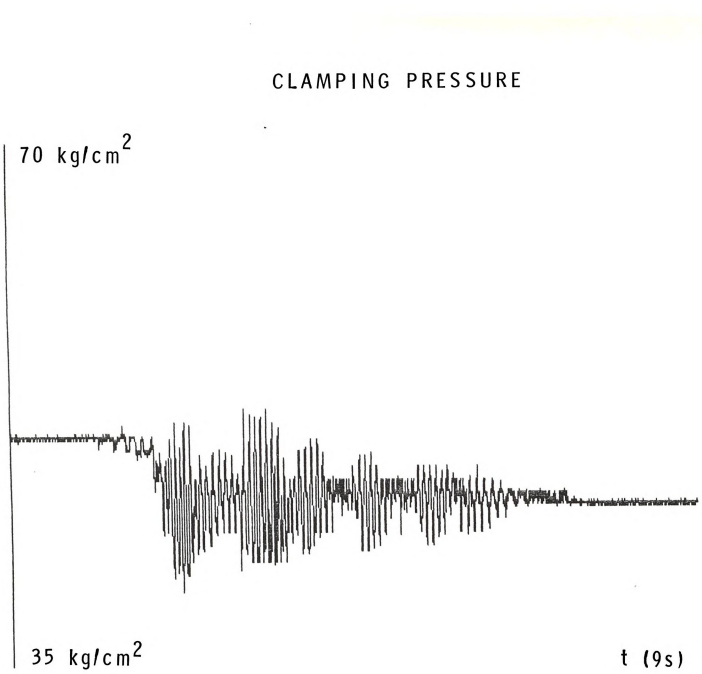

Figure 5.13 Clamping cylinder pressure trace revealing peak pressures during shake harvesting of cherry trees. Test: Theta, 14.0 Hz, 11 cm (4.5 in) Tree.

Table 5.4. Clamping cylinder pressures resulting from trunk shaking cherry trees (Target pressure = 49.3 kg/cm^2 (700 psi)).

Tree ID	Weight Frequency (Hz)	Beginning Pressure	Minimum Pressure	Maximum Running	Maximum Startup	Deviation	Average Pressure	Ending Pressure
			11 cm (4.5 in.) Diameter Trunks					
1	9.3	49.7 (706)	44.5 (631)	47.8 (678)	50.6 (718)	3.3 (47)	47.1 (668)	45.9 (651)
2	9.3	48.0 (681)	42.1 (598)	48.8 (692)	48.7 (691)	6.6 (94)	46.8 (664)	46.0 (653)
3a	9.3	44.0 (624)	40.3 (572)	43.6 (619)	44.0 (624)	3.3 (47)	42.1 (598)	42.1 (598)
3b	9.3	51.8 (735)	47.9 (680)	53.2 (755)	53.0 (752)	5.3 (75)	49.7 (705)	49.7 (705)
1	14.0	50.7 (719)	40.2 (571)	52.6 (746)	-	12.3 (175)	47.2 (670)	46.1 (655)
2	14.0	51.6 (733)	41.3 (586)	55.6 (789)	52.5 (745)	14.3 (203)	49.7 (705)	49.6 (704)
3a	14.0	53.3 (756)	43.0 (611)	58.8 (835)	53.3 (756)	15.8 (224)	50.6 (718)	49.8 (707)
3b	14.0	53.3 (757)	44.3 (629)	59.5 (845)	54.2 (769)	15.2 (216)	52.3 (743)	51.8 (736)
			16 cm (6.5 in.) Diameter Trunks					
4	9.3	49.7 (706)	44.7 (635)	53.4 (765)	50.4 (716)	9.2 (130)	49.3 (700)	49.3 (700)
5	9.3	51.4 (730)	46.4 (659)	53.3 (756)	-	6.8 (97)	49.3 (700)	48.6 (690)
6a	9.3	52.8 (750)	47.2 (670)	55.6 (789)	-	8.4 (119)	50.0 (710)	49.8 (707)
6b	9.3	50.1 (711)	44.6 (633)	54.9 (780)	50.9 (723)	10.4 (147)	49.0 (696)	48.3 (685)
4	14.0	56.4 (800)	50.4 (716)	-	-	-	55.0 (780)	53.4 (765)
5	14.0	44.0 (625)	36.2 (514)	53.2 (755)	-	17.0 (241)	45.1 (640)	42.3 (600)
6a	14.0	55.9 (793)	51.1 (725)	60.2 (855)	-	9.2 (130)	54.5 (774)	53.5 (760)
6b	14.0	49.9 (708)	39.0 (553)	60.9 (865)	-	22.0 (312)	47.9 (680)	47.9 (680)

had occurred. However, the opposite is true and is verified by the following argument.

As the clamp is locked up, the pad is put under sudden stressed compression. The pad does not have the freedom to conform in a 'bind free' state. As the shake begins, the pad can 'unwind' and continue conformation around the tree. This process can be termed 'pad relaxation'. As the pad 'relaxes', the clamp arm moves closer to the tree by a very small amount, as referenced in the previous section as clamp arm tightening. The clamp's hydraulic circuit is locked on the pressure side during shake by a pilot operated check valve. Since the pressure sensor monitors the closing pressure side of the clamp's hydraulic circuit, a tightening or closing of the clamp arm is indicated by pressure relief in the cylinder (Figure 5.10). Therefore, at the end of a tree shake, the clamp arm has moved inward to tighten to within 4 mm with an average clamp pressure reduction of 2.4 kg/cm^2 (34 psi).

Some pressure fluctuation would normally be expected due to hose elasticity and air in the hose and cylinder. This appears to range from 0.2-0.4 kg/cm^2 (3-6 psi).

Assuming little leak in the check valve with a fixed initial pressure, the changes in pressure in the cylinder must be accounted for by the changes due to air

in the hoses and cylinder and the hose elasticity, changes in tree diameter due to bark compression, and changes caused by arm movement (pad relaxation). The change due to normal fluctuations in the circuit is negligible for practical purposes. Thus, the pressure is related to the movement of the arm which can be thought of as a function of two variables: 1) movement due to 'pad relaxation' and 2) movement due to the resultant of the applied and resistive forces. With this in mind, cylinder clamp pressures can be converted into forces directed in the -X direction (c.f. Figure 4.5) radially inward on the tree. This is only a unidirectional force on the tree since the low pressure side of the dual action clamp cylinder was not monitored.

The hydraulic clamp cylinder has a 7.62 cm (3.00 in) inside diameter with a 3.18 cm (1.25 in) diameter rod. The net pressure area is 5.84 cm^2 (0.91 in^2). Forces may be calculated from F=PA. The results of the force calculation are shown in Table 5.5.

The average force over all tests was 18110 N (4070 lb), a difference of only 85 N (19 lb) from the desired force of 18190 N (4089 lb) (which has a standard deviation of 1195 N (268 lb)). Maximum forces were 20500 N (4609 lb) on the 9.3 Hz shake and 22220 N (4994 lb) on the 14.0 Hz shake. Maximum force deviation was 5820 N (1309 lb) at 14.0 Hz on the 11 cm trees and 8110 N (1823

Table 5.5. Forces generated by clamping cylinder pressures on a tree trunk in the -X direction. All forces in Newtons (pounds-force). (Target force = 18190N (4089 lb)).

Tree ID	Weight Frequency (Hz)	Beginning Force	Minimum Force	Maximum Dynamic	Maximum Startup	Deviation	Average Force	Ending Force
				11 cm (4.5 in.) Diameter Trunks				
1	9.3	18340 (4124)	16390 (3686)	17630 (3960)	18660 (4194)	1220 (274)	17360 (3902)	16910 (3803)
2	9.3	17690 (3978)	15540 (3493)	17980 (4042)	17954 (4036)	2440 (549)	17250 (3879)	16970 (3814)
3a	9.3	16210 (3645)	14860 (3341)	16080 (3616)	16210 (3645)	1220 (275)	15540 (3493)	15540 (3493)
3b	9.3	19100 (4293)	17670 (3972)	19620 (4410)	19540 (4393)	1950 (438)	18320 (4118)	18320 (4118)
1	14.0	18680 (4200)	14840 (3335)	19380 (4358)	-	4550 (1023)	17410 (3914)	17020 (3826)
2	14.0	19040 (4282)	15230 (3423)	20500 (4609)	19360 (4352)	5280 (1186)	18450 (4148)	18290 (4112)
3a	14.0	25800 (4416)	15880 (3569)	21700 (4878)	19640 (4416)	5820 (1309)	18660 (4194)	18370 (4130)
3b	14.0	19670 (4422)	16340 (3674)	21960 (4936)	19980 (4492)	5610 (1262)	19300 (4340)	19120 (4300)
				16 cm (6.5 in.) Diameter Trunks				
4	9.3	18340 (4124)	16500 (3709)	19880 (4469)	18600 (4182)	3380 (760)	18190 (4089)	18190 (4089)
5	9.3	18970 (4264)	17120 (3850)	19640 (4416)	-	2520 (566)	18190 (4089)	17930 (4031)
6a	9.3	19490 (4381)	17410 (3914)	20500 (4609)	-	3091 (695)	18450 (4147)	18370 (4130)
6b	9.3	18470 (4153)	16450 (3698)	20270 (4556)	18790 (4223)	3880 (867)	18080 (4066)	17800 (4001)
4	14.0	20790 (4673)	18600 (4182)	-	-	-	20270 (4556)	19880 (4469)
5	14.0	16240 (3651)	13350 (3003)	19620 (4410)	-	6260 (1407)	16630 (3738)	15590 (3505)
6a	14.0	20600 (4632)	18840 (4235)	22220 (4994)	-	3380 (759)	20110 (4521)	19750 (4439)
6b	14.0	18400 (4136)	14370 (3230)	22470 (5053)	-	8110 (1823)	17670 (3972)	17670 (3972)

lb) occurring at 14 Hz on the 16 cm trees. Radial force from these observed pressures could be a potential cause for bark damage (Frahm et al., 1982). The smaller trees are more prone to damage and concern growers greatly.

5.5 Real Time Mass Position

Recording the times the rotating masses were in selected positions was done in anticipation of eventual correlation of possible cause and effect. Proximity sensors, placed on the shaft mounts of the rotating masses, produced pulse traces of the passing of each individual mass center of gravity. Typical pulse traces are shown in Figures 5.14-5.19. The proximity sensors are of the coil type. Therefore, pulse height was proportional to rotational speed (and frequency); pulse spacing was inversely proportional with frequency. This is evident when comparing Figure 5.14 and Figure 5.16. The 14.0 Hz test displays larger, more closely spaced pulses than the 9.3 Hz test. Non-uniform rotation of each mass can also be seen from the plots. The "phasing" of the masses is a result of the centrifugal resistance of the system as "seen" by the vibration generating rotating masses; the resistance corresponds to the activity of the tree and shaker body.

Several things can be deduced from the traces of Figures 5.14 to 5.19. The masses quickly begin to spin

MASS FREQUENCY

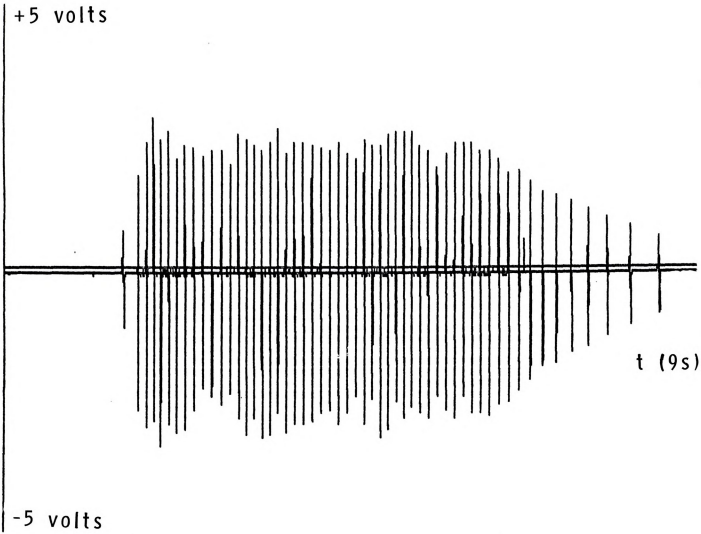

Figure 5.14 Real time proximity trace of rotating mass A with no tree in the clamp. Pulse height and spacing both indicate rotational velocity. Test: Eta, 9.3 Hz, No Tree.

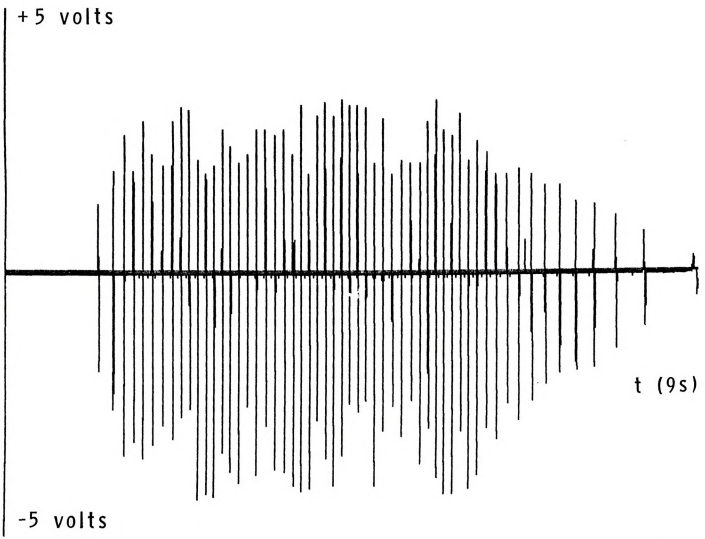

Figure 5.15 Real time proximity trace of rotating mass B with no tree in the clamp. Pulse height and spacing both indicate rotational velocity. Test: Eta, 9.3 Hz, No Tree.

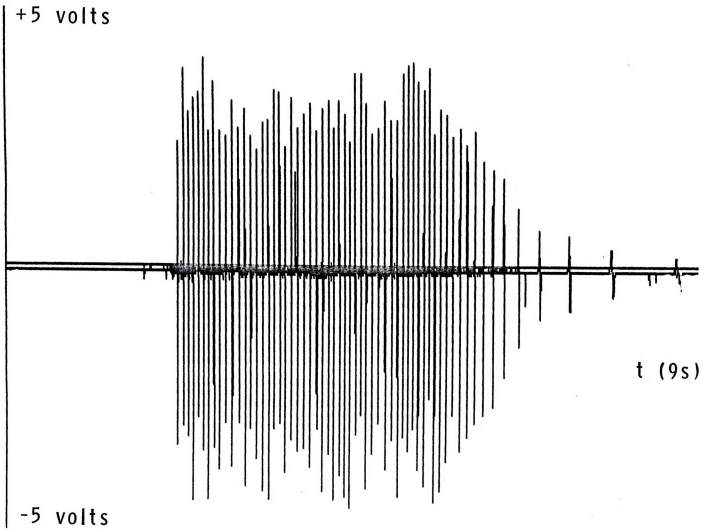

Figure 5.16 Real time proximity trace of rotating mass A with no tree in the clamp. Pulse height and spacing both indicate rotational velocity. Test: Zeta, 14.0 Hz, No Tree.

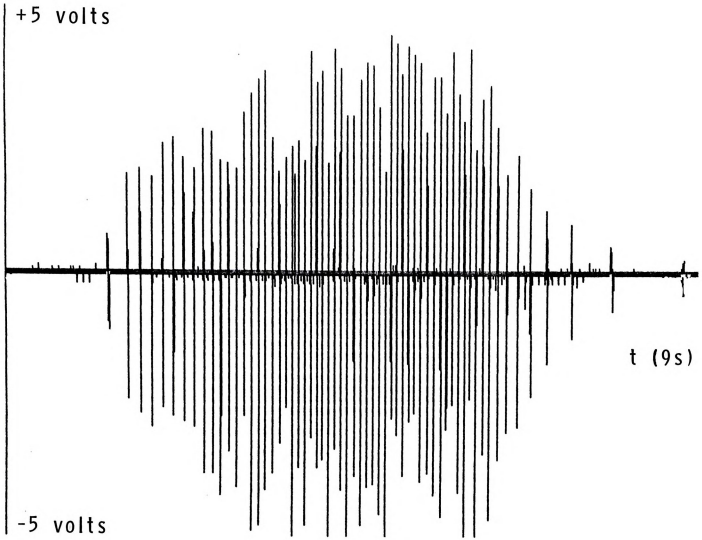

Figure 5.17 Real time proximity trace of rotating mass B with no tree in the clamp. Pulse height and spacing both indicate rotational velocity. Test: Zeta, 14.0 Hz, No Tree.

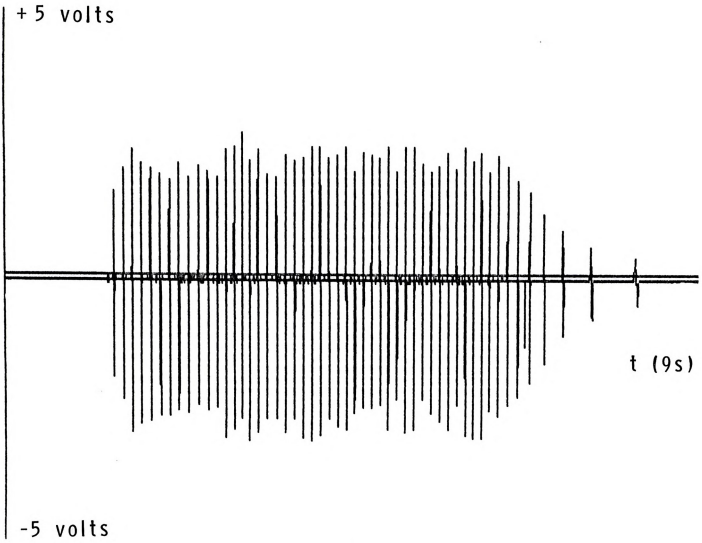

Figure 5.18 Real time proximity trace of rotating mass A with a 11 cm (4.5 in) tree in the clamp. Test: Omicron, 9.3 Hz, 11 cm (4.5 in) Tree.

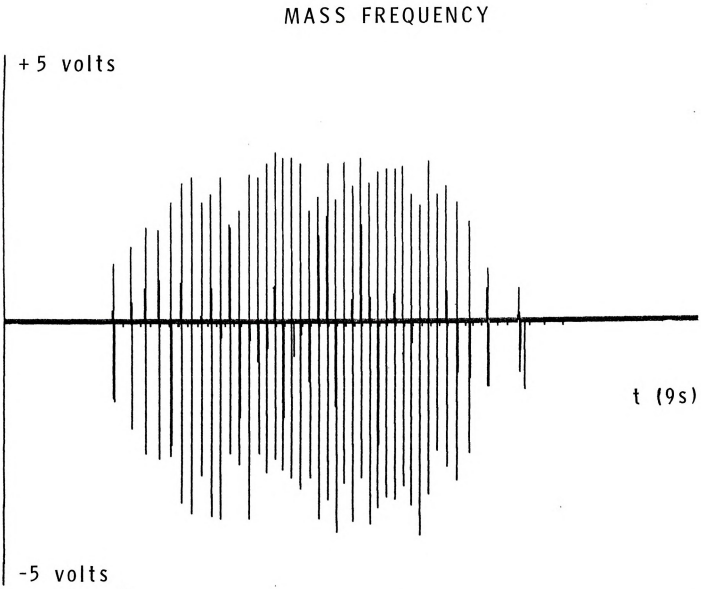

Figure 5.19 Real time proximity trace of rotating mass B with a 11 cm (4.5 in) tree in the clamp. Test: Omicron, 9.3 Hz, 11 cm (4.5 in) Tree.

when hydraulically engaged, thus creating a large acceleration. Since force is proportional to acceleration, a large initial force on the tree may be expected. With the tree just beginning to oscillate, it must pass through its first fundamental natural frequency (around 1 Hz). The possibility then exists that if this large force creates the properly directed 'detrimental' vector while the system is at the first resonant frequency, a large impact could occur resulting in longitudinal or tangential pad slip on the bark or radial crushing of the tree tissues.

The tree must react to the driving force with a resistance vector at the base of the tree (the ground structure). The inertia and damping of the upper branching structure of the tree also contributes to resistance to the driving force. Normal forcing by the wind causes the tree to bend as a cantilever with the base of the tree as the point of pivot. However, imparted force at the trunk by a fruit harvester tends to cause a whipping of the tree structure starting at the point-of-force application, then migrating to the top of the tree where it is dampened by the leaves and branches (the "fly-rod" effect). This bending imparted near the base of the tree trunk is not a normal application in nature. This may cause unforeseen strain in the inner tissues.

The maximum arm displacements as measured by the LVDT (Figures 5.5-5.8) tend to verify this theory by the existence of maximum arm displacement during the transient up-to-speed operation. This start-up transient maximum also occurs in the clamp pressure plots.

In the next section, it will be shown that maximum shaker motor pressure occurs at start-up of the rotating masses. This time period apparently involves the largest excitation forces which must be transferred to the shaker body with direct connection to the tree.

The opposite is seen to hold during the transient shut-down period. As oil flow is reduced to zero in the drive motor, the eccentric masses come to a halt at a moderate deceleration. Though there appears to be less (negative) acceleration associated with the shut-down transient, there still exists a (negative) acceleration and a resistive force both of which can reach high values when the driving frequency passes through the resonant frequency of the shaker-plus-tree. This being the case, damage in this time period is also a potential hazard.

5.6 Centrifugal System Reactance

The phase relationship of the spinning masses is best understood by observation of the pulse diagrams discussed previously (Figures 5.14-5.19). Some additional information on timing and centrifugal resistance can be

obtained from studying the input pressure to the hydraulic motors during the rotation period.

Some typical output traces for rotating mass B are shown in Figures 5.20-5.25. Observation of the free shake plot shows a cyclic resistance-compliance response to shake. The average timing between compliance or low resistance effects for the free shake case is 1.3 s. This indicates a frequency of 0.8 Hz. This could be the result of a beat frequency between the two masses.

The secondary low pressure dips would indicate another secondary system response of compliance. Noting the fact that the shaker mass is approximately 100 times that of the rotating masses, it may be reasonable to conclude that the primary 'no resistance' points are where forces from the rotating masses were directed in line with the current motion of the shaker. The secondary 'low resistance' points could then be the coincident rotation vectors of the two masses encountering an opposing machine displacement. Peak pressures could occur when the masses were nearly 180 degrees out of synchronization resulting in low amplitude, undefined shaker displacements. However, these pressure changes could also be the result of an unequal distribution of fluid to the motors, as well as the different requirements of each motor dependent on the reactance of the other mass, the shaker motion, and the tree motion.

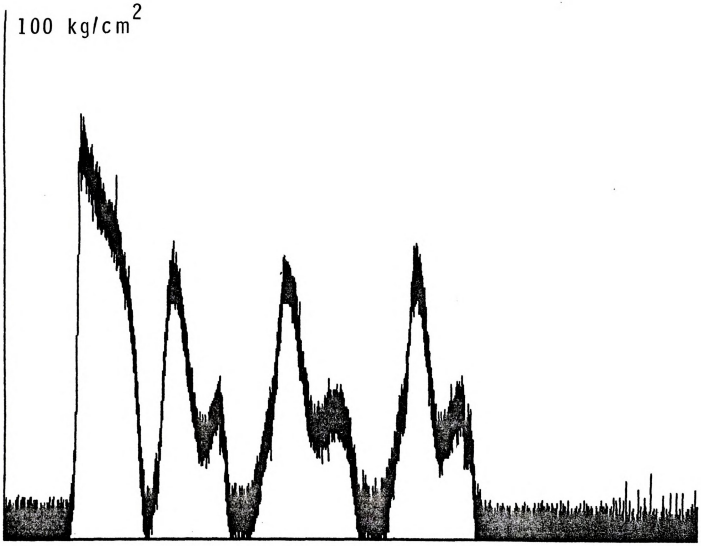

Figure 5.20 Pressure plot of drive motor B on the trunk shaker harvester with no tree in the clamp. Operational speed set at 9.3 Hz. Test: Eta.

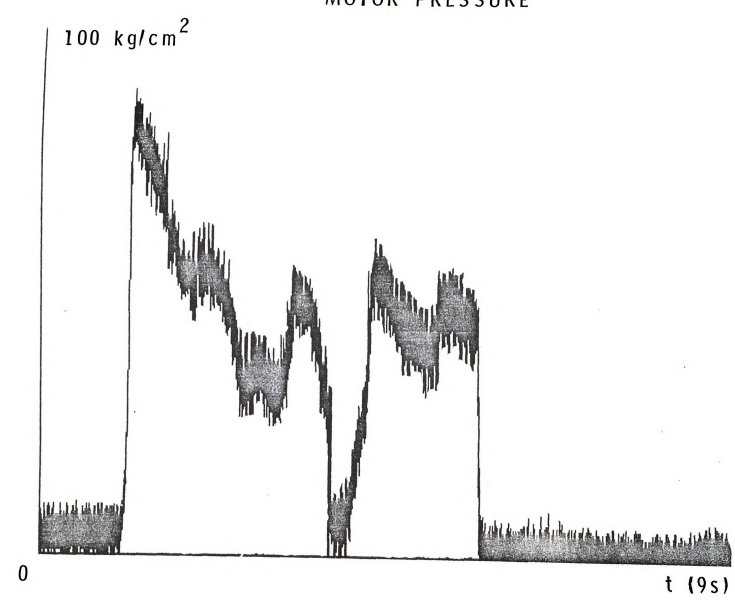

Figure 5.21 Pressure plot of drive motor B on the trunk shaker harvester with no tree in the clamp. Operational speed set at 14.0 Hz. Test: Zeta.

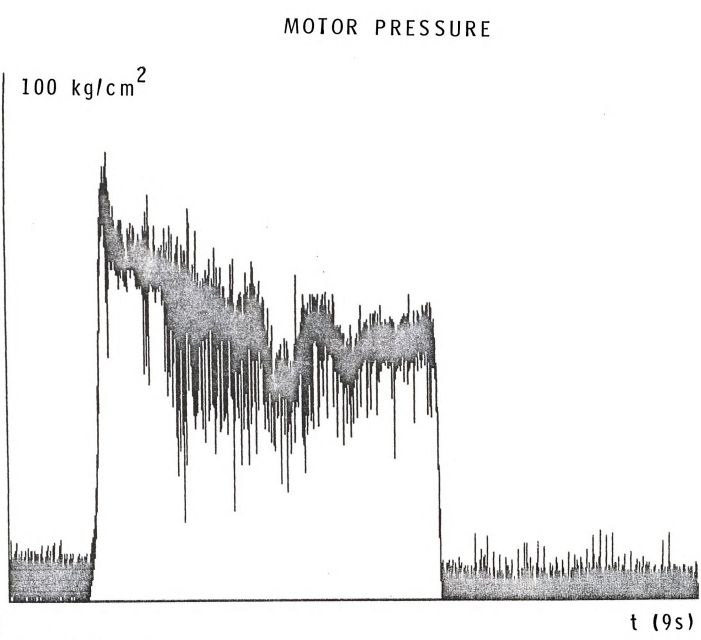

Figure 5.22 Pressure plot of drive motor B on the trunk shaker harvester with a 11 cm (4.5 in) tree in the clamp. Operational speed set at 9.3 Hz. Test: Omicron.

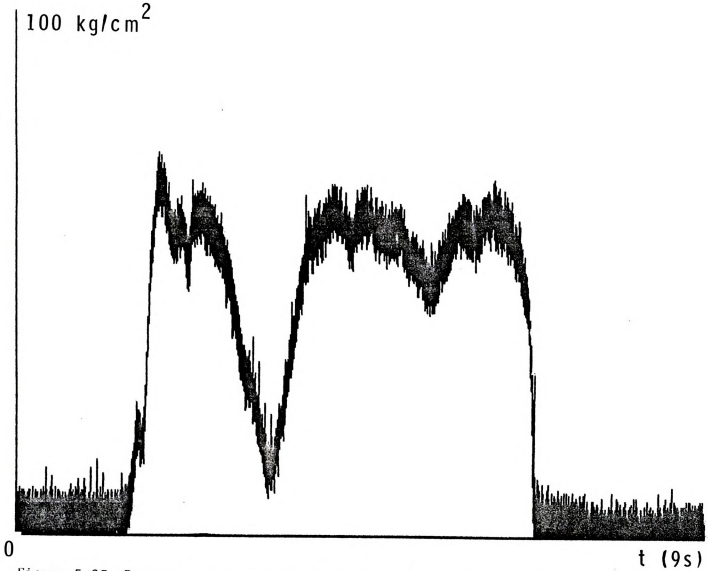

Figure 5.23 Pressure plot of drive motor B on the trunk shaker harvester with a 16 cm (6.5 in) tree in the clamp. Operational speed set at 9.3 Hz. Test: Alpha.

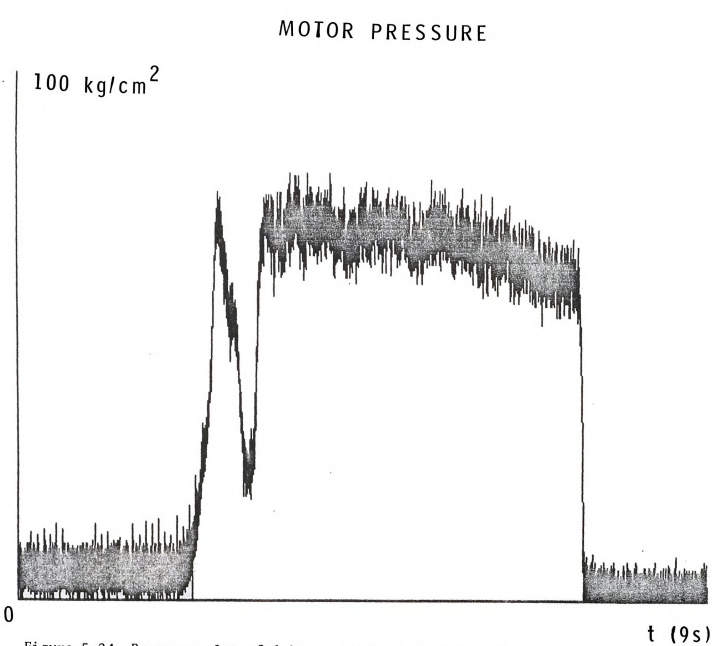

Figure 5.24 Pressure plot of drive motor B on the trunk shaker harvester with a 16 cm (6.5 in) tree in the clamp. Operational speed set at 14.0 Hz. Test: Delta.

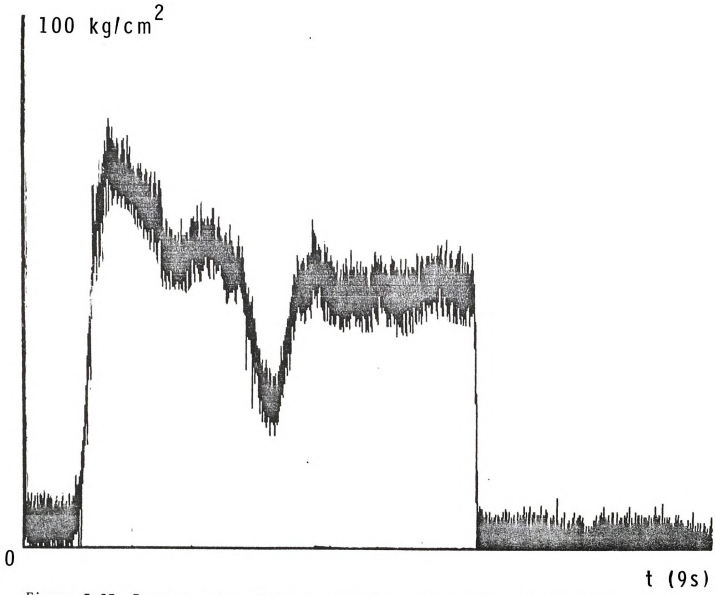

Figure 5.25 Pressure plot of drive motor B on the trunk shaker harvester with a 11 cm (4.5 in) tree in the clamp. Operational speed set at 14.0 Hz. Test: Theta.

The plot of pressure within a system where a tree is mounted reveals maximum pressure at start-up as expected. One other maximum pressure case occurs as observed in Figure 5.24. This reveals a short period during the shake when a very low pressure minimum occurs. This minimum can be attributed to a synchronization of the masses, the shaker, and tree. The extent of the minimum gives an indication of the significance of this phase relation. However, this minimum could have resulted from the second mass engaging and drawing more hydraulic fluid to start rotating. In Figure 5.23, the pressure falls to a very low level just after a short period of resistance-compliance and resistance-only. This minimum suggests resonance with the clamped tree. In all cases, after one occurrence of a very low minimum, the pressure tends to reach a stable operating level. Further tree resonance effects are not apparent when the tree is being shaken at a frequency above its fundamental resonant frequency. Pressures need to be monitored at other points in the hydraulic circuit before any conclusions can be made.

When the shaker is shut down, hydraulic pressure is immediately removed from the drive motor. Therefore, no information is received about shaker action and reaction at shut-down.

The value of quasi-steady state operating

pressure is in the range of 49-63 kg/cm^2 (700-900 psi) while startup and recovery maxima reach 92 kg/cm^2 (1300 psi). in some cases with minima of 11-21 kg/cm^2 (150-300 psi). This great variability in pressure relates to varied power requirements for shaker operation.

5.7 Acceleration to Displacement

The objective of this study is to characterize forces imposed upon a cherry tree trunk by the dynamic action of an eccentric mass trunk shaker. Observation of the pressures generated in the clamping cylinder provide some insight into the magnitude of these forces. The simulation of real world dynamic displacements in the laboratory environment may, however, present a more realistic account as to the stress and strain undergone by the bark of a tree.

Accelerometers on the tree and shaker were to resolve X, Y, and Z displacements. Accelerometer data were quickly and accurately accumulated by the ADC operating system for digital processing. Digital integration of the accumulated accelerometer signals, however, produced non-uniform velocity and displacement waveforms. Several of the acceleration waves are shown in Figures 5.26-5.31 for comparison.

The analytical procedure allowed numerical piecewise quadratic integration over the displacement

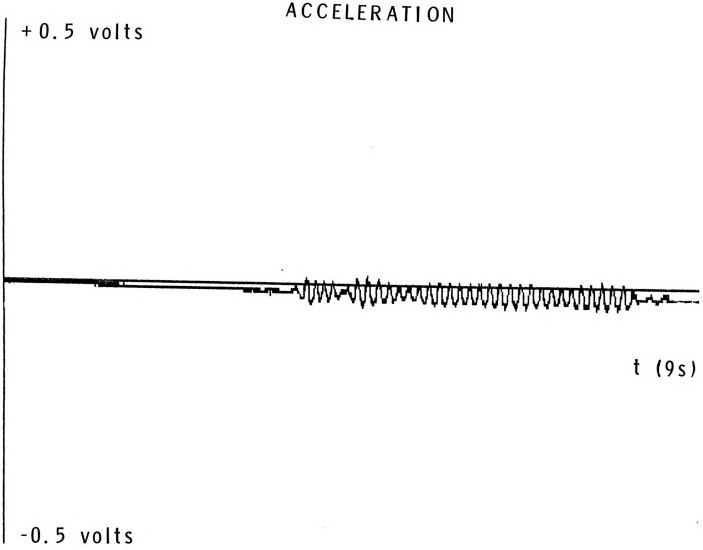

Figure 5.26 Uncalibrated acceleration trace from the -X direction sensor on the tree. Channel 2. Test: Alpha, 9.3 Hz, 16 cm (6.5 in) Tree.

16 cm (6.5 in) Tree..

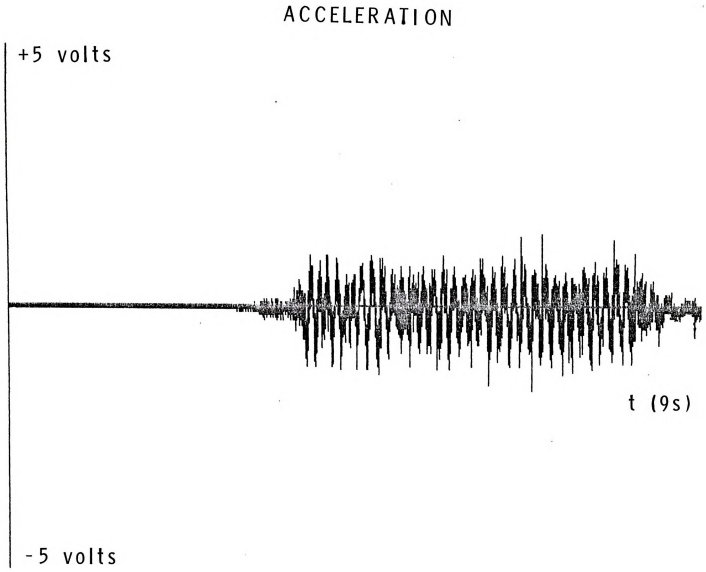

Figure 5.27 Uncalibrated acceleration trace from the +X direction sensor at the center of gravity on the shaker. Channel 4. Test: Alpha, 9.3 Hz, 16 cm (6.5 in) Tree.

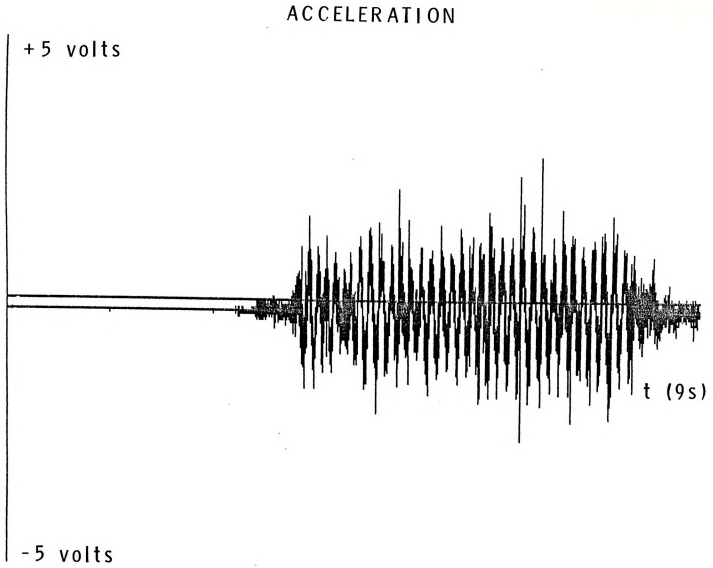

Figure 5.28 Uncalibrated acceleration trace from the +X direction sensor at the bark-pad interface on the shaker. Channel 6. Test: Alpha, 9.3 Hz, 16 cm (6.5 in) Tree.

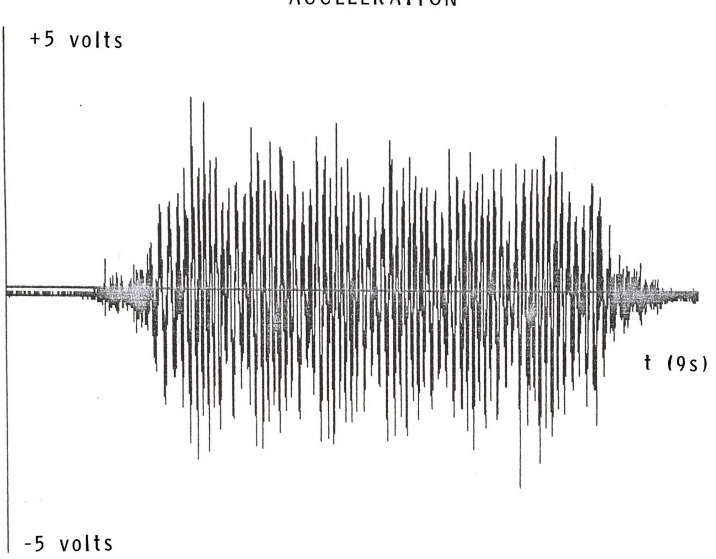

Figure 5.29 Uncalibrated acceleration trace from the +X direction sensor at the bark-pad interface on the shaker. Channel 6. Test: Beta, 14.0 Hz, 16 cm (6.5 in) Tree.

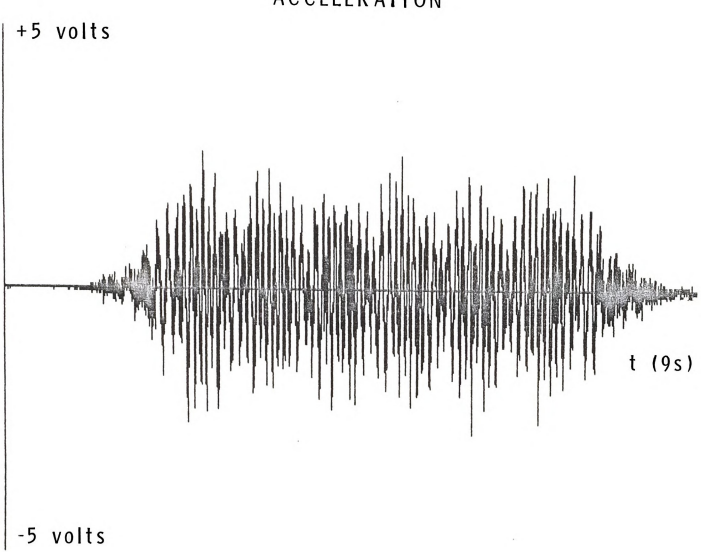

Figure 5.30 Uncalibrated acceleration trace from the +X direction sensor at the center of gravity on the shaker. Channel 4. Test: Beta, 14.0 Hz, 16 cm (6.5 in) Tree.

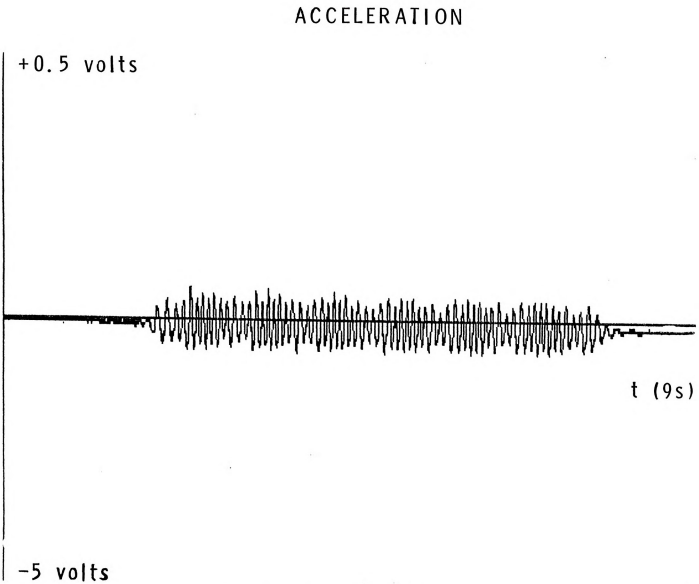

Figure 5.31 Uncalibrated acceleration trace from the -X direction sensor on the tree. Channel 2. Test: Beta, 14.0 Hz, 16 cm (6.5 in) Tree.

waveforms of interest. Constant and linear offsets in velocity and displacement data were removed by standard linear regression techniques. Non-linear offsets were removed by piecewise linear approximations. Signal bias, evident in some traces, was apparently a result of capacitive charging or discharging of amplifiers in the system, as well as the possible aliasing of unwanted high frequency signals. This effect was a typical exponential decay. The exponential time constant appeared to be much greater than the acquisition period of 9 s. This made estimation of the curve amplitude and time constant difficult. Subsequent removal of an estimated curve by exponential fitting did not account for all the observed distortion. Exact piecewise quadratic fitting removed the offset better than the estimated exponential fit and was thus employed on the data which evidenced this interference.

The acceleration trace was characterized by many points per time period. As a signal was integrated, the number of points was reduced. Theoretically then, piecewise linear regression would work better in the acceleration than in the integrals of acceleration. This was indeed the case, and was the reason for removing suspected offsets in acceleration. Unmatched slopes, however, caused discontinuities in the integrals. Therefore, this method was abandoned.

The final resolution for analysis was the subtraction of a line from 'all' data points in the acceleration and velocity. This provided translation of the base curve without distorting the vibratory information which was superimposed on it. The data were integrated to displacement as shown in the series of Figures 5.32-5.38. In Figure 5.36, the desired curve is practically hidden by the integrated offsets until the data are fitted piecewise linear to filter out all but the vibratory information. In the final step, the data are calibrated. A typical resultant displacement curve is shown in Figure 5.38.

The discontinuities arise from unmatched slopes at segment endpoints, as well as the general linear fit that provides a somewhat inadequate model of the non-linear waveform upon which the displacement wave of interest lies. The peak-to-peak displacement of the wave has not been altered by this procedure. The same method was used on the calibration data obtained from the lathe-driven displacement calibration. In this respect, all data would be subjected to the same processes, and that which is transformed on one trace is tranformed on the other.

Repeating this procedure, Figures 5.39-5.44 show the results of several calibrated displacement traces. Though some distortion due to piecewise filtering is

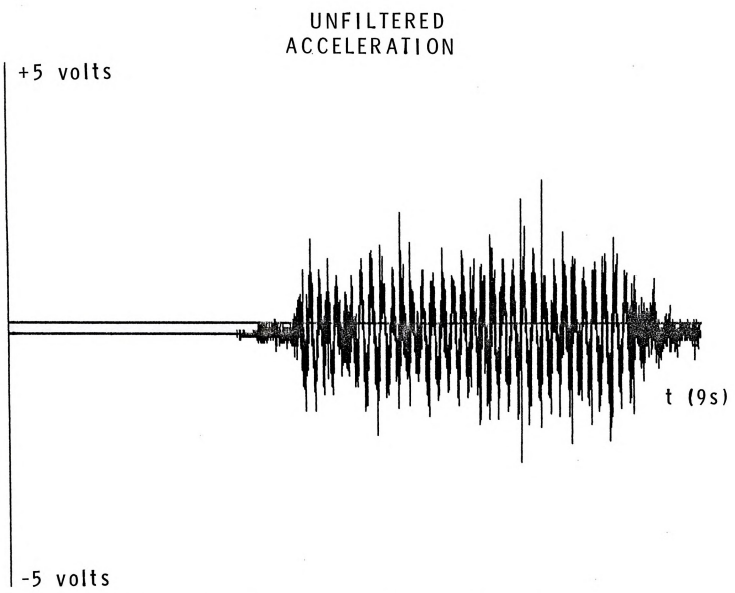

Figure 5.32 Uncalibrated acceleration trace from the +X direction sensor at the bark-pad interface on the shaker. Channel 6. Test: Alpha, 9.3 Hz, 16 cm (6.5 in) Tree.

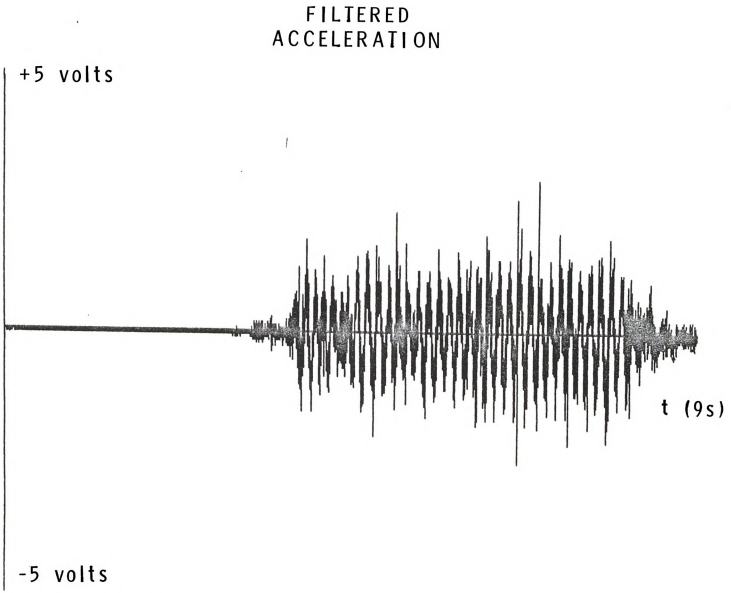

Figure 5.33 Acceleration trace from Figure 5.32 with a single line regressed on all data points and subtracted (Channel 6).

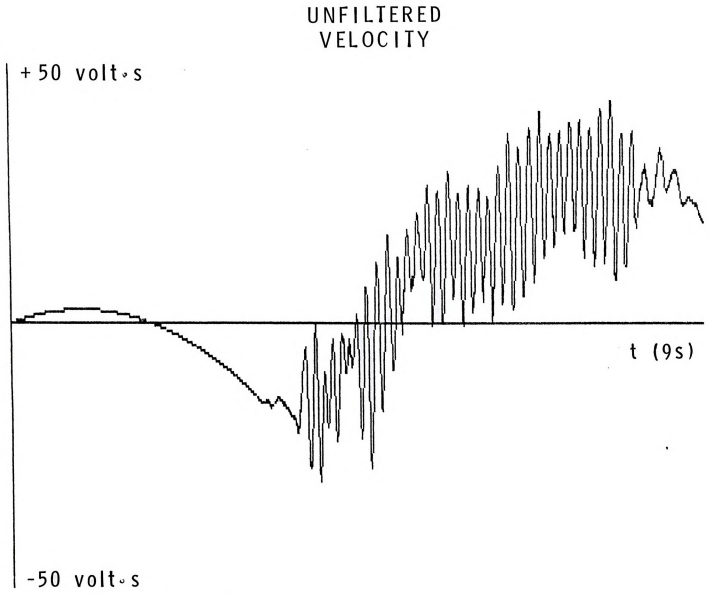

Figure 5.34 Velocity trace from the integration of the acceleration curve of Figure 5.33. Integration was conducted using piecewise quadratic methods (Channel 6).

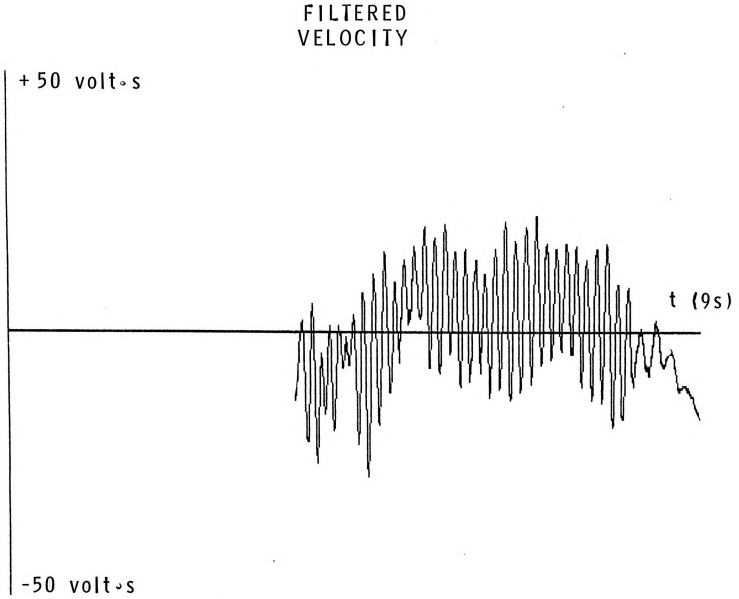

Figure 5.35 Velocity curve from Figure 5.34 with the front end drift integral removed and a single line regressed on the remaining points. Subtraction of the regressed line translates the base value (Channel 6).

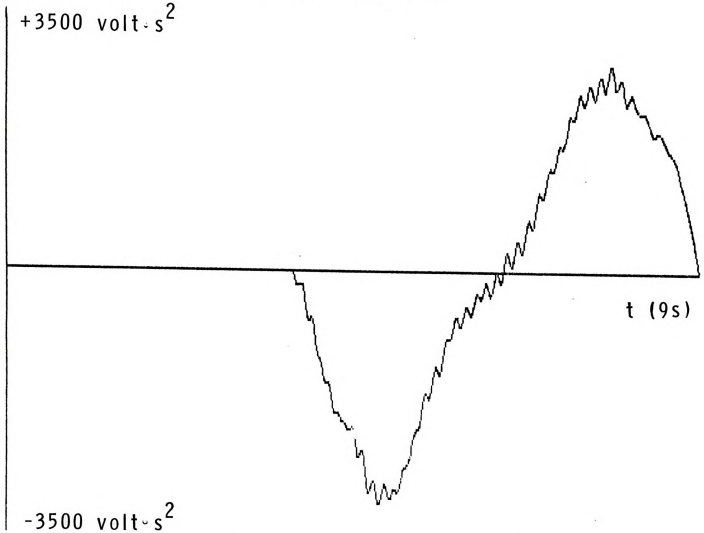

Figure 5.36 Displacement curve from the integration of the velocity curve shown in Figure 5.35. Note the single cycle underlying the desired waveform. (Channel 6).

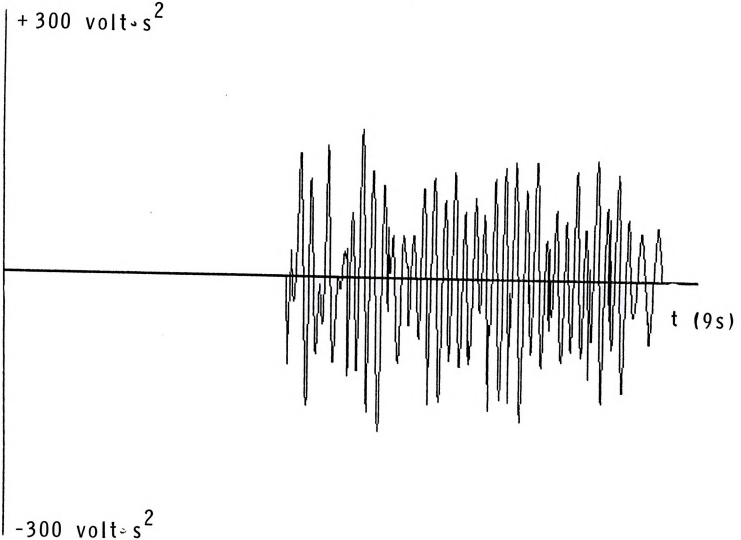

Figure 5.37 Uncalibrated displacement curve from Figure 5.36 where lines regressed on 50 data points per interval were removed to translate the base value. This removes the low frequency wave viewed in the previous figure (Channel 6).

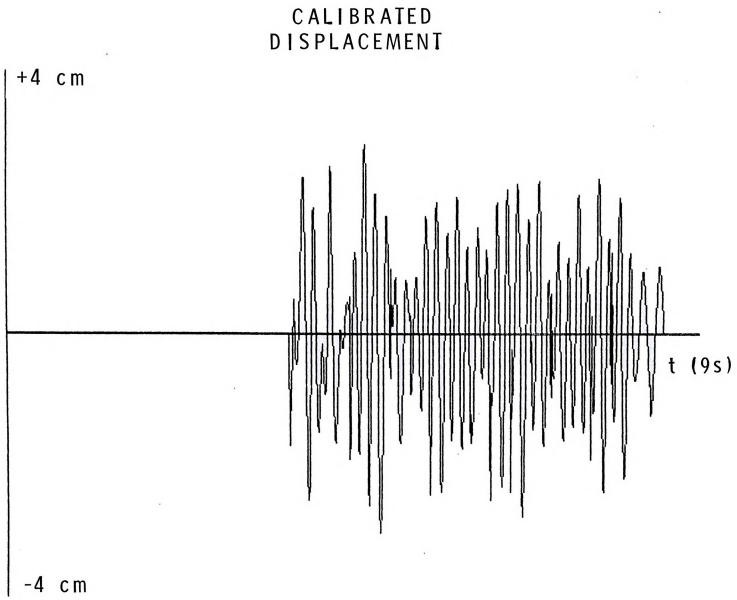

Figure 5.38 Final calibrated displacement curve for Channel 6 in this test.
Test: Alpha, 9.3 Hz, 16 cm (6.5 in) Tree.

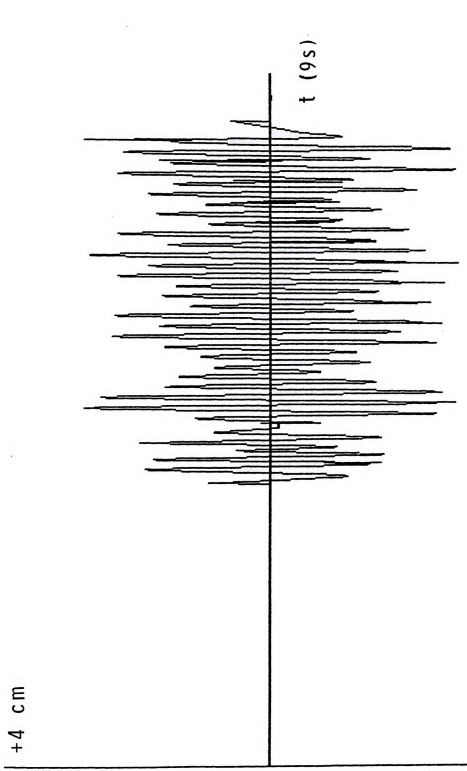

Figure 5.39 Displacement trace from integrated accelerometer channel 2. Sensor is in the -X direction on the tree. Test: Alpha, 9.3 Hz, 16 cm (6.5 in) Tree.

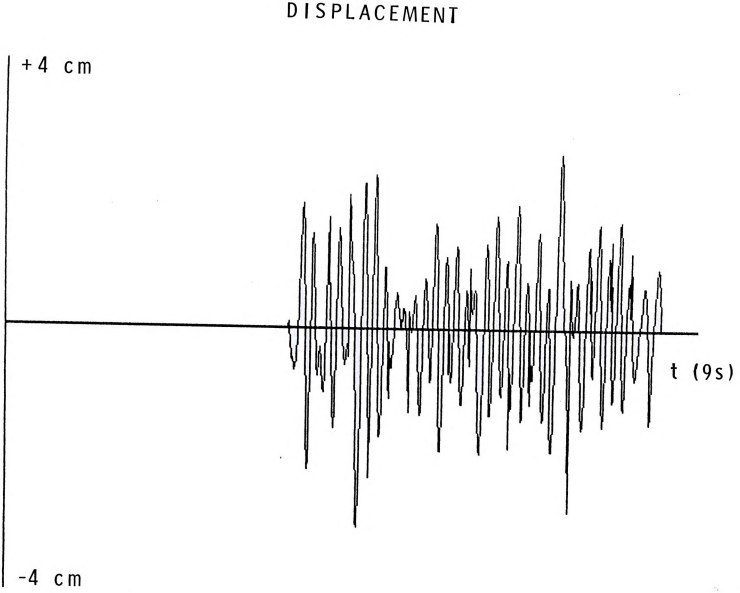

Figure 5.40 Displacement trace from integrated accelerometer channel 4. Sensor is in the +X direction at the center of gravity on the shaker. Test: Alpha, 9.3 Hz, 16 cm (6.5 in) Tree.

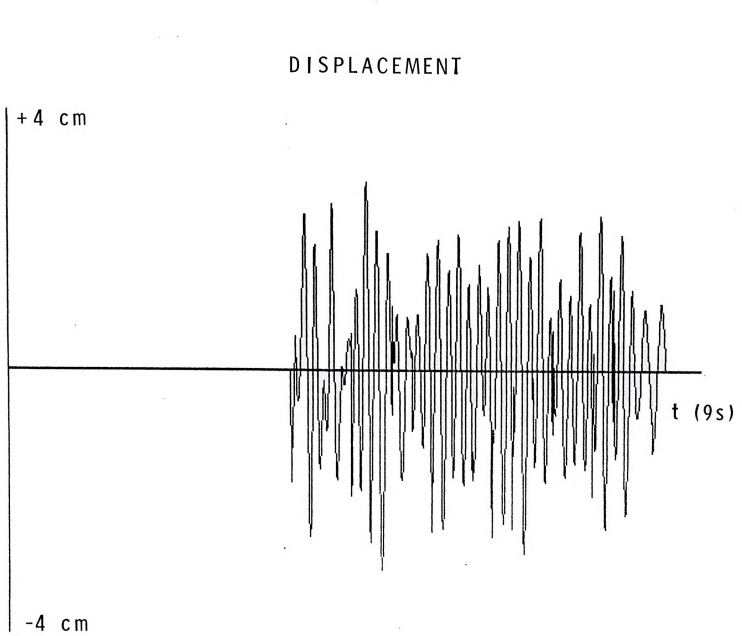

Figure 5.41 Displacement trace from integrated accelerometer channel 6. Sensor is in the +X direction at the bark-pad interface on the shaker. Test: Alpha, 9.3 Hz, 16 cm (6.5 in) Tree.

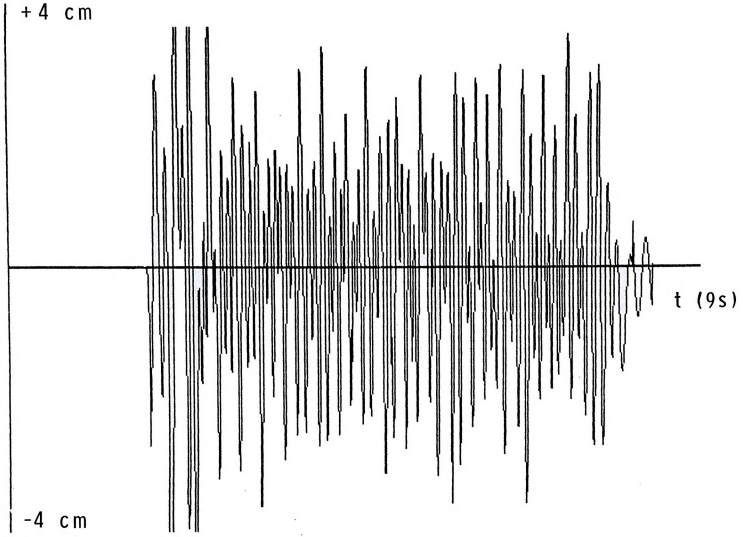

Figure 5.42 Displacement trace from integrated accelerometer channel 2. Sensor is in the -X direction on the tree. Test: Beta, 14.0 Hz, 16 cm (6.5 in) Tree.

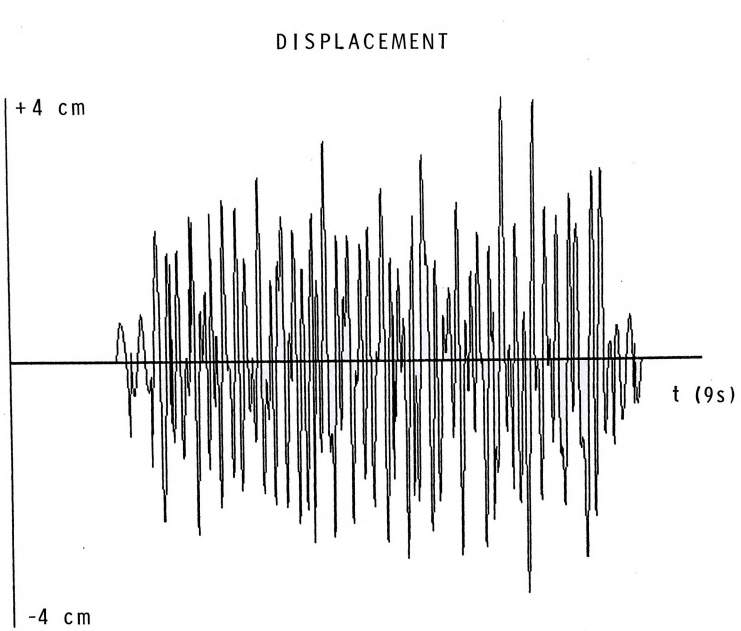

Figure 5.43 Displacement trace from integrated accelerometer channel 4. Sensor is in the +X direction at the center of gravity on the shaker. Test: Beta, 14.0 Hz, 16 cm (6.5 in) Tree.

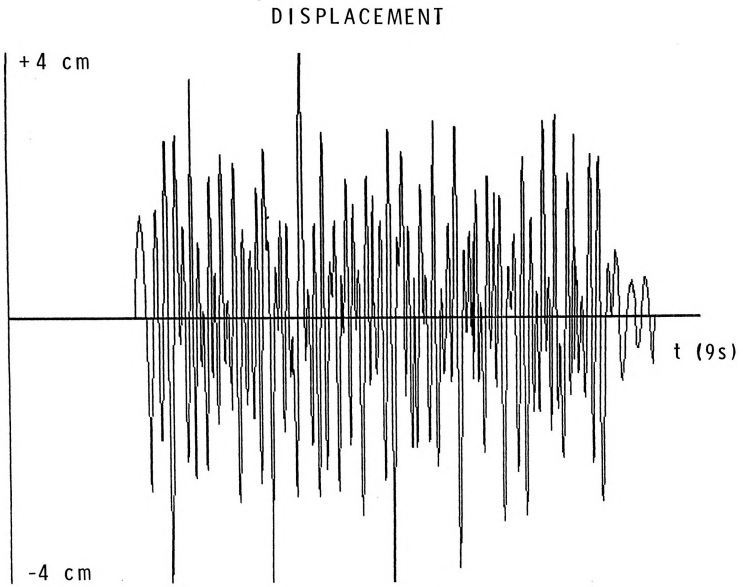

Figure 5.44 Displacement trace from integrated accelerometer channel 6. Sensor is in the +X direction at the bark-pad interface on the shaker. Test: Beta, 14.0 Hz, 16 cm (6.5 in) Tree.

apparent, the peak-to-peak displacements of the waves reach 5-6 cm on the shaker (channel 6) and 6-7 cm on the tree (channel 2). These large displacements were not evident from visual observation of shaker operation. It is not unreasonable to believe that these displacements actually occurred. With the shaker operating at this frequency, the human eye could only perceive an average value. Furthermore, it appears that displacement of the free shake test (no tree) was smaller than when the shaker was attached to the tree. This is not totally unforeseeable either, for the tree may feasibly act as a resonator causing the shaker and tree to shake more violently than the free shaker itself.

The relative amplitudes of these displacements appear to agree with one another, especially in the quasi-steady state region (between start-up and shut-down). The displacements of channels 4 and 6 (Figures 5.40, 5.41, 5.43, 5.44) which are both on the rigid shaker body, agree quite well. These channels differ only slightly from channel 2, the transducer in the corresponding direction on the tree. These observations are reasonable evidence that the method of analysis did not distort the amplitude or time scale of these transducer signals. It is favorable that all data are consistent in response to this analysis procedure. It may be that the difference between displacements in

corresponding directions are most important. At this stage, the calibration of the difference for absolute units of distance needs further validation.

As evidenced by the LVDT, the clamping cylinder pressure sensor, and the motor drive pressure sensor, an obvious maximum occurs just after start-up on the shaker. This is significant evidence that possible damage to fruit trees by trunk shakers may occur at the beginning of the shake cycle. Redesigning this machine to reduce the start-up maximum may be a solution to eliminating the major concern in damage potential.

The epicyclic trunk shaker patterns develop cyclic displacement amplitudes in any given direction. This provides efficiency in fruit removal by varying direction and amplitude of shake. The changing of magnitude and direction at a frequency incompatable with tree response may induce excessive forces on the trunk.

In hardware, integration is part of an amplified feedback filtering process. The method of numerical piecewise quadratic integration in software fills the roll of the hardware amplified feedback. There is no filtering using this software method, however. Slight problems in discrete signal-sampling result when the sampling frequency approaches the minimum required sampling frequency. Ideal impulse sampling becomes less important when integrating, even though a slight discrete bias still

remains. Aliasing of data signals was not an obvious problem. The integration of acceleration does evidence underlying low frequency waveforms for which we see an aliasing by superposition. These low frequency signals could represent a frequency of a difference of the rotational frequencies of the individual masses. Low order tree response may also be involved, as well as vibrational response of the carrier (the tractor) to the shaker vibration.

High order polynomial regression on the data may well remove any underlying frequencies that are not of importance in analysis of the immediate response of the tree. High order regression, however, has a tendency to add its own characteristics of 'overshoot' and 'ringing'. The final analysis requires a digital filter. Though these are available, more computer processing power than I had available is required.

5.8 Discrete Time Domain

The problem of discrete time signal analysis is approached in voluminous literature. To produce a system that would accurately characterize a real-world, high speed event and reproduce it without distortion requires much time, effort and equipment. The problems arising in the data acquisition system I constructed were typical of a discrete time domain analysis, though not simple to

solve. Several problems occurring both in software and hardware can be solved with a great increase in system reliability.

In this system, three different models of accelerometers were employed. This required three different models of impedance amplifiers to convert from charge to voltage. The use of different sensors and amplifiers with amplifiers having individual settings and characteristics, required different range settings on the ADC. As the range settings are varied, the time required to make a conversion changes. Sensitivity of these varied amplifiers also becomes a problem as the capacitive drift and response time will vary. Drift is then more apparent with low output transducers and can saturate signals. High impedance amplifiers are noise attractive and if not properly shielded and grounded, result in non-decodeable output.

In this system, improper grounding in the field allowed static charge build-up in the van. Temperature and moisture changes in the environment greatly affected the operation of the amplifiers. The first test was conducted on a hot, dry day in September. After a weekend rain, the air was cool and humid, requiring that all amplifiers go through a warm-up period, followed by sensitivity readjustment.

All cables were shielded, twisted pair with most

signals carried as charge. Measuring the voltage on unused lines within a twisted pair evidenced some crosstalk. Preliminary tests in the laboratory revealed no measurable interference between two simultaneously operating lines within a pair.

The ADC was operated at 21 KHz, which is 1 KHz above the manufacturer's suggested limit rating. A faster ADC may have eliminated some variable, spurious signals evidenced on some channels.

The 6502 system was programmed to accept data, store in memory, and reprogram the ADC for another conversion. Direct Memory Access (DMA), which is not present on this system, may have provided a better means of collecting the information. A faster processor would also have allowed for some further front end data processing in the areas of averaging and filtering.

The present system operates with 256 Kbytes of "Random-Access-Memory" which is present in segmented banks. This amount was adequate to hold a short 2 Kbyte assembly language collection routine, the standard operating system, and 210 Kbytes of data. However, when a 35 Kbyte analysis routine was written that also required several sizeable external procedures, 256 Kbytes of RAM were a critical limiting factor. Data had to be read piecewise from disk. Reading time accumulates fast when the disk is required to operate a minimum of 2 s each

time. The greatest limitation to the analysis package, which was UCSD Pascal-encoded, was the operational speed. A simple linear regression on one data channel (7020 points) required 50 s. The 2 MHz operating system (which actually operates at 1.4 MHz) was adequate for data collection at the limited ADC operating speed of 21 KHz, but truely requires a dedicated processor and increased volatile memory for data processing.

5.9 Future Systems

The major problem encountered in this analysis occurred because the incoming signal was not filtered and the existing processor lacked the capability to handle such digital signal conditioning. Therefore, all incoming frequencies were digitized, leaving an unreal task for a small system to decode. A future system should begin with charge amplifiers constructed in the accelerometer package itself. Though such charge amplifiers require a constant current source, the output would be reliable and less susceptible to external noise. This would also eliminate the problems of external charge amplifiers with variable settings and power supplies. Shielded cables are always required, as they were in this system.

Ideal accelerometer signal sampling would involve the immediate conversion to a frequency domain where signal filtering can be easily carried out. Time domain

sampling would be adequate if front end hardware filters were available. Hardware integration would be an improvement where only the final desired signal (displacement) would be sampled for reconstruction and calibration. The major drawback with front end hardware filters and integrators is that each is constructed of amplifiers which are prone to drift and external noise interference.

In my experiment, electric power in the field was obtained with a 12VDC to 120VAC sine wave inverter powered by a vehicle battery charged by an alternator. Static charge build-up in the vehicle body, discharge of the vehicle power supply, and noise from the inverter electronics contributed to the erratic signals. There are now available microprocessor systems with large internal volatile memories capable of operating an ADC or other peripheral equipment on a 5 VDC power supply with low current input. These systems are portable, and semi-sealed. As part an improved package, accelerometers with 9 VDC batteries as the amplifier current source have been available for a long time.

Therefore, if time domain sampling is a must, as many error sources as possible should be eliminated, for the real world will inherently add complexity to the situation.

CHAPTER 6

SUMMARY

A method was devised by which dynamically impressed stress and strain in fruit tree bark caused by mechanical shakers could be determined. Imposed stress and strain of bark could then be compared to known tolerances to determine if the biological limits of the cell strength in bark and cambium had been exceeded. This process involved a) digitally obtaining real-time accelerations of a tree and shaker b) software processing the accelerations into meaningful rigid body displacements and c) simulating maximum conditions under a laboratory environment to determine stress and strain. This aspect of the investigation dealt with the dynamic acceleration analysis of tree and shaker.

A vibratory trunk shaker was instrumented with transducers to evaluate bark damage potential from real-time displacements during tree vibration. Calculations were made to theoretically insure sensor capability of acquiring the rapidly changing signals. Sensing elements detected X, Y, and Z acceleration of tree and shaker, clamping cylinder pressure, mass position and

linear displacement of the clamp cylinder. Operating frequencies for harvesting cherry trees were 9.3 Hz and 14.0 Hz. A conventional shaker was used; it was operated in typical grower fashion.

A 2 Mhz 6502 microprocessor-controlled data acquisition system was developed. A machine language operating program provided a user-friendly interface to the high speed data acquisition addressable controls in field maneuvers. A 12 bit analog-to-digital converter provided 0.024% resolution on analog inputs. The calculated collection rate was 10,240 bytes per second. The actual operating rate was 21,491 bytes per second, providing a 110% increase in waveform characterization accuracy; essentially twice the Nyquist folding frequency. Total points collected were 98,301 in 9.148 seconds. Actual shaking interval was 3-5 seconds, allowing characterization of the transient start and stop activity. Transducers were calibrated in the laboratory calibrated under similar operating conditions. Data collected from all transducers were calibrated and plotted.

Pressure in the clamping cylinder remained quite constant during shaking tests with an average deviation of less than 1.0% from the recommended setting. This correlated well with linear displacement measurements of the clamping jaw. Deviation from the null position was 1 mm on the average. Major deviations occurred in the first

fraction of a second of shake and was attributed to the dynamic settling of the shaker pad. Deviation beyond this setting was indicative of a cushioned beating action on the tree. Results indicated that a maximum amplitude of clamp arm movement was 7 mm but overall averaged 2-4 mm. The maximum was normally evident just after the pad 'relaxed' into position and the arm adjusted its grip on the tree. In all cases, a small overall closing of the clamp was observed.

Clamping cylinder pressure agreed with clamp arm movement in that the pressure decreased slightly by the end of the test, indicating an inward arm motion. The start-up transient again revealed a pressure maximum reaching a peak-to-peak difference of 22 kg/cm^2 (312 psi) in one worst case with a normal range of 3.5-14.1 kg/cm^2 (50-200 psi) peak-to-peak deviation. Clamp pressure was converted to force in the 'pull' (-X) direction only and displayed an average range of 'pull' forces of 17,350-20,000 N (3900-4500 lb).

Motor pressure showed more variability indicating the forcing action necessary to overcome the total system resistance and reactance. Minima occurred upon shaker start-up showing the possibility of a system resonance state of 'compliance' which could reasonably be the condition of critical bark damaging force I seek.

Proximity sensors verified actual quasi-steady

state operating frequencies as being within 10% of those calculated. These sensors also revealed a rapid start-up of mass rotation which translates to a massive and complex acceleration pattern.

When attached to the tree, shaker displacement maxima occurred most often during startup of the shaking mechanism, probably because the forced frequency of vibration coincided with the lowest natural frequency of the tree. Harmonic magnification of system displacement could have resulted in potentially destructive reactive forces. When passing out of this frequency, reduced shaker displacements may have required unusual resistive forces by the tree. These harmonic vibrations were not evident in shaker shutdown, possibly due to the no-power state of the mass drivers allowing the slowing mass to seek a minimum energy level.

Real-time displacement maxima of the tree and shaker were desired. Numerical double integration of acceleration data using a piecewise quadratic fitting procedure was only partly successful. Limitations of the hardware in the analysis system prevented accurate integration of imperfect time-based signals. Stray signals, introduced from sources such as transducer amplifier drift, ADC amplifier or capacitive drift, poor system grounding, and electrical power supply spikes distorted several acceleration traces to the extent that

they could not be decoded. Suggestions for an improved system are given where acquisition speed and system reliability could be increased and data quantity could be decreased. The existing software can be improved. The 6502 processor is still not capable of handling a frequency domain analysis, but with proper equipment and appropriate data preparation and formatting, this task could be easily accomplished on another computer.

No visible bark damage was evident in any harvesting tests conducted on tart cherry trees with this vibration system. Internal tree damage, which may have occurred, was not detectable at this time due to a lack of sufficient sensing technology.

CHAPTER 7

CONCLUSIONS

1. A high-speed microprocessor-based data acquisition system was assembled capable of monitoring and digitizing 14 analog signals, each at a rate of 767 points per second. A 14 Hz analog sine wave could be characterized by 54 points per cycle with 0.024% resolution and 0.049% quantization accuracy.

2. Acceleration data could be integrated digitally employing a piecewise quadratic fitting procedure. Superposition of unwanted frequencies in the acceleration waveform required high speed processing in the time or frequency domain which was not feasible with the 6502 based system. Hardware inaccuracies could also have caused intermediate acquisition errors. Methods to overcome these errors are discussed.

3. Limited decoding power for the complex acceleration traces prevented direct determination of shaker body and tree displacements. Natural frequency interference (shaker "gallop") from the tree on shaker startup was prominent in producing large clamping arm displacements of up to 7 mm amplitude. Evidence of a

'compliance state' is prominent in the clamp pressure, motor pressure, and mass position diagrams.

4. No evidence of exterior bark damage to tart cherry trees was observed immediately after shaking with machine parameters set at grower, manufacturer and researcher recommmendations. Delayed indications are still a possibility.

DISCLAIMER: Shaking forces may differ with shaker design and pattern of application. Bark strength of cherry trees may differ due to climate, soil, location and cultural practice. Consequently, acceptable harvester tree accelerations (determining stress and strain) in one orchard may be detrimental to another orchard. Different orchard production practices and shaker operation procedures may be necessary to minimize bark damage. The conclusions reached herein should be generalized to include other orchards and conditions only with great caution.

CHAPTER 8

RECOMMENDATIONS FOR FUTURE RESEARCH

1. System Software: Integration of acceleration data to displacement using numerical piecewise quadrature works well for 'ideal' data. Acceleration data such as those collected in this experiment are not ideal; they evidence superimposed frequencies, amplifier drift and possible high frequency aliasing. A 2 MHz microcomputer system programmmed in a high level language (Pascal in this experiment) does not have the power to perform the needed filtering and frequency analysis (such as a Fast Fourier Transform) to separate the complex data traces into meaningful physical events. Hence, machine level data acquisition routines should be revised to do some filtering (sampling) to reduce the quantity of data and then store the data in a format acceptable for transmission to larger computers. The data acquisition program should accept keyboard input of channel-gain sequences. Future data acquisition systems must be considered on the basis of programming ease, memory management, processing time, and compatability with other processors.

2. Instrumentation: The acquisition of analog signals in digital form requires that the conditioned signals be present at the analog-to-digital converter. Microcomputers have the capability of operating on conditioned signals only with simple algorithms; larger processors are needed for complex digital signal analysis. A computer may utilize a megabyte of memory and require a dedicated processor to analyze the data (7000 points per test) of this experiment. Operating speeds of 8 MHz or better may be needed to perform the spectral analyses required to filter out unwanted signals. Therefore, signal conditioning such as filtering, amplification, and integration should be done in hardware. Care must be taken, however, when using amplifiers and other integrated circuit equipment for these tasks since most electronic hardware is prone to temperature effects, moisture effects, offset errors, linear and non-linear drift and saturation. Mismatching between the amplifier impedance and the transducer capacitance can also distort the signal. The choice is between the difficulties involved in hardware signal conditioning and software signal decoding. Matching transducers to hardware for amplification, integration, and filtering with a final stage of digital filtering and calibration may increase the accuracy and and speed of

analysis in this system.

3. Stress and Strain: Finding peak displacements is only a first step in the determination of a cause for bark damage to cherry trees. The peak displacement information should enable estimation of stress and strain imposed on the tree by the shaker by simulating peak displacements between a trunk shaker and a model tree in the laboratory and measuring contact pressures and contact area between them at the pad.

4. Injury Detection: Better methods are needed to determine the existence of and to quantify the extent of damaged tree tissue. Visual observations are only sufficient to determine if external damage has occurred. A nondestructive method to sense and evaluate sub-clinical damage immediately after shaking is needed so that changes can be made to reduce or eliminate damage.

5. Sensor Development: As knowledge is gained on the static and dynamic characteristics of production and harvest systems, sensor packages will be required to detect mechanical and biological information and relay this information immediately to controllers or test instruments. Such sensor packages, capable of detecting specific basic data on plant growth and response

to external stimuli, will also be valuable in future research on the preservation of critical high-investment crops.

APPENDIX A

6502 ASSEMBLY LANGUAGE DATA COLLECTION OPERATING PROGRAM

APPENDIX A

6502 ASSEMBLY LANGUAGE DATA COLLECTION OPERATING PROGRAM

```
;================PROGRAM ADI13 INTERPRETER===============

        .ABSOLUTE               ;Interpreter is absolute
        .NOPATCHLIST            ;Assembler directive
        .NOMACROLIST            ;Assembler directive
        .PROC   ADI13           ;Procedure returns no value

;.........................FILE HEADER.....................

START   .EQU    0A000           ;Start loading address A000
        .ORG    START-0E        ;Header info. leads interp.
        .ASCII  "SOS NTRP"      ;Header for kernel recog.
        .WORD   0000            ;Opt. header length = 0
        .WORD   START           ;Starting address of prgm.
        .WORD   CODELEN         ;Length of operating code
        JMP     BEGIN           ;Start pt. of operating prgm.

;...................MACRO FOR SOS CALLS..................

        .MACRO  SOS
        BRK
        .BYTE   %1
        .WORD   %2
        .ENDM

;.................EQUATE FOR CALL NUMBERS.................

GETTIME .EQU    063             ;Get Time SOS Call Number
OPEN    .EQU    0C8             ;Open SOS Call Number
CLOSE   .EQU    0CC             ;Close SOS Call Number
READ    .EQU    0CA             ;Read SOS Call Number
WRITE   .EQU    0CB             ;Write SOS Call Number
REQSEG  .EQU    040             ;Reqseg SOS Call Number

;.....................USER ZERO PAGE.....................

RBUF1   .EQU    050             ;Buffer pointer in 0050
RBUF2   .EQU    052             ;Buffer pointer in 0052
RBUF3   .EQU    054             ;Buffer pointer in 0054
RBUF4   .EQU    056             ;Buffer pointer in 0056
RBUF5   .EQU    058             ;Buffer pointer in 0058
RBUF6   .EQU    060             ;Buffer pointer in 0060

TIMEB1  .BLOCK  48,0            ;Store time in 72 bytes
TIMEB2  .EQU    TIMEB1+12       ;Time pointer for Time2
TIMEB3  .EQU    TIMEB2+12       ;Time pointer for Time3
TIMEB4  .EQU    TIMEB3+12       ;Time pointer for Time4
```

APPENDIX A

6502 ASSEMBLY LANGUAGE DATA COLLECTION OPERATING PROGRAM

```
;::::::::::::::::::::::::::::::::::::::::::::::::::::::::::::
;::::::::::::::::::ANALOG ADI13 USER PROGRAM:::::::::::::::::
;::::::::::::::::::::::::::::::::::::::::::::::::::::::::::::

BEGIN   .EQU    *               ;Address of prgm. start
        JSR     OPENCON         ;Open console for Rd/Wrt
        LDA     CREF            ;Load console ref number
        STA     RDREF           ;for reading
        STA     WRREF           ;and writing
        STA     PRREF           ;and prompt start
        STA     NPREF           ;and prompt repeat
        STA     SCRREF          ;and screen on/off

        JSR     OPENAD          ;Open A-D for Rd/Wrt
        LDA     ADREF           ;Load A-D ref num
        STA     ADREF1          ;for reading 65K bytes
        STA     ADREF2          ;and another 65K bytes
        STA     ADREF3          ;and another 65K bytes

RDWPRT  SOS     WRITE, PROMPT   ;Write beginning prompt

RDCHAR  SOS     READ, RDLIST    ;Read a console key
        LDA     RDCNT           ;Was one read?
        BEQ     RDCHAR          ;Branch/no and reread

        LDA     BUFFER          ;Load the Ascii key code
        CMP     #11             ;Quit?          (CTL Q)
        BEQ     FINISH
        CMP     #53             ;Collect?       (S)
        BEQ     COLLECT
        CMP     #50             ;Load disks?    (P)
        BEQ     LOADSK
        JMP     RDWPRT          ;Wait for a valid key

FINISH  SOS     0CC, HBLK1      ;Close all files
        SOS     065, HBLK2      ;Terminate

HBLK1   .BYTE   01              ;Close Call table
HBLK2   .BYTE   00              ;Close ALL files & terminate

COLLECT JSR     ALLSEG          ;Release and allocate memory
        JSR     SCROFF          ;Turn off screen for speed
        SOS     GETTIME, TIME1  ;Get time from sys. clock
        SOS     READ, RDATA1    ;Read 65K bytes and return
        SOS     GETTIME, TIME2  ;Get time again
        SOS     READ, RDATA2    ;Read 65K bytes and return
```

APPENDIX A

6502 ASSEMBLY LANGUAGE DATA COLLECTION OPERATING PROGRAM

```
        SOS     GETTIME, TIME3  ;Get time again
        SOS     READ, RDATA3    ;Read 65K bytes and return
        SOS     GETTIME, TIME4  ;Get time again
        SOS     WRITE, NEWPT    ;Write prompt for next job
        JMP     RDCHAR          ;Wait for next order

LOADSK  JSR     CREATE          ;Create file set on disks
        JSR     OPENDK          ;Open disk files
        SOS     WRITE, DATA1    ;Write 32K out
        SOS     WRITE, DATA2    ;Write 32K out
        SOS     WRITE, DATA3    ;Write 32K out
        SOS     WRITE, DATA4    ;Write 32K out
        SOS     WRITE, DATA5    ;Write 32K out
        SOS     WRITE, DATA6    ;Write 32K out
        SOS     WRITE, TIME     ;Write time out
        JSR     CLOSDK          ;Close files
        JSR     ALLSEG          ;Release and allocate memory
        JMP     RDWPRT          ;Wait for next order

;::::::::::::::::::::::::::::::::::::::::::::::::::::::::::::::
;:::::::::::::::::::::::END OF MAIN PRGM:::::::::::::::::::::::
;::::::::::::::::::::::::::::::::::::::::::::::::::::::::::::::

;---------SEGMENT RELEASE & ALLOCATION  SUBROUTINE--------

ALLSEG  SOS     045, RELS       ;Release Segment Call number
                                ;Table RELS
        SOS     REQSEG, RSEG1   ;Request first seg in B:00
        BNE     HOLD            ;Errors in getting memory?
        SOS     WRITE, WRLIST   ;Send OK signal to screen
        LDX     BASE1           ;Load bb in X
        LDA     BASE1+1         ;Load pp in A
        JSR     FIXADDR         ;Fix addresses for driver
        STX     RBUF1+1601      ;Store bb in extend page
        STA     RBUF1+1         ;Store pp in hi byte pter

        SOS     REQSEG, RSEG2   ;Request second seg in B:02
        BNE     HOLD            ;Errors in getting memory?
        SOS     WRITE, WRLIST   ;Send OK signal to screen
        LDX     BASE2           ;Load bb in X
        LDA     BASE2+1         ;Load pp in A
        JSR     FIXADDR         ;Fix addresses for driver
        STX     RBUF3+1601      ;Store bb in extend page
        STA     RBUF3+1         ;Store pp in hi byte pter

        SOS     REQSEG, RSEG3   ;Request third seg in B:04
        BNE     HOLD            ;Errors in getting memory?
```

APPENDIX A

6502 ASSEMBLY LANGUAGE DATA COLLECTION OPERATING PROGRAM

```
        SOS     WRITE, WRLIST   ;Send OK signal to screen
        LDX     BASE3           ;Load bb in X
        LDA     BASE3+1         ;Load pp in A
        JSR     FIXADDR         ;Fix addresses for driver
        STX     RBUF5+1601      ;Store bb in extend page
        STA     RBUF5+1         ;Store pp in hi byte pter

        LDX     #01             ;Set up pointer for Write
        LDA     #20             ;32k seg B:01 P:20
        JSR     FIXADDR         ;Fix addresses for driver
        STX     RBUF2+1601      ;Store bb in extend page
        STA     RBUF2+1         ;Store pp in hi byte pter

        LDX     #03             ;Set up pointer for Write
        LDA     #20             ;32k seg B:03 P:20
        JSR     FIXADDR         ;Fix addresses for driver
        STX     RBUF4+1601      ;Store bb in extend page
        STA     RBUF4+1         ;Store pp in hi byte pter

        LDX     #05             ;Set up pointer for Write
        LDA     #20             ;32k seg B:05 P:20
        JSR     FIXADDR         ;Fix addresses for driver
        STX     RBUF6+1601      ;Store bb in extend page
        STA     RBUF6+1         ;Store pp in hi byte pter

        LDA     #0              ;Zero lo byte of pointers
        STA     RBUF1
        STA     RBUF2
        STA     RBUF3
        STA     RBUF4
        STA     RBUF5
        STA     RBUF6
        RTS                     ;Return from subroutine

HOLD    SOS     WRITE, PROMPT   ;Scroll out prompt as
        JMP     HOLD            ;note of memory error

RSEG1   .BYTE   04              ;Request Seg (4 params)
BASE1   .WORD   2000            ;Base bb=00 pp=20 (ppbb)
        .WORD   9F01            ;Limit bb=01 pp=9F
        .BYTE   11              ;Seg ID (Interp data)
        .BYTE   00              ;Seg Num (result)

RSEG2   .BYTE   04              ;Request Seg (4 params)
BASE2   .WORD   2002            ;Base bb=02 pp=20 (ppbb)
        .WORD   9F03            ;Limit bb=03 pp=9F
        .BYTE   11              ;Seg ID (Interp data)
```

APPENDIX A

6502 ASSEMBLY LANGUAGE DATA COLLECTION OPERATING PROGRAM

```
         .BYTE   00              ;Seg Num (result)

RSEG3    .BYTE   04              ;Request Seg (4 params)
BASE3    .WORD   2004            ;Base bb=04 pp=20 (ppbb)
         .WORD   9F05            ;Limit bb=05 pp=9F
         .BYTE   11              ;Seg ID (Interp data)
         .BYTE   00              ;Seg Num (result)

RELS     .BYTE   01              ;Release seg (1 param)
         .BYTE   00              ;Release all except sys. code

;------------------SUBROUTINE FIXADDRESSES----------------

FIXADDR  CPX     #0              ;Zero bank?
         BEQ     SZBANK          ;Branch/yes to 8F fix
         CPX     #0F             ;Low S bank?
         BEQ     SZBANK          ;Branch/yes to 8F fix
         CPX     #10             ;High S bank?
         BEQ     SZBANK          ;Branch/yes to 8F fix
         TAY                     ;Temp move pp to Y
         TXA                     ;Temp move bb to A
         CLC                     ;Fix GENERAL CASE
         ADC     #7F             ;XX=$80+bb-1
         TAX                     ;Move bb back to X
         TYA                     ;Move pp back to A
         CLC
         ADC     #60             ;NNNN=pp00+$6000
         RTS
SZBANK   LDX     #8F             ;Zero bank or S bank
         RTS

;------- PARAMETER LISTS FOR CALLS IN THE MAIN PRGM ------

BUFFER   .BYTE   00              ;Send CR, LF, +, CR, LF
CRBUFF   .BYTE   0D, 0A, 2B, 0D, 0A

RDLIST   .BYTE   04              ;Read keyboard table (4 params)
RDREF    .BYTE   00              ;Read reference number (value)
         .WORD   BUFFER          ;Read data buffer
         .WORD   0001            ;Request count
RDCNT    .WORD   0000            ;Transfer count (result)

WRLIST   .BYTE   03              ;Write to cons. table (3 params)
WRREF    .BYTE   00              ;Write reference number (value)
         .WORD   CRBUFF          ;Write data buffer
WCNT     .WORD   0005            ;Request count
```

APPENDIX A

6502 ASSEMBLY LANGUAGE DATA COLLECTION OPERATING PROGRAM

```
;-----------------SUBROUTINE OPENCONSOLE-----------------

OPENCON SOS      OPEN, COLIST    ;Open console for read & write
        RTS                      ;Table COLIST

COLIST  .BYTE    04              ;Open (4 params)
        .WORD    CNAME           ;Pathname pointer
CREF    .BYTE    00              ;Reference Number (result)
        .WORD    COPLIST         ;Optional list pointer
        .BYTE    01              ;Optional list length
COPLIST .BYTE    03              ;Required access (Read & Write)

CNAME   .BYTE    08              ;Pathname Length
        .ASCII   ".CONSOLE"      ;Pathname


;-------------------SUBROUTINE OPENAD--------------------

OPENAD  SOS      OPEN, ADLIST    ;Open A-D for read & write
        RTS                      ;Table ADLIST

ADLIST  .BYTE    04              ;Open (4 params)
        .WORD    ADNAME          ;Pathname pointer
ADREF   .BYTE    00              ;Reference Number (result)
        .WORD    ADPLIST         ;Optional list pointer
        .BYTE    01              ;Optional list length
ADPLIST .BYTE    03              ;Required access (Rd & Wrt)

ADNAME  .BYTE    06              ;Pathname length
        .ASCII   ".ADI13"        ;Pathname

;-----------------SUBROUTINE SCREENOFF-----------------

SCROFF  SOS      WRITE, SCRLIST  ;WRITE call for screen on/off
        RTS                      ;Table SCRLIST

SCRLIST .BYTE    03              ;WRITE (3 params)
SCRREF  .BYTE    00              ;Reference number (value)
        .WORD    DOCODE          ;Data buffer pointer
        .WORD    0002            ;Request count (value bytes)

DOCODE  .BYTE    0E, 0A          ;Code to turn off screen
                                 ;"SO" = Hex "OE" = Dec "14"
                                 ;Read to console turns it on

;----------------------TIME TABLES-----------------------
```

APPENDIX A

6502 ASSEMBLY LANGUAGE DATA COLLECTION OPERATING PROGRAM

```
TIME1   .BYTE   01              ;Get time (1 param)
        .WORD   TIMEB1          ;Buffer pointer

TIME2   .BYTE   01              ;Get time (1 param)
        .WORD   TIMEB2          ;Buffer pointer

TIME3   .BYTE   01              ;Get time (1 param)
        .WORD   TIMEB3          ;Buffer pointer

TIME4   .BYTE   01              ;Get time (1 param)
        .WORD   TIMEB4          ;Buffer pointer

;-------------------READ DATA TABLES----------------------

RDATA1  .BYTE   04              ;Read (4 params)
ADREF1  .BYTE   00              ;Reference number (value)
        .WORD   RBUF1           ;Data buffer pointer
        .WORD   0FFFE           ;Request count (65,534 bytes)
        .WORD   0000            ;Transfer count (result)

RDATA2  .BYTE   04              ;Read (4 params)
ADREF2  .BYTE   00              ;Reference number (value)
        .WORD   RBUF3           ;Data buffer pointer
        .WORD   0FFFE           ;Request count (65,534 bytes)
        .WORD   0000            ;Transfer count (result)

RDATA3  .BYTE   04              ;Read (4 params)
ADREF3  .BYTE   00              ;Reference number (value)
        .WORD   RBUF5           ;Data buffer pointer
        .WORD   0FFFE           ;Request count (65,534 bytes)
        .WORD   0000            ;Transfer count (result)

;-------------------CREATE DISK TABLES--------------------

CREATE  SOS     0C0, CREAT1     ;Create file #1
        SOS     0C0, CREAT2     ;Create file #2
        SOS     0C0, CREAT3     ;Create file #3
        SOS     0C0, CREAT4     ;Create file #4
        SOS     0C0, CREAT5     ;Create file #5
        SOS     0C0, CREAT6     ;Create file #6
        SOS     0C0, CREAT7     ;Create file #7
        RTS

CREAT1  .BYTE   03              ;Create (3 params)
        .WORD   F1              ;pathname pointer
        .WORD   0000            ;optional list pointer
        .BYTE   00              ;optional list length
```

APPENDIX A

6502 ASSEMBLY LANGUAGE DATA COLLECTION OPERATING PROGRAM

```
CREAT2  .BYTE   03              ;Create (3 params)
        .WORD   F2              ;pathname pointer
        .WORD   0000            ;optional list pointer
        .BYTE   00              ;optional list length

CREAT3  .BYTE   03              ;Create (3 params)
        .WORD   F3              ;pathname pointer
        .WORD   0000            ;optional list pointer
        .BYTE   00              ;optional list length

CREAT4  .BYTE   03              ;Create (3 params)
        .WORD   F4              ;pathname pointer
        .WORD   0000            ;optional list pointer
        .BYTE   00              ;optional list length

CREAT5  .BYTE   03              ;Create (3 params)
        .WORD   F5              ;pathname pointer
        .WORD   0000            ;optional list pointer
        .BYTE   00              ;optional list length

CREAT6  .BYTE   03              ;Create (3 params)
        .WORD   F6              ;pathname pointer
        .WORD   0000            ;optional list pointer
        .BYTE   00              ;optional list length

CREAT7  .BYTE   03              ;Create (3 params)
        .WORD   F7              ;pathname pointer
        .WORD   0000            ;optional list pointer
        .BYTE   00              ;optional list length

F1      .BYTE   09              ;Pathname length
        .ASCII  ".D1/DATA1"     ;Pathname file one
F2      .BYTE   09              ;Pathname length
        .ASCII  ".D1/DATA2"     ;Pathname file two
F3      .BYTE   09              ;Pathname length
        .ASCII  ".D1/DATA3"     ;Pathname file three
F4      .BYTE   09              ;Pathname length
        .ASCII  ".D1/DATA4"     ;Pathname file four
F5      .BYTE   09              ;Pathname length
        .ASCII  ".D2/DATA5"     ;Pathname file five
F6      .BYTE   09              ;Pathname length
        .ASCII  ".D2/DATA6"     ;Pathname file six
F7      .BYTE   08              ;Pathname length
        .ASCII  ".D2/TIME"      ;Pathname file seven

;-----------------SUBROUTINE OPENDISKS-----------------
```

APPENDIX A

6502 ASSEMBLY LANGUAGE DATA COLLECTION OPERATING PROGRAM

```
OPENDK  SOS     OPEN, OPEND1    ;Open disk files
        LDA     DREF1           ;Load disk reference number
        STA     DATAR1          ;Store for Rd/Write
        SOS     OPEN, OPEND2    ;Open disk file 2
        LDA     DREF2           ;Load disk reference number
        STA     DATAR2          ;Store for Rd/Write
        SOS     OPEN, OPEND3    ;Open disk file 3
        LDA     DREF3           ;Load disk reference number
        STA     DATAR3          ;Store for Rd/Write
        SOS     OPEN, OPEND4    ;Open disk file 4
        LDA     DREF4           ;Load disk reference number
        STA     DATAR4          ;Store for Rd/Write
        SOS     OPEN, OPEND5    ;Open disk file 5
        LDA     DREF5           ;Load disk reference number
        STA     DATAR5          ;Store for Rd/Write
        SOS     OPEN, OPEND6    ;Open disk file 6
        LDA     DREF6           ;Load disk reference number
        STA     DATAR6          ;Store for Rd/Write
        SOS     OPEN, OPEND7    ;Open disk file 7
        LDA     DREF7           ;Load disk reference number
        STA     DATAR7          ;Store for Rd/Write
        RTS

OPEND1  .BYTE   04              ;Open (4 params)
        .WORD   F1              ;Pathname pointer
DREF1   .BYTE   00              ;Reference Number (result)
        .WORD   DKOPT           ;Optional list pointer
        .BYTE   01              ;Optional list length

OPEND2  .BYTE   04              ;Open (4 params)
        .WORD   F2              ;Pathname pointer
DREF2   .BYTE   00              ;Reference Number (result)
        .WORD   DKOPT           ;Optional list pointer
        .BYTE   01              ;Optional list length

OPEND3  .BYTE   04              ;Open (4 params)
        .WORD   F3              ;Pathname pointer
DREF3   .BYTE   00              ;Reference Number (result)
        .WORD   DKOPT           ;Optional list pointer
        .BYTE   01              ;Optional list length

OPEND4  .BYTE   04              ;Open (4 params)
        .WORD   F4              ;Pathname pointer
DREF4   .BYTE   00              ;Reference Number (result)
        .WORD   DKOPT           ;Optional list pointer
        .BYTE   01              ;Optional list length
```

APPENDIX A

6502 ASSEMBLY LANGUAGE DATA COLLECTION OPERATING PROGRAM

```
OPEND5   .BYTE   04              ;Open (4 params)
         .WORD   F5              ;Pathname pointer
DREF5    .BYTE   00              ;Reference Number (result)
         .WORD   DKOPT           ;Optional list pointer
         .BYTE   01              ;Optional list length

OPEND6   .BYTE   04              ;Open (4 params)
         .WORD   F6              ;Pathname pointer
DREF6    .BYTE   00              ;Reference Number (result)
         .WORD   DKOPT           ;Optional list pointer
         .BYTE   01              ;Optional list length

OPEND7   .BYTE   04              ;Open (4 params)
         .WORD   F7              ;Pathname pointer
DREF7    .BYTE   00              ;Reference Number (result)
         .WORD   DKOPT           ;Optional list pointer
         .BYTE   01              ;Optional list length

DKOPT    .BYTE   03              ;Open for Read/Write

;--------------------DISK WRITE TABLES--------------------

DATA1    .BYTE   03              ;Write (3 params)
DATAR1   .BYTE   00              ;Reference Number (value)
         .WORD   RBUF1           ;Data buffer pointer
         .WORD   8000            ;Transfer 32,768 bytes

DATA2    .BYTE   03              ;Write (3 params)
DATAR2   .BYTE   00              ;Reference Number (value)
         .WORD   RBUF2           ;Data buffer pointer
         .WORD   7FFE            ;Transfer 32,766 bytes

DATA3    .BYTE   03              ;Write (3 params)
DATAR3   .BYTE   00              ;Reference Number (value)
         .WORD   RBUF3           ;Data buffer pointer
         .WORD   8000            ;Transfer 32,768 bytes

DATA4    .BYTE   03              ;Write (3 params)
DATAR4   .BYTE   00              ;Reference Number (value)
         .WORD   RBUF4           ;Data buffer pointer
         .WORD   7FFE            ;Transfer 32,766 bytes

DATA5    .BYTE   03              ;Write (3 params)
DATAR5   .BYTE   00              ;Reference Number (value)
         .WORD   RBUF5           ;Data buffer pointer
         .WORD   8000            ;Transfer 32,768 bytes
```

APPENDIX A

6502 ASSEMBLY LANGUAGE DATA COLLECTION OPERATING PROGRAM

```
DATA6    .BYTE   03              ;Write (3 params)
DATAR6   .BYTE   00              ;Reference Number (value)
         .WORD   RBUF6           ;Data buffer pointer
         .WORD   7FFE            ;Transfer 32,766 bytes

TIME     .BYTE   03              ;Write (3 params)
DATAR7   .BYTE   00              ;Reference Number (value)
         .WORD   TIMEB1          ;Data buffer pointer
         .WORD   0048            ;Transfer 72 bytes

;-----------------SUBROUTINE CLOSE DISKS----------------

CLOSDK   LDA     DREF1           ;Load Ref Num 1 to Close
         JSR     CLSUB
         LDA     DREF2           ;Load Ref Num 2 to Close
         JSR     CLSUB
         LDA     DREF3           ;Load Ref Num 3 to Close
         JSR     CLSUB
         LDA     DREF4           ;Load Ref Num 4 to Close
         JSR     CLSUB
         LDA     DREF5           ;Load Ref Num 5 to Close
         JSR     CLSUB
         LDA     DREF6           ;Load Ref Num 6 to Close
         JSR     CLSUB
         LDA     DREF7           ;Load Ref Num 7 to Close
         JSR     CLSUB
         RTS

CLSUB    STA     CLREF           ;Store Ref Num of file
         SOS     CLOSE, CLLIST   ;Close file
         RTS

CLLIST   .BYTE   01              ;CLOSE  (1 param)
CLREF    .BYTE   00              ;File Ref Num to Close

;-----------------------ASCII CODING--------------------

SPRMT    .EQU    *
         .BYTE   0D, 0A, 0A
         .ASCII  ".............DISKS LOADED............."
         .BYTE   0D, 0A
         .ASCII  "        S: START COLLECTION"
         .BYTE   0D, 0A
         .ASCII  "    CTL Q: QUIT"
         .BYTE   0A, 09, 09, 09, 5B, 09, 5D, 08, 08
SPCNT    .EQU    *-SPRMT
```

APPENDIX A

6502 ASSEMBLY LANGUAGE DATA COLLECTION OPERATING PROGRAM

```
PROMPT   .BYTE   03              ;Write (3 params)
PRREF    .BYTE   00              ;Reference Number (value)
         .WORD   SPRMT           ;Data buffer pointer
         .WORD   SPCNT           ;Request count (value)

NPRMT    .EQU    *
         .BYTE   0D, 0A, 0A
         .ASCII  ".........COLLECTION COMPLETE........."
         .BYTE   0D, 0A
         .ASCII  "        P: DATA TO DISK"
         .BYTE   0D, 0A
         .ASCII  "        S: CLEAR/RECOLLECT"
         .BYTE   0D, 0A
         .ASCII  "   CTL Q: QUIT"
         .BYTE   0A, 09, 09, 09, 5B, 09, 5D, 08, 08
NPCNT    .EQU    *-NPRMT

NEWPT    .BYTE   03              ;Write (3 params)
NPREF    .BYTE   00              ;Reference Number (value)
         .WORD   NPRMT           ;Data buffer pointer
         .WORD   NPCNT           ;Request count (value)

;++++++++++++++++++++++++++++++++++++++++++++++++++++++++++++

CODELEN  .EQU    *-START         ;Calc. codelength for Header
         .END                    ;End Program (Assembly)

;++++++++++++++++++++++++++++++++++++++++++++++++++++++++++++
```

APPENDIX B

6502 ASSEMBLY LANGUAGE ANALOG-TO-DIGITAL CONVERTER DEVICE DRIVER PROGRAM

APPENDIX B

6502 ASSEMBLY AND SOS LANGUAGE DRIVER FOR THE ANALOG TO DIGITAL CONVERTER

```
;==================ADI13 CHARACTER DRIVER=================

          .PROC  ADI13              ;Procedure returns no values
          .NOPATCHLIST              ;Assembler directive
          .NOMACROLIST              ;Assembler directive

;.......................SOS EQUATES.......................

ALLOCSIR .EQU    1913               ;Allocate Internal Resource
DEALCSIR .EQU    1916               ;Deallocate Internal Resource
SELC800  .EQU    1922               ;Select/Deselect I/O space
SysErr   .EQU    1928               ;report error to system
EREG     .EQU    0FFDF              ;Environment Register
BREG     .EQU    0FFEF              ;Bank Register

REQCODE  .EQU    0C0                ;Request Code
SOSUNIT  .EQU    0C1                ;Unit Number
SOSBUF   .EQU    0C2                ;Buffer Pointer
REQCNT   .EQU    0C4                ;Requested Byte Count
BREAD    .EQU    0C8                ;Bytes Read Returned by D_READ

;......... ..............ZERO PAGE.......................

RETCNT   .EQU    0D1                ;Returned Request Code

;.....................SOS ERROR CODES.....................

XREQCODE .EQU    20                 ;Invalid request code
XNOTOPEN .EQU    23                 ;Device Not Open
XNOTAVAIL .EQU   24                 ;Device Not Available
XNORESRC .EQU    25                 ;Resource Not Available
XBADOP   .EQU    26                 ;Invalid Operation
XIOERROR .EQU    27                 ;I/O Error
XNODRIVE .EQU    28                 ;Drive Not Connected

;........................MACROS.........................

          .MACRO switch
          .IF     "%1" <> ""        ;If Parameter 1 Is Present
           LDA      %1              ;Load A With Switch Index
          .ENDC
          .IF     "%2" <> ""        ;If Parameter 2 Is Present
           CMP      #%2+1           ;Check Bounds
           BCS      $010
          .ENDC
           ASL      A
           TAY
           LDA      %3+1,Y          ;Get Switch Index From Table
```

APPENDIX B

6502 ASSEMBLY AND SOS LANGUAGE DRIVER FOR THE ANALOG TO DIGITAL CONVERTER

```
          PHA
          LDA     %3,Y
          PHA
          .IF   "%4" <> "*"       ;If Parameter 4 Is Omitted
          RTS                     ;Go to Code
          .ENDC
$010      .ENDM

;.....................FORCE 1 Mhz Mode.................

          .MACRO setlmhz
          LDA     EREG            ;Load Environment Register
          ORA     #80             ;Set 6th bit to 1
          STA     EREG            ;Restore Environment Reg.
          .ENDM

;.....................FORCE 2 Mhz Mode.................

          .MACRO set2mhz
          LDA     EREG            ;Load Environment Register
          AND     #7F             ;Set 6th bit to 0
          STA     EREG            ;Restore Environment Reg.
          .ENDM

;....INCREMENT 3 BYTE ADDRESS & CHECK FOR BAD ADDRESSES....

          .MACRO INCADR
          INC     %1              ;Increment Low Byte
          BNE     $310            ;If not zero, then OK
          INC     %1+1            ;If Low Byte = 0, Inc. Hi Byte
          LDA     %1+1            ;Load the hi byte for check
          CMP     #0A0            ;Are we in SOS Hi Address?
          BEQ     $120            ;If so, fix it
$110      CMP     #00             ;Are we in SOS Lo Address?
          BNE     $310            ;If not, leave
          SEC                     ;If so, fix it
          ROR     %1+1            ;Reset upper byte of Address
          INC     %1+1401         ;Increment to next bank
          JMP     $310            ;Leave
$120      LDY     %1+1401         ;Where in SOS Hi are we?
          CPY     #8F             ;Are we in Bank Zero?
          BNE     $130            ;If not, repair differently
          LDA     #80             ;If so, do general fixup
          STA     %1+1            ;Set Hi Byte to 80
          STA     %1+1401         ;Set Bank Extension to 80
          JMP     $310            ;Leave
$130      CMP     #00             ;Are we in SOS zero page?
          BNE     $310            ;If not, leave
```

APPENDIX B

6502 ASSEMBLY AND SOS LANGUAGE DRIVER FOR THE ANALOG TO DIGITAL CONVERTER

```
            SEC                     ;If so, Reset Hi Byte
            ROR     %1+1            ;of Address
            INC     %1+1401         ;And Increment bank Extension
$310        .ENDM                   ;Leave Macro

;.....................INCREMENT A WORD MACRO.................

            .MACRO  INW
            INC     %1              ;Increment Lo Byte
            BNE     $210            ;If not zero, leave
            INC     %1+1            ;If Lo is zero, Inc. Hi Byte
$210        .ENDM

;.............DEVICE IDENTIFICATION BLOCK (DIB).............

DIB         .WORD   0000            ;Link to System
            .WORD   Entry           ;User Program Entry Point
            .BYTE   06              ;Name Count
            .ASCII  ".ADI13          " ;Device Name (15 Chars)
            .BYTE   80              ;Active, No Page Alignment

DIB_SLOT
            .BYTE   0FF             ;Slot Number (User Select)
            .BYTE   00              ;Unit Number
            .BYTE   064             ;Type (Char), R/W, Parallel
            .BYTE   01              ;Subtype for Parallel Card
            .BYTE   00              ;Filler

DIB_BLOCKS
            .WORD   0000            ;# Blocks (None=char device)
            .WORD   0000            ;Manufacturer
            .WORD   100A            ;Release-Preliminary (ALPHA)

;.....................DCB LENGTH AND DCB..................

DCB         .WORD   1               ;One Byte for Now

DEBUG       .BYTE   80              ;Debugging On(80)/Off(00) Flg

;.....................LOCAL STORAGE.....................

INITOK      .BYTE   XNORESRC        ;Init went OK(00)/Error Code
SLOTCN      .BYTE   00              ;Compute CNxx and Store On Init
SLOTCX      .BYTE   00              ;Compute COxO and Store On Init
DIBPTR      .WORD   DIB             ;Indicate this device
OPENFLG     .BYTE   00              ;Open/Close Flag
ADSLOT      .BYTE   00              ;Store Slot Num*$10
```

APPENDIX B

6502 ASSEMBLY AND SOS LANGUAGE DRIVER FOR THE ANALOG TO DIGITAL CONVERTER

```
NLFLAG    .BYTE   00              ;NEWLINE Mode Flag (80/00)
NLCHAR    .BYTE   00              ;NEWLINE Character Storage

;.........................SIR TABLE.........................

SIRADDR   .WORD   SIRTABL         ;Address of System Internal Res.
SIRTABL   .BYTE   10,0,0,0,0      ;Set System Parameters
SIRCNT    .EQU    *-SIRTABL       ;Length of SIR Table

;........CHANNEL AND GAIN BUFFER FOR DATA COLLECTION.......

CHGA      .BYTE   70              ;Channel  0    -.1 to .1 SSA 0
          .BYTE   71              ;         1    -.1 to .1 SSA 1
          .BYTE   72              ;         2    -.1 to .1 SSA 2
          .BYTE   43              ;         3    - 5 to  5 GRA 3
          .BYTE   44              ;         4    - 5 to  5 GRA 4
          .BYTE   45              ;         5    - 5 to  5 GRA 5
          .BYTE   46              ;         6    - 5 to  5 GRA 6
          .BYTE   47              ;         7    - 5 to  5 GRA 7
          .BYTE   48              ;         8    - 5 to  5 GRA 8
          .BYTE   7B              ;        11    -.1 to .1 LVDT
          .BYTE   4C              ;        12     -5 to  5 TACH A
          .BYTE   4D              ;        13     -5 to  5 TACH B
          .BYTE   3E              ;        14      0 to .1 PRESS M A
          .BYTE   0F              ;        15      0 to  5 PRESS CLP

CHX       .BYTE   00              ;Buffer for Selection

;************************************************************
;************* MAIN ENTRY POINT FOR THE DRIVER ************
;************************************************************

Entry     LDA     REQCODE         ;Request Code?

;.......A D_INIT CALL (CODE 8) SKIPS THE SLOT SET UP........

          CMP     #8              ;D_INIT Call?
          BEQ     DOIT            ;Perform D_INIT Processing

;.IF DEBUGGING IS ENABLED, PUT ADDRESS IN (18)FD, FE and FF

          LDA     DEBUG           ;Load Debug Status
          BEQ     $10             ;Skip if Disabled
          LDA     BREG            ;Load Bank Select
          STA     0FF             ;Store in Bank Register
          LDA     DIBPTR          ;Load Device Address
          STA     0FD             ;Store Lo Byte In FD
          LDA     DIBPTR+1        ;Load Hi Byte Address
```

APPENDIX B

6502 ASSEMBLY AND SOS LANGUAGE DRIVER FOR THE ANALOG TO DIGITAL CONVERTER

```
         STA     0FE             ;Store Hi Byte in FE

;.INITIALIZE OK? YES=ZERO, OTHERWISE WE HAVE THE ERROR CODE

$10      LDA     INITOK          ;Load Initialization Status
         BEQ     $60             ;If OK, then continue

;....INITIALIZATION FAILED. RETURN ERROR CODE AND LEAVE....

$50      JSR     SysErr          ;Go to SOS Error Routine

;..........SUBROUTINE CALLING TO DISPATCH DUTIES..........

         JSR     DOIT            ;Determine What To Do
         RTS

;....SUBROUTINE TO DISPATCH DUTIES DEPENDING ON REQCODE....

DOIT     .EQU    *               ;Start Subroutine Address

         switch  REQCODE,8,DOTABL ;Dispatch Duty Roster

BADREQ   LDA     #XREQCODE       ;Invalid Request
         JSR     SysErr          ;Go to SOS Error Routine

BADOP    LDA     #XBADOP         ;Invalid Operation
         JSR     SysErr          ;Go to SOS Error Routine

NOTOPEN  LDA     #XNOTOPEN       ;Device is not Open
         JSR     SysErr          ;Go to SOS Error Routine

;..........DISPATCH TABLE FOR DOIT SUBROUTINE.............

DOTABL   .WORD   DRead-1         ;0 Read
         .WORD   BADREQ-1        ;1 Unused
         .WORD   BADREQ-1        ;2 Unused
         .WORD   BADREQ-1        ;3 Unused
         .WORD   BADREQ-1        ;4 Unused
         .WORD   BADREQ-1        ;5 Unused
         .WORD   DOpen-1         ;6 Open the Device
         .WORD   DClose-1        ;7 Close the Device
         .WORD   DInit-1         ;8 Init

;.................D_INIT CALL PROCESSING.................
;..........CALLED AT SYSTEM INITIALIZE TIME ONLY..........

DInit    LDA     DIB_SLOT        ;Load the Device Slot Number
         BMI     $1              ;Invalid if it's Negative
```

APPENDIX B

6502 ASSEMBLY AND SOS LANGUAGE DRIVER FOR THE ANALOG TO DIGITAL CONVERTER

```
         ORA     #0C0            ;Set Up Code
         STA     SLOTCN          ;Store for later Reference

;.........CHECK THE SLOT TO SEE IF A CARD IS THERE.........

         setlmhz                 ;Slow Down For I/O Access
         LDA     DIB_SLOT        ;Get Slot Number
         JSR     SelC800         ;Try to Select It
         BCS     $1              ;No, we can't

;.......COMPUTE C0X0 FOR THIS SLOT AND SAVE FOR ACCESS......

         LDA     DIB_SLOT        ;Load the Slot Number
         CLC                     ;Clear the Carry Register
         ROL     A
         ROL     A
         ROL     A
         ROL     A               ;Calc Slot*16 to Point to AD
         STA     ADSLOT          ;Wherever It Is
         ADC     #80             ;C080 + (Slot * 16)
         STA     SLOTCX          ;Store in Slot Locater

;......DESELECT DEVICE, MARK ALL ACCEPTABLE AND LEAVE......

         LDA     #0               ;Prepare OK Code in Accum.
         STA     INITOK           ;All is Well
         JSR     SelC800          ;Deselect the Device
         RTS

;................SOMETHING WRONG AT THE SLOT..............

$1       LDA     #XNODRIVE       ;Load Bad Drive Code
         BNE     $3

;..........SYSTEM INTERNAL RESOURCES NOT AVAILABLE.........

$2       LDA     #XNORESRC       ;Load No Resources Code

;...........PUT CODE IN INITOK AND REPORT ERROR............

$3       STA     INITOK          ;Something went wrong
         JSR     SysErr          ;Go to SOS Error Routine

;................D_OPEN CALL PROCESSING.................

;...ALLOCATE RESOURCES, RESET DEVICE, & PREPARE FOR DATA...

DOpen    LDA     OPENFLG         ;Open Already?
```

APPENDIX B

6502 ASSEMBLY AND SOS LANGUAGE DRIVER
FOR THE ANALOG TO DIGITAL CONVERTER

```
          BEQ     $1              ;No

;.................ALREADY OPEN, SEND MESSAGE.................

          LDA     #XNOTAVAIL      ;Not Available Code
          JSR     SysErr          ;Go to SOS Error Routine

;.....COMPUTE AND ALLOCATE SYSTEM INTERNAL RESOURCES.......

$1        LDA     DIB_SLOT        ;Load Slot Number
          CLC
          ADC     SIRTABL         ;SIR=16+Slotnumber
          STA     SIRTABL         ;Store in SIR Pointer
          LDA     #SIRCNT         ;Load length of SIRTABL
          LDX     SIRADDR         ;Load X with lo byte Address
          LDY     SIRADDR+1       ;Load Y with hi byte Adress
          JSR     AllocSIR        ;Go to SOS Allocation Routine
          BCS     $2              ;Resources Not Available

;.................MARK DEVICE OPEN AND LEAVE.................

          LDA     #80             ;Load OPEN DEVICE Code
          STA     OPENFLG         ;Store in Open Flag
          RTS

;.................RESOURCES NOT AVAILABLE...................

$2        LDA     #XNORESRC       ;Load No Resources Code
          JSR     SysErr          ;Go to SOS Error Routine

;...................D_CLOSE PROCESSING.....................

;....CLEAN UP, COMPLETE WRITES, DEALLOCATE ALL, & LEAVE....

DClose    LDA     OPENFLG         ;Device Open?
          BNE     $1              ;Br/Yes
          JMP     NotOpen         ;Report if Not Open

;......CLEAN UP I/O, DISABLE INTERRUPTS, FREE THE SLOT......

$1        LDA     #SIRCNT         ;Load System Int. Res.
          LDX     SIRADDR         ;Load SIR Lo Byte Address
          LDY     SIRADDR+1       ;Load SIR Hi Byte Address
          JSR     DealcSIR        ;Deallocate Resources
          LDA     #0              ;Prepare to Close
          STA     OPENFLG         ;Mark This Device CLOSED
          RTS
```

APPENDIX B

6502 ASSEMBLY AND SOS LANGUAGE DRIVER FOR THE ANALOG TO DIGITAL CONVERTER

```
;.......CHECK INITIALLY FOR BUFFER POINTER ANOMOLIES.......

;                00XX bank N -> 80XX bank N-1
;                               20XX bank 8F if N was 0
;                FFXX bank N -> 7FXX bank N+1

Fixup     LDA     SOSBUF+1          ;Load MSB of Buffer Pointer
          BEQ     $2                ;If Zero, Fix It
          CMP     #0FF              ;Is it Another Problem?
          BEQ     $3                ;Br/Yes and Fix It
          RTS

$2        LDA     #80               ;00XX -> 80XX
          STA     SOSBUF+1          ;Fix and Restore
          DEC     SOSBUF+1401       ;Bank N -> Bank N-1
          LDA     SOSBUF+1401       ;Was It Bank Zero?
          CMP     #7F               ;(80) Before the Decrement
          BNE     $4                ;Br/No, All Fixed
          LDA     #20               ;If it was Zero, Change Both
          STA     SOSBUF+1          ;The MSB of the Buffer Address
          LDA     #8F               ;And The
          STA     SOSBUF+1401       ;Bank Number for Bank 8F
          BNE     $4                ;Always Branches

$3        CLC
          ROR     SOSBUF+1          ;FFXX-> 7FXX
          INC     SOSBUF+1401       ;Bank N -> Bank
$4        RTS

;..................D_READ CALL PROCESSING.................

DRead     LDA     OPENFLG           ;Check to See If Device Open
          BNE     $1                ;Br/Yes Open
          JMP     NotOpen           ;Else Report Error

;..............ZERO THE NUMBER OF BYTES READ..............

$1        LDA     #0                ;Prepare to Zero
          STA     RETCNT            ;Zero Lower Byte
          STA     RETCNT+1          ;Zero Upper Byte
          STA     CHX               ;Zero Channel-Gain Pointer

;..............CHECK BUFFER ADDRESS FOR PROBLEMS..........

          JSR     FixUp             ;Check and Fix Buffer Address

;..............COMPLIMENT REQUESTED BYTE COUNT...........
```

APPENDIX B

6502 ASSEMBLY AND SOS LANGUAGE DRIVER FOR THE ANALOG TO DIGITAL CONVERTER

```
            LDA     #0FF            ;Form One's Compliment
            EOR     REQCNT          ;By Exclusive-Or
            STA     REQCNT          ;Easier To Increment
            LDA     #0FF            ;And Test For Zero
            EOR     REQCNT+1        ;Same for Hi Byte
            STA     REQCNT+1        ;And Store

          set2mhz                   ;Set Fast Speed

;.......READ LOOP - CHECK FOR BYTE COUNT TERMINATION.......

RLOOP       INC     REQCNT          ;Increment Req. Count
            BNE     $2              ;Br/Not Zero
            INC     REQCNT+1        ;Increment Hi Byte
            BNE     $2              ;Br/Not Zero
            JMP     Rdend           ;End On Bytecount Done

;...COLLECT TRANSDUCER DATA, PUT IN BUFFER, INC. REQCOUNT..

$2          LDX     CHX             ;Load CHGA pointer
            LDA     CHGA, X         ;Load CHGA CODE into Accum.
            LDY     ADSLOT          ;Load Slot Offset
            STA     0C080,Y         ;False Store to Settle Voltages

            LDX     #08             ;Delay Constant
LOOPX       DEX                     ;Decrement Constant
            BNE     LOOPX           ;Delay 45 Microsec Settling

            STA     0C080,Y         ;Write to $C080 + SLOT * $16
            PHA                     ;Delay for Data Return
            PLA
            PHA
            PLA

            INY                     ;Inc for Hi Byte
            LDA     0C080,Y         ;Get Data Hi Byte
            AND     #0F             ;Knock Off Upper Nibble
            LDY     #0              ;Indirect Pointer
            STA     (SOSBUF), Y     ;Store Byte
            INCADR  SOSBUF          ;Inc. the Pointer
            INW     RETCNT          ;Inc. Return Count

            INC     REQCNT          ;Increment the Reqcount
            BNE     BITE2           ;Br/Not Zero
            INC     REQCNT+1        ;Increment Hi Byte
            BEQ     Rdend           ;Terminate on Byte Count

BITE2       LDY     ADSLOT          ;Load Slot Offset in Y
```

APPENDIX B

6502 ASSEMBLY AND SOS LANGUAGE DRIVER FOR THE ANALOG TO DIGITAL CONVERTER

```
            LDA     0C080,Y         ;Get Data Lo Byte
            LDY     #0              ;Prepare to Store
            STA     (SOSBUF), Y     ;Store Lo Byte (8 bits)
            INCADR  SOSBUF          ;Inc. the Pointer
            INW     RETCNT          ;Inc. Return Count

MORE        INC     CHX             ;Inc CHGA Pointer
            LDA     CHX             ;Load to Test (CHX=Chan. read)
            CMP     #0E             ;Read Last One? 0E=14
            BNE     RJUMP           ;Have we done 14 channels yet?
            LDA     #0              ;If so, Reset CHGA Pointer
            STA     CHX
RJUMP       JMP     RLOOP           ;And Read More Data

;.TERMINATE ON BYTE COUNT, INFORM USER OF NUMBER AND LEAVE.

Rdend       LDY     #0              ;Prepare to Return Read Count
            LDA     RETCNT          ;LSB of Returned Byte Count
            STA     (BREAD),Y       ;Store for Return to User
            INY                     ;Prepare to Do Hi Byte
            LDA     RETCNT+1        ;And Load It In
            STA     (BREAD),Y       ;And Return It

            RTS                     ;That's All The Reading!
            .END                    ;End of Device Driver Prgm.

;*************************************************************
;                          END PROGRAM
;*************************************************************
```

BIBLIOGRAPHY

BIBLIOGRAPHY

Adrian, P. A. and R. B. Fridley. 1958. Mechanical Fruit Tree Shaking. Calif. Agric. 12(10):3,15.

Adrian, P. A. 1962. Minimizing Bark Injury with Mechanical Shakers. Calif. Agric. 16(1):3.

Adrian, P. A. and R. B. Fridley. 1963a. Shaker Clamp Design as Related to Allowable Stresses of the Tree Bark. ASAE Paper No. 63-121. Am. Soc. of Agr. Eng., St. Joseph, MI 49085.

Adrian, P. A., R. B. Fridley, and C. Lorenzen. 1963b. Forced Vibration of a Tree Limb. ASAE Paper No. 63-642D. Am. Soc. of Agr. Eng., St. Joseph, MI 49085.

Adrian, P. A. 1964. The Forced Vibration of a Tree Limb. M.S. Thesis, Univ. of Calif., Davis.

Adrian, P. A., R. B. Fridley and D. Chaney. 1965a. Testing Permanent Fasteners. Calif. Agric. 19(8):10-11.

Adrian, P. A., R. B. Fridley, D. H. Chaney and K. Uriu. 1965b. Shaker-Clamp Injury to Fruit and Nut Trees. Calif. Agric. 19(8):8-10.

Agricultural Engineering Research Division (AERD). 1964. Mechanizing the Harvesting and Orchard Handling of Fruits. USDA, ARS, Spec. Rep. 22-88. Feb.

Alder, Y., A. Foux and U. M. Peiper. 1976. Experimental Investigation of Orange Tree Dynamics under Mechanical Shaking. J. Agr. Eng. Res. 21(2):121-131.

Beljakov, V., P. Manolov and A. Nikolov. 1979. Effect of Mechanical Harvesting using Tree Shakers on the Root System and Physiological Processes of Fruit Trees. Selskostopanska Tehnika 16(6):3-14.

Brown, G. K. 1980. Harvest Mechanization Status for Horticultural Crops. ASAE Paper No. 80-1532. Am. Soc. of Agr. Eng., St. Joseph, MI 49085.

Brown, G. K. 1982. Res. Leader USDA. Mich. State Univ., E. Lansing, MI 48824. Personal Communication.

Brown, G. K. (Ed.). 1983. Status of Harvest Mechanization of Horticultural Crops. ASAE Special Publication 0383, 78 pp. Am. Soc. of Agr. Eng., St. Joseph, MI 49085.

Brown, G. K., J. R. Frahm, R. L. Ledebuhr and B. F. Cargill. 1982. Bark Damage when Trunk Shaking Cherry Trees. ASAE Paper No. 82-1557. Am. Soc. of Agr. Eng., St. Joseph, MI 49085.

Brown, G. K., J. E. Neibauer, T. Kornecki and B. H. Zandstra. 1983. Small Farm Fruit and Vegetable Machinery Survey. ASAE Paper No. 83-1081. Am. Soc. of Agr. Eng., St. Joseph, MI 49085.

Bruhn, H. D. 1969. Mechanized Cherry Harvesting and the Relation of Applied Acceleration to Performance. From 'Mechanization of Harvesting Fruits' by J. H. Levin. Proceedings of the 3rd Section Theme 5 VII Int'l. Cong. Agr. Eng., Oct. 6-9, 1969, Baden-Baden, West Germany.

Bukovac, M. J. 1983. Too Much Shaking - A Costly Tool for Cherry Growers. Great Lakes Fruit Growers News, May.

Bukovac, M. J. 1984. Prof. of Horticulture. Mich. State Univ., E. Lansing, MI 48824. Personal Communication.

Bundat, J. S. and A. G. Piersol. 1971. Random Data: Analysis and Measurement Procedures. John Wiley and Sons, Inc., New York, NY. pp. 228-231, 287.

Cargill, B. F., G. K. Brown and M. J. Bukovac. 1982. Factors Affecting Bark Damage to Cherry Trees by Harvesting Machines. Mich. State Univ., CES, AEIS Bull. No. 471. June, 6 pp.

Conte, S. D. and C. de Boor. 1980. Elementary Numerical Analysis. Third Edition. McGraw Hill Book Co., New York, NY. pp. 303-345.

Davis, C. C. and J. T. Blake. 1937. Chemistry and Technology of Rubber. Reinhold Publishing Corp., New York, NY.

Devay, J. E., W. H. English, F. L. Lukezic and H. J. O'Reilly. 1960. Mallet Wound Canker of Almond Trees. Calif. Agric. 14(8):8-9.

Devay, J. E., F. L. Lukezic, W. H. English, W. J. Moller and B. W. Parkinson. 1965. Ceratocystis Canker of Stone Fruit Trees. Calif. Agric. 19(10):2-4.

Devay, J. E., F. L. Lukezic, W. H. English, K. Uriu and C. J. Hansen. 1962. Ceratocystis Canker. Calif. Agric. 16(1):2-3.

Diener, R. G., F. H. Buelow and S. K. Ries. 1965. A Plane Area Method for Estimating the Weight of Living Fruit Trees. Quart. Bull. 47(4):527-532. Mich. Agr. Expt. Sta., E. Lansing, MI 48824.

Diener, R. G., J. H. Levin and B. R. Tennes. 1968. Directional Strength Properties of Cherry, Apple and Peach Bark ad the Influence of Limb Mass and Diameter on Bark Damage. Trans. of the ASAE 11(6):788-791.

Doeblin, E. O. 1983. Measurement Systems: Application and Design. Third Edition. McGraw Hill Inc., New York, NY. pp. 73, 134, 317-323.

Drake, S. R. 1983. Introduction to the Symposium - The Influence of Mechanical Harvesting on the Quality of Horticultural Crops. Hort Sci. 18(4):Spec. Insert p.406.

Ellis, R. and D. Gulick. 1978. Calculus with Analytic Geometry. Harcourt Brace Jovanovich Inc., New York, NY. pp. 363-371.

Esau, K. 1965. Plant Anatomy. John Wiley and Sons, Inc. New York, NY.

Frahm, J. R., G. K. Brown and L. J. Segerlind. 1983. Mechanical Properties of Trunk Shaker Pads. ASAE Paper No. 83-1078. Am. Soc. of Agr. Eng., St. Joseph, MI 49085.

Friday, D. and P. Friday. 1983. Personal Communication. Hartford, MI 49057.

Friday Tractor Company. 1982-83. Sales Literature and Personal Communication. Hartford, MI 49057.

Fridley, R. B. and P. A. Adrian. 1960. Some Aspects of Vibratory Fruit Harvesting. Agricultural Engineering 41(1):28-31.

Fridley, R. B., G. K. Brown and P. A. Adrian. 1970. Strength Characteristics of Fruit Tree Bark. Hilgardia 40(8):205-223.

Gaston, H. P., J. H. Levin and R. T. Whittenberger. 1966. How to Use Cherry Harvesting Machines. Coop. Ext. Serv. Bull. 532. Farm Sci. Series, Mich. State Univ., E. Lansing, MI 48824.

Gentry, J.P. 1980. Mechanical Harvesting Desert Grown Grapefruit. ASAE Paper No. 80-1042. Am. Soc. of Agr. Eng., St. Joseph, MI 49085.

Halderson, J. L. 1966. Fundamental Factors in Mechanical Cherry Harvesting. Trans. of the ASAE 9(5):681-684.

Hedden, S. L., J. D. Whitney and D. B. Churchill. 1983. Trunk Shaker Removal of Oranges. ASAE Paper No. 83-1079. Am. Soc. of Agr. Eng., St. Joseph, MI 49085.

Hussain, A. A., G. E. Rehkugler and W. W. Gunkel. 1975. Tree Limb Response to a Periodic Discontinuous Sinusoidal Displacement. Trans. of the ASAE 18(4):614-617.

Hutton, R. J. and G. A. Brown. 1981. Evaluation of a Whole Tree Fruit Harvester for Mechanical Harvesting of Processing Fruits in the Murrumbidgee Irrigation Areas, N.S.W. Dept. of Agric. New South Wales Tech. Bull. 24.

Kronenberg, H. G. 1964. Possibilities for Mechanical Fruit Harvesting. J. Agr. Eng. Res. 9(2):194-196.

Levin, J. H., H. P. Gaston, S. L. Hedden and R. T. Whittenberger. 1960. Mechanizing the Harvest of Red Tart Cherries. Quarterly Bulletin 42(4):42-60. Michigan State University Agr. Expt. Station, East Lansing, MI 48824. May.

Lyons, C. G., Jr. and K. S. Yoder. 1981. Poor Anchorage of Deeply Planted Peach Trees. Hort Science 16(1):48-49.

Memmler, D. K. 1934. The Science of Rubber. Reinhold Publishing Corp., New York, New York.

Michigan Department of Agriculture. 1979. Michigan Fruit Tree Survey 1978. 65 pp. P. O. Box 20008, Lansing, MI 48901.

Michigan Department of Agriculture. 1983a. Michigan Agricultural Statistics. 80 pp. P. O. Box 20008, Lansing, MI 48901.

Michigan Department of Agriculture. 1983b. Michigan Orchard and Vineyard Survey 1982. 49 pp. P.O. Box 20008, Lansing, MI 48901.

Millier, W. F., J. v. d. Werken and J. A. Throop. 1983. A Recoil-Impact Shaker for Semi-Dwarf Apple Trees. ASAE Paper No. 83-1080. Am. Soc. of Agr. Eng., St. Joseph, MI 49085.

Peterson, D. L. and G. E. Monroe. 1977. Continuously Moving Shake-Catch Harvester. Trans. of the ASAE 20(2):202-205, 209.

Peterson, D. L. 1984. Mechanical Harvester for High Density Orchards. Presented at the Int'l. Symposium on Fruit, Nut, and Vegetable Harvesting Mechanization, Oct. 5-12, 1983, Tel Aviv, Israel.

Priestly, J. H. 1930. Studies in the Physiology of Cambial Activity III. "The Seasonal Activity of the Cambium". New Phytologist 29:316-354.

Tennes, B. R. and G. K. Brown. 1981. The Design, Development, and Testing of a Sway Bar Shaker for Horticultural Crops---A Progress Report. ASAE Paper No. 81-1059. Am. Soc. of Agr. Eng., St. Joseph, MI 49085.

Yamamoto, H. 1979. Study on the Response of Tree to be Forced to Vibrate. Sci. Rept. Agr. Kobe Univ. 13:301-311. Kobe Daigaku, Nogaku-bu, Japan.

Yung, C. and R. B. Fridley. 1975. Simulation of Vibration of Whole Tree Systems using Finite Elements. Trans. of the ASAE 18(3):475-481.